Trait-based Approaches to Marine Microbial Ecology

by

Andrew David Barton

Submitted to the Department of Earth, Atmospheric, and Planetary Science
in partial fulfillment of the requirements for the degree of

Doctor of Philosophy

at the

MASSACHUSETTS INSTITUTE OF TECHNOLOGY

September 2011

Author .....
Department of Earth, Atmospheric, and Planetary Science
June 1, 2011

Certified by .....
Michael J. Follows
Senior Research Scientist
Thesis Supervisor

Accepted by .....
Maria T. Zuber
E. A. Griswold Professor of Geophysics
Head of Department

Trait-based Approaches to Marine Microbial Ecology

by

Andrew David Barton

Submitted to the Department of Earth, Atmospheric, and Planetary Science
on September 1, 2011, in partial fulfillment of the
requirements for the degree of
Doctor of Philosophy

Abstract

The goal of this thesis is to understand how the functional traits of species, biotic interactions, and the environment jointly regulate the community ecology of phytoplankton.

In Chapter 2, I examined Continuous Plankton Recorder observations of diatom and dinoflagellate abundance in the North Atlantic Ocean and interpreted their community ecology in terms of functional traits, as inferred from laboratory- and field-based data. A spring-to-summer ecological succession from larger to smaller cell sizes and from photoautotrophic to mixotrophic and heterotrophic phytoplankton was apparent. No relationship between maximum net growth rate and cell size or taxonomy was found, suggesting that growth and loss processes nearly balance across a range of cell sizes and between diatoms and dinoflagellates.

In Chapter 3, I examined a global ocean circulation, biogeochemistry, and ecosystem model that indicated a decrease in phytoplankton diversity with increasing latitude, consistent with observations of many marine and terrestrial taxa. In the modeled subpolar oceans, seasonal variability of the environment led to the competitive exclusion of phytoplankton with slower growth rates and to lower diversity. The relatively weak seasonality of the stable subtropical and tropical oceans in the global model enabled long exclusion timescales and prolonged coexistence of multiple phytoplankton with comparable fitness. Superimposed on this meridional diversity decrease were "hot spots" of enhanced diversity in some regions of energetic ocean circulation which reflected a strong influence of lateral dispersal.

In Chapter 4, I investigated how small-scale fluid turbulence affects phytoplankton nutrient uptake rates and community structure in an idealized resource competition model. The flux of nutrients to the cell and nutrient uptake are enhanced by turbulence, particularly for big cells in turbulent conditions. Yet with a linear loss form of grazing, turbulence played little role in regulating model community structure and the smallest cell size outcompeted all others because of its significantly lower R^* (the minimum nutrient requirement at equilibrium). With a quadratic loss form of grazing, however, the coexistence of many phytoplankton sizes was possible and turbulence played a role in selecting the number of coexisting size classes and the dominant size class. The impact of turbulence on community structure in the ocean may be greatest in relatively nutrient-deplete regions that experience episodic inputs of turbulence kinetic energy.

Thesis Supervisor: Michael J. Follows
Title: Senior Research Scientist

Acknowledgments

I would like to thank my collaborators, thesis committee members, and funding sources. The work in Chapter 2 was done in collaboration with Zoe Finkel (Mt. Allison University; she is primarily responsible for the cell size database), David Johns (Sir Alister Hardy Foundation for Ocean Science; David helped me sort out phytoplankton taxonomy), Mick Follows (MIT), and Ben Ward (MIT). The Sir Alister Hardy Foundation for Ocean Science kindly provided the Continuous Plankton Recorder data. Also, Per Juel Hansen (University of Copenhagen) was very helpful in putting together the trophic strategy database. The work in Chapter 3 was done in collaboration with Stephanie Dutkiewicz (MIT), Glenn Flierl (MIT), Mick Follows, and Jason Bragg (CSIRO). Oliver Jahn's (MIT) work with high resolution ocean-ecosystem models was helpful in interpreting the diversity patterns. The work in Chapter 4 was done in collaboration with Mick Follows and Ben Ward. In particular, I would like to thank Mick for his enthusiasm, ongoing support, and clear intellectual guidance. Thank you to the members of my thesis committee–John Marshall (MIT), Heidi Sosik (WHOI), Glenn Flierl, and Mick Follows–for your counsel. And thank you also to all the current and past members of the Follows lab group. Lastly, thank you to the Gordon and Betty Moore Foundation's Marine Microbiology Initiative and to the National Science Foundation for supporting my PhD.

To my family, M., T., M., and L.: with you on the Kern, I learned to love and question nature. To G.K.: may we always raise a lush and merry garden together. Now, let's all get out there together and enjoy warm summer days, Willow Lake, and incense cedars.

Contents

Chapter 1

Introduction

1.1 Summary

The term "phytoplankton" refers to a diverse group of largely photoautotrophic, single-celled organisms that live primarily in sunlit, surface waters (Falkowski et al., 2004). Taken together, marine phytoplankton account for roughly half the primary production on Earth (Field et al., 1998), and consequently they play key roles in marine ecosystems, global biogeochemical cycles, and the climate system. They constitute the base of the marine food chain, and are of great importance to humans because of the goods and services provided by marine ecosystems (Worm et al., 2006). The role of phytoplankton in marine ecosystems, global biogeochemical cycles, and the climate system depends not just on their total biomass, but also on what kinds of phytoplankton are present and their relative abundance through space and time (Cushing, 1989; Cullen et al., 2002). Thus, a greater understanding of the community ecology of marine phytoplankton has direct bearing on the study of complex, global processes.

The goal of this thesis is to understand how the functional traits of constituent species, their biotic interactions, and the environment jointly regulate the community ecology of phytoplankton. To this end, I employ a combination of data and models, which I describe in detail in each of the following chapters. I examine compilations of laboratory- and field-based data describing phytoplankton traits, as well as field observations of the abundances of species within diverse phytoplankton communities. I develop idealized, zero-dimensional models and examine complex global simulations where the net population growth of phytoplankton depends on their functional traits, environmental conditions, and loss processes, such as grazing. In these models, where appropriate I have investigated both bottom-up phytoplankton ecological processes and top-down processes such as losses to zooplankton grazing, as both perspectives are important in regulating the phytoplankton community (Armstrong, 1994; Ward et al., 2011). The general approach is to have data analysis and modeling complement and inform each other, and I have written each of the following chapters such that they can be read independently from the rest.

In the Introduction, I review briefly the role of phytoplankton in marine ecosystems and biogeochemical cycles, and discuss why the diversity of phytoplankton has a crucial impact on these processes. I then describe what is known about phytoplankton diversity and biogeography, focusing on groups of phytoplankton, such as diatoms, dinoflagellates, and picophotoautotrophs (e.g., *Prochlorococcus*, , and picoeukaryotes), that are discussed in this thesis. I introduce key phytoplankton traits that govern their community ecology,

and describe how they are often constrained by phytoplankton size. Lastly, I outline the main questions and goals of each chapter and summarize the methodology used.

1.1.1 Where do Phytoplankton Grow? A First Look

Data indicating the mean concentration of chlorophyll *a* for the biosphere during September 1997 through August 1998, as inferred by the SeaWiFS satellite, tell a good deal about where and why phytoplankton flourish (Fig. 1.1). Chlorophyll *a* is an important photosynthetic pigment used by phytoplankton to collect light to power photosynthesis, and is an imperfect but useful proxy for the total phytoplankton biomass present in the surface ocean. When viewed from this broad, mean perspective, it is apparent that phytoplankton are unevenly distributed over the ocean surface. In particular, one notices greater phytoplankton biomass in the cooler subpolar ocean gyres than in the warmer, lower latitude subtropical gyres. Ignoring for the moment processes such as losses to predation and respiration, this distribution of phytoplankton biomass can be understood, to first order, by considering a simplified reaction describing phytoplankton biosynthesis (Anderson, 1995):

$$106CO_2 + 16HNO_3 + H_3PO_4 + 78H_2O + light \longrightarrow C_{106}H_{175}O_{42}N_{16}P + 150O_2 \quad (1.1)$$

In this view, a cell incorporates inorganic forms of carbon (CO_2), nitrogen (HNO_3), and phosphorous (H_3PO_4; as well other micronutrients, such as iron) in the presence of light to make organic matter ($C_{106}H_{175}O_{42}N_{16}P$) and oxygen ($O_2$). The availability of light and nutrients (C, N, and P) constrains where phytoplankton may photosynthesize and grow. Whereas light is most abundant at the ocean surface and decays with depth, nutrients are plentiful at depth and depleted at the surface by biological activity (I discuss this process below), and the contrasting vertical availability of these resources is evident in patterns of phytoplankton biomass. For example, in the vast expanses of the subtropical oceans with little surface chlorophyll (Fig. 1.1), there is typically abundant light but little surface nutrients because of the stable density stratification of the water column and wind-driven, downwelling vertical motion (Williams and Follows, 2011). In these nutrient limited regions, phytoplankton may become abundant either deeper in the water column (~100m depth), where both nutrients and light are available (e.g., Partensky et al., 1999; Huisman et al., 2006), or in response to localized upwelling zones or other physical processes that sporadically deliver nutrients to the surface (e.g., Chavez and Barber, 1987; McGillicuddy et al., 2007). By contrast, in the subpolar gyres (areas of relatively high chlorophyll in Fig. 1.1), the wind-driven vertical motion is upwards, the surface ocean is relatively well-mixed, and nutrient delivery to the surface tends to be greater. However, light varies seasonally, and with additional light in spring, photosynthesis proceeds and phytoplankton "bloom." The ambient nutrient concentration is drawn down by the rapid growth and may be replenished by later mixing events (some organic matter leaves the surface, as I describe below). A large range of other factors, including environmental temperature, the recycling of primary productivity in the surface, sinking of phytoplankton cells, predation, and respiration, enrich this conceptual picture, but to a first order, considering light and nutrient availability explains a great deal about the distribution of phytoplankton biomass.

1.1.2 Phytoplankton and Biogeochemical Cycles

Phytoplankton play a key role in global biogeochemical cycles and the climate system because of their ability to transport carbon and other elements from the surface ocean, which

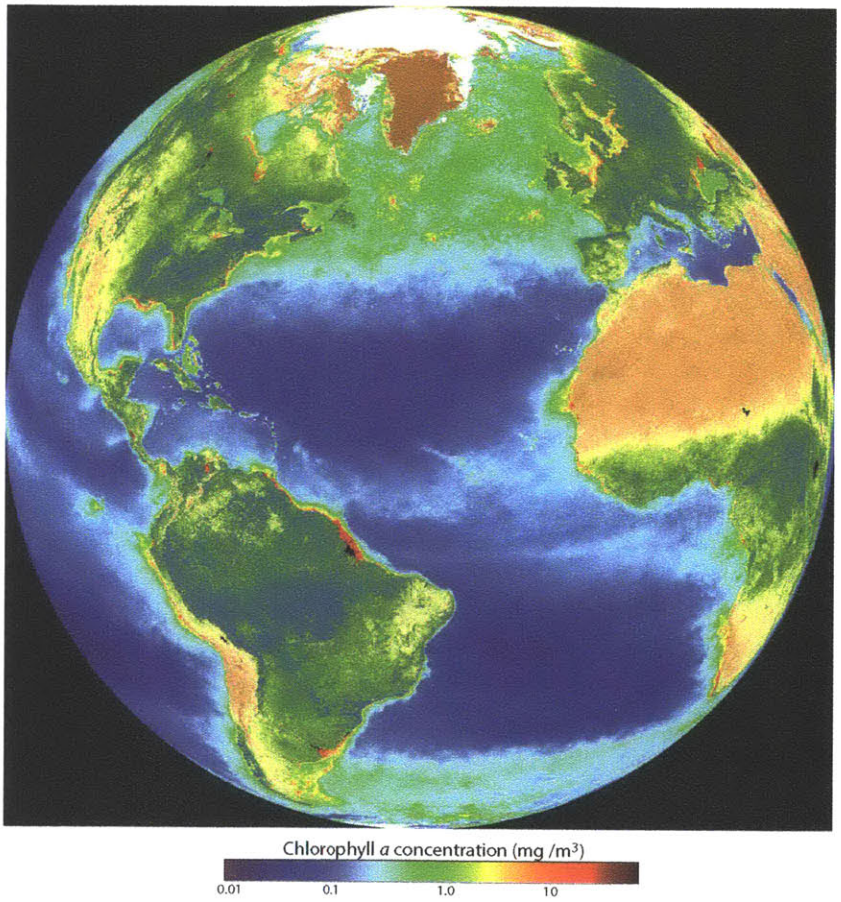

Figure 1.1: Mean SeaWiFS chlorophyll a concentration (mg m^{-3}) for September 1997 through August 1998, NASA Ocean Color Gallery, http://oceancolor.gsfc.nasa.gov/.

is in near constant contact with the atmosphere, to the deep ocean and sediments, which are isolated from the atmosphere for a much longer duration (Falkowski et al., 1998; Sigman and Boyle, 2000; Sarmiento and Gruber, 2006; Williams and Follows, 2011). In Fig. 1.2, I show a very simplified schematic of some of the possible pathways for phytoplankton primary production at a given location in the ocean. This is by no means a complete picture, but is helpful in discussing the importance of phytoplankton ecology to global-scale processes (see Sarmiento and Gruber, 2006 and Williams and Follows, 2011 for a more complete picture). First, at each level in the ocean, lateral transport is possible and is mediated by biological processes, such as migrations of fish and zooplankton, and physical processes, such as transport due to currents and mixing. Second, much of the surface primary productivity is recycled locally. Elements contained in dead or predated phytoplankton, their predators, and exudates are ultimately returned to inorganic, bioavailable forms through a complex array of biological and chemical transformations, and an appreciation for the importance of this surface recycling has grown over the last few decades (Azam et al., 1983; Sherr and Sherr, 1994; Pomeroy et al., 2007). Third, some portion of surface primary production makes its way into the deeper waters, either by physical transport or mixing, gravitational sinking of phytoplankton, predators, or other particles such as fecal pellets, or through biological movements such as zooplankton and fish migrations. This process has been coined the "biological pump", and its character varies strongly in space and time (Ducklow et al., 2001; Sarmiento and Gruber, 2006). It tends to deplete the surface of nutrients and is responsible for the characteristic increase of nutrients with depth. Fourth, most of the primary production entering the deep ocean will be remineralized (again, by complex biological and chemical pathways) back into inorganic form and ultimately be returned to the surface, and a very small fraction of the surface primary productivity is buried in marine sediments. Superimposed on this marine component of the schematic is the equilibration of the surface ocean with the atmosphere; carbon dioxide, for instance, fluxes into or out of the surface ocean depending on the concentration gradient (e.g., Wanninkhof, 1992). The rates of exchange between and amounts of carbon and other elements in each reservoir are determined, in part, by ecosystem processes, and thus ecosystems play a key role in biogeochemical cycles and climate.

1.2 Phytoplankton Diversity

In the previous section I considered phytoplankton as though they were one, generic group, whereas in fact they are quite diverse, and the biogeochemical function of the ecosystem depends not only on the total primary productivity, but also on how many species are present and their relative abundances (e.g., Laws et al., 2000; Doney et al., 2004; Cullen et al., 2007; Ptacnik et al., 2008). There are at least 25,000 identified species of phytoplankton spanning 8 major divisions or phyla (Falkowski et al., 2004), though the actual number of species may be much higher (Pedrós-Alió, 2006; Armbrust, 2009). They span a broad range in size ($\sim 10^0 - 10^8 \mu m^3$ in cell volume), morphology, behavior, and biochemistry (Tomas et al., 1997; Taylor et al., 2008; Fig. 1.3), and they inhabit all the world's surface marine waters. Relatively little is known, however, about the patterns of marine phytoplankton diversity. This is perhaps surprising considering the important role that diversity plays in ecosystem resilience, stability (e.g., Vallina and LeQuéré, 2011), and function (e.g., Ptacnik et al., 2008). Here I review what little is known about how phytoplankton diversity varies in the ocean, and introduce the primary mechanisms that are thought to play a role in

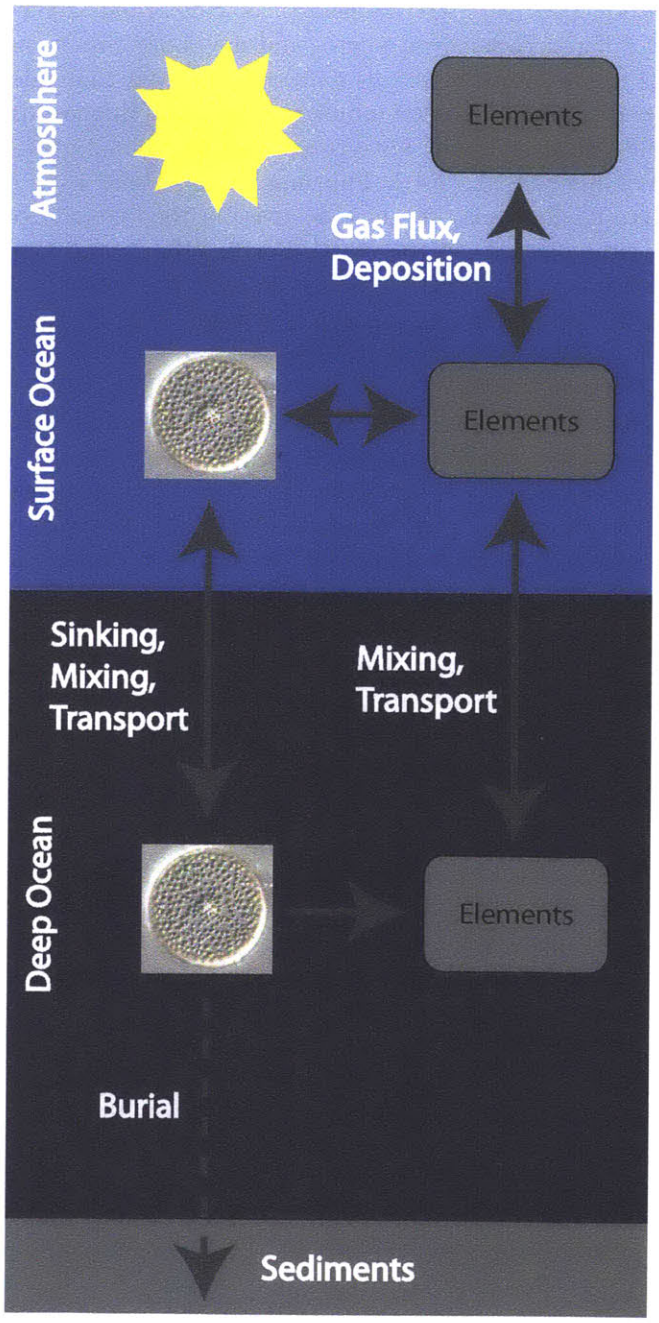

Figure 1.2: Idealized representation of important pathways for phytoplankton biomass (left) and bioavailable forms of important elements, such as C, N, P, and Fe (right). For a more complete picture, see Sarmiento and Gruber (2006) and Williams and Follows (2011).

regulating the diversity of many types of organisms.

A large range of marine and terrestrial taxa exhibit a decrease in species diversity with increasing latitude (Currie, 1991; Angel, 1993; Hillebrand, 2004; Fig. 1.4). While there are important differences between micro- and macroorganisms, such as the ease and range of dispersal (Finlay, 2002), it is now generally believed that microbes have similar ecological patterns and processes as seen in macroorganisms (Hughes Martiny et al., 2006). Studies employing molecular methods have revealed a meridional gradient in diversity for bacterioplankton (Pommier et al., 2007; Fuhrman et al., 2008; Fig. 1.4B). Microscope-based studies of phytoplankton also reveal a decrease in the diversity of coccolithophorids from subtropical to subpolar seas in the North Pacific (Honjo and Okada, 1974) and the South Atlantic (Cermeño et al., 2008a). Along an Atlantic transect (the Atlantic Meridional Transect), diatoms exhibited a different pattern (Cermeño et al., 2008a), with "hot spots" of enhanced diversity associated with productive regions (at $\sim$15°N, close to the African coast, and at $\sim$40°S, in the South Atlantic). A related study found no clear relationship between phytoplankton diversity and latitude in a compilation of Atlantic observations, but this study did not include the smallest phytoplankton, which tend to be abundant in the tropics, and subarctic latitudes (Cermeño et al., 2008b). Overall, though, the relatively sparse observational evidence suggests a meridional decline in the diversity of marine microbes including at least some taxa of phytoplankton, as well as regional "hot spots" for some taxonomic groups. However, more marine observations are needed to confirm these patterns.

What regulates these large-scale patterns of diversity? Even for relatively well-studied terrestrial taxa, this question remains the subject of great debate (e.g., Rohde, 1992). The picture is murkier still for less studied systems and taxa such as marine phytoplankton. The mechanisms for maintaining the diversity of life on Earth have long interested ecologists (Hutchinson, 1959; Hutchinson, 1961), and the explanations for the meridional diversity gradient have been classified as historical, evolutionary, or ecological in nature (Mittelbach et al., 2007; Fuhrman et al., 2008). Historical explanations invoke events and changes in Earth history, such as Milankovitch cycles, in setting current species diversity. Evolutionary explanations examine the rates of speciation and extinction and their balance through time (MacArthur and Wilson, 1967; Allen et al., 2006). Ecological explanations include trophic interactions (e.g., Paine, 1966), spatial and temporal heterogeneity of habitats (e.g., Hutchinson, 1961; MacArthur and MacArthur, 1961), internal oscillations and chaotic interactions among competing species (e.g., Huisman and Weissing, 1999), the area and geometry of habitats (e.g., Colwell and Hurtt, 1994), and the impact of total primary productivity (Irigoien et al., 2004; see Chapter 3 Appendices for a more detailed review). However, there is, as yet, no single accepted explanation for what causes diversity patterns, and it is likely that multiple mechanisms act in concert to bring about the observed patterns. With respect to marine phytoplankton, for which we have relatively few data and studies on diversity patterns, the mechanisms underlying their diversity patterns are almost completely unknown.

1.3 Phytoplankton Biogeography

From this great degree of diversity, groups of phytoplankton with similar characteristics or biogeochemical function can be organized (LeQuéré et al., 2005; Follows and Dutkiewicz, 2011). Though the exact definitions of these groups are extremely fluid, generalizations can be made about their typical spatial distribution, or biogeography (Longhurst, 1998),

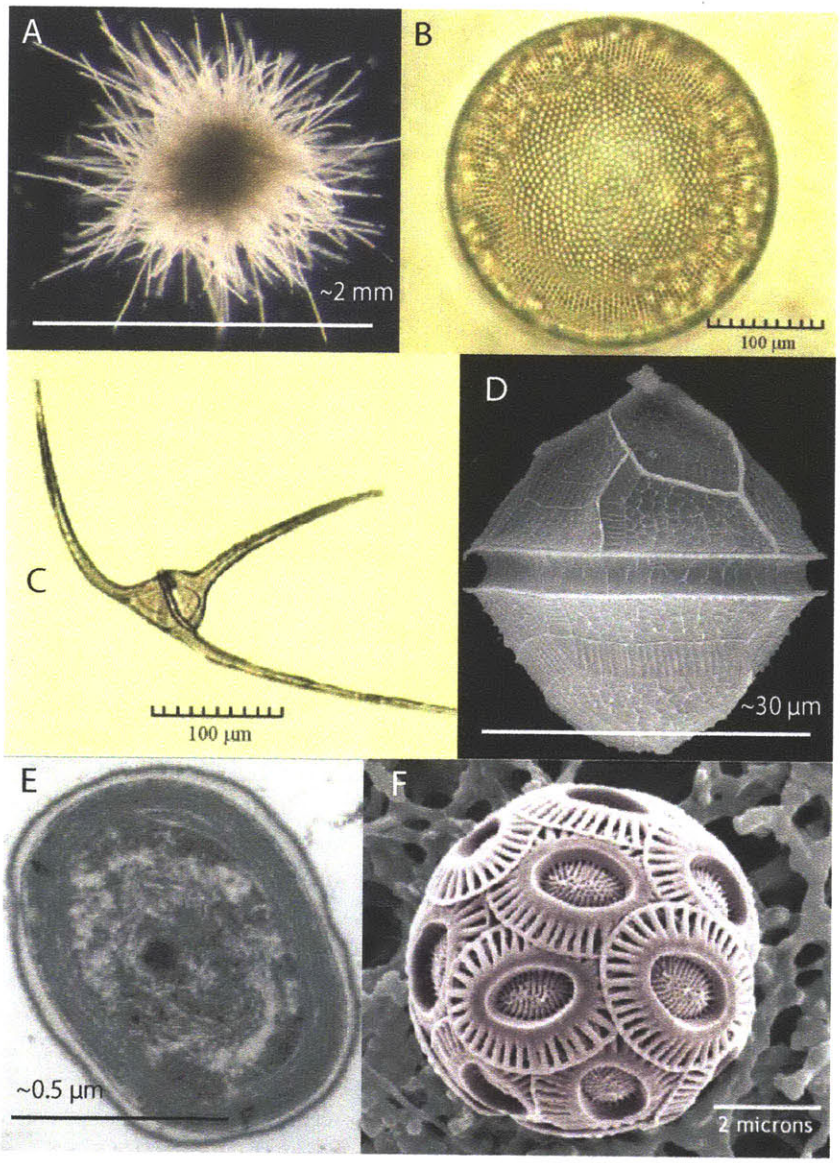

Figure 1.3: A range of phytoplankton species, images not to scale. A) Colony of the nitrogen-fixing cyanobacterium, *Trichodesmium thibautii* (Waterbury, 2004), B) Diatom, *Coscinodiscus oculus iridis* (Matishov et al., 2000), C) Dinoflagellate, *Ceratium arcticum* (Matishov et al., 2000), D) Heterotrophic dinoflagellate, *Protoperidinium latistriatum* (Scott, 2011), E) Cyanobacterium, *Prochlorococcus* (Waterbury, 2004), and F) Coccolithophore, *Emiliania huxleyi* (Geisen, 2011).

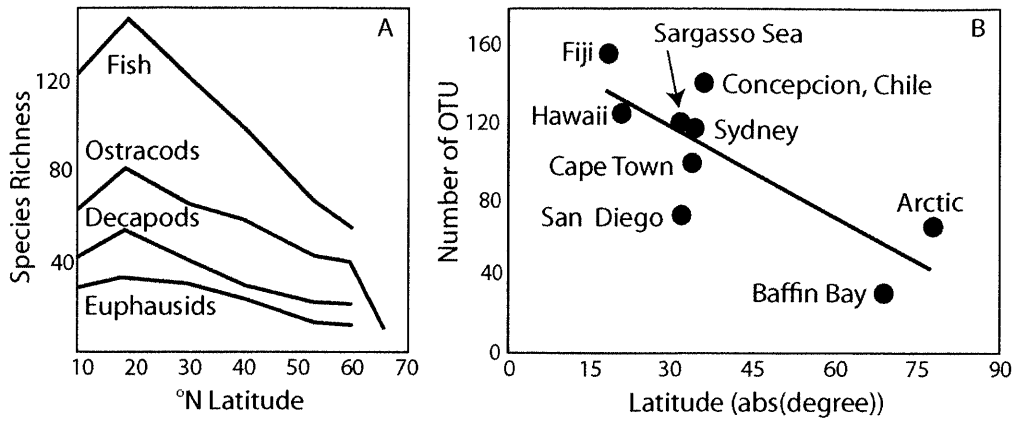

Figure 1.4: A) Species richness, or diversity, in several marine taxonomic groups, including fish, ostracods, decapods, and euphausids. Similar patterns are common among terrestrial taxa. Figure redrawn from Angel (1993). B) Number of operational taxonomic units (OTU) among marine bacterioplankton, including photosynthetic cyanobacteria. An OTU is defined as the bacterioplankton strains having $\geq$ 97% 16S rRNA gene sequence identity, and is often treated as a proxy for "species". Figure redrawn from Pommier et al. (2007).

and biogeochemical functions. Several groups, notably the diatoms, dinoflagellates, and picophotoautotrophs, are discussed in this thesis. Generally speaking, marine ecosystems characterized by the dominance of diatoms or dinoflagellates and picophotoautotrophs are quite different in nature of mineral export and recycling. Diatoms are, on average, relatively large phytoplankton cells (~5-200μm in equivalent spherical diameter, or ESD) that require silica to form their frustules, and they are typically most conspicuous in turbulent, nutrient-rich waters such as upwelling zones, coastal zones, or in spring bloom conditions (Barber and Hiscock, 2006; Cermeño et al., 2008a). Diatom blooms typically terminate because of nutrient limitation, grazing, or sedimentation from the water column (reviewed in Sarthou et al., 2005). Because of their size, dense frustules, and high, episodic abundance, diatoms are thought to be relatively efficient at exporting organic matter from the surface to ocean depths, as well as in feeding higher trophic levels (Ryther, 1969; Cushing, 1989).

Dinoflagellates are relatively large phytoplankton (~5-200μm), though they tend to be more abundant in nutrient-deplete conditions, either in oligotrophic seas or in post-bloom conditions (Margalef, 1978). A notable exception to this pattern are harmful algal blooms of dinoflagellates, which tend to occur in low turbulence, but high nutrient, regimes (Smayda, 1997; Smayda and Reynolds, 2001). Picophotoautotrophs, such as *Prochlorococcus*, *Synechococcus*, and picoeukaryotes, are small (~0.5-5μm) but extremely abundant phytoplankton that tend to be most numerous in relatively nutrient-poor conditions, though *Synechococcus* tends to favor slightly higher nutrient levels (Zubkov et al., 1998). Deep chlorophyll maximums (~100m) found in many subtropical zones consist largely of picophotoautotrophs. Compared with ecosystems dominated by diatoms, dinoflagellate and picophotoautotroph-dominated ecosystems are thought to have a greater fraction of organic matter recycled within the surface layers (Azam et al., 1983; Laws et al., 2000). Dinoflagellates and picophotoautotrophs are not always found together, but are in many cases (Margalef, 1978).

Even in this simple division of the ocean into two separate regimes reflecting some of the diversity of phytoplankton, one can see the impact of phytoplankton communities on biogeochemical cycles. There are, of course, many other important groups of phytoplankton not considered here, including coccolithophores (Cermeño et al., 2008a), small flagellates (Zubkov and Tarran, 2008), *Phaeocystis* spp. (Verity et al., 1988), and others, but I focus on those described above. Many of the mechanisms and hypotheses discussed in the following chapters may be general enough to extend beyond these primary groups.

1.4 Phytoplankton Functional Traits

Why do diatoms, dinoflagellates, and picophotoautotrophs grow when and where they do? The makeup of ecological communities is thought to be regulated by the interplay of constituent species functional traits, biotic interactions, and the environment (McGill et al., 2006; Litchman and Klausmeier, 2008), and this perspective has a long history in terrestrial (e.g., Westoby and Wright, 2006) and marine ecology (e.g., Margalef, 1978). Environmental gradients in parameters that impact phytoplankton fitness, such as temperature, light, and nutrients, are pervasive features in the ocean, and occur on a range of spatial and temporal scales, from short-lived, small-scale fluid turbulence (Karp-Boss et al., 1996) to long-term, global climate change. Inter- and intraspecific biotic interactions include predation, production of toxins for mediating predation and competition, viral infection, and other factors (Armstrong, 1994; Smayda, 1997; Fuhrman, 1999). But what are functional traits?

A functional trait is defined as an organism characteristic that determines its fitness through its effects on growth, reproduction, and survival (Violle et al., 2007). For phytoplankton, functional traits include light and nutrient acquisition and use (Aksnes and Egge, 1991), predator avoidance (Kiørboe, 2008), morphological variation (such as size, shape, and motility), temperature sensitivity (e.g., Eppley, 1972), and reproductive strategies (Litchman and Klausmeier, 2008). Traits should vary strongly between species and be measurable on continuous scales (McGill et al., 2006). For example, classifying phytoplankton "singled-celled" may not be a useful trait. Importantly, we also need to know something of the trade-offs among traits (e.g., Litchman et al., 2007); in effect, one species cannot be optimal at everything, or it would dominate everywhere at all times. For phytoplankton, progress has been made toward uncovering the crucial traits and trade-offs among traits that regulate their net population growth and community ecology, often by analyzing compilations of laboratory data from many taxa (Tang, 1995; Litchman et al., 2007).

In the following chapters, I consider a number of phytoplankton traits, including those that are rather descriptive and relatively straight-forward, such as phytoplankton cell size (μm^3) and trophic strategy (ranging from photoautotrophic to heterotrophic). For these more descriptive traits, my collaborators and I have mined the literature for published studies describing phytoplankton cell size and trophic strategy (see Chapter 2 for more details). Other traits describing growth and uptake rates and nutrient storage perhaps make the most sense when considered in the context of equations describing algal growth. Here, I introduce the Droop (1968), or variable internal stores, model, but other models of algal growth, including the Monod model (Monod, 1950), use traits in a similar manner (Verdy et al., 2009 and others have related the two models). Consider a community with i phytoplankton types (X_i, cells m^{-3}) competing for one limiting nutrient (N, μmolN m^{-3}) in a chemostat. Phytoplankton may uptake (V_i, μmolN cell^{-1} day^{-1}) and store nutrients in an internal quota (Q_i, μmolN cell^{-1}). Uptake follows Michaelis-Menten kinetics, and the

internal quota is depleted through cellular division (μ_i, day^{-1}). Cells may die (m, day^{-1}) or be diluted (D, day^{-1}). The equations are:

$$\frac{dX_i}{dt} = \mu_i X_i - mX_i - DX_i \tag{1.2}$$

$$\frac{dQ_i}{dt} = V_i^{max}\frac{N}{N+k_i} - \mu_i Q_i \tag{1.3}$$

$$\frac{dN}{dt} = D(N_o - N) - \sum_i V_i^{max}\frac{N}{N+k_i}X_i \tag{1.4}$$

$$\mu_i = \mu_i^{max}(1 - \frac{Q_i^{min}}{Q_i}) \tag{1.5}$$

where N_o (μmolN m^{-3}) is the input nutrient concentration. Phytoplankton biomass (P_i, μmolN m^{-3}) is X_iQ_i. The functional traits describing each model phytoplankton are as follows: maximum potential division rate (μ_i^{max}, day^{-1}); minimum internal nutrient quota (Q_i^{min}, μmolN cell^{-1}); maximum nutrient uptake rate (V_i^{max}, μmolN cell^{-1} day^{-1}); and the half-saturation nutrient concentration (k_i, μmolN m^{-3}), or the nutrient concentration at which $V = 0.5V^{max}$. In the context of the quota model, μ^{max} is a cellular division rate. However, when using a biomass formulation for the time rate of change in phytoplankton biomass (μmolN m^{-3} day^{-1}; Chapter 2 and 3), I will refer to μ^{max} simply as a growth rate, which may include cellular growth and division.

These functional traits often scale with cell volume: $x = bV^a$, where V is cell volume and coefficients a and b are observed to hold across many orders of magnitude in data compilations. For example, laboratory studies for all phytoplankton types taken together reveal that μ^{max} scales with cell volume such that $b = 3.49$ and $a = -0.15$ (Tang, 1995; Fig. 1.5). In this allometric context, smaller cells grow faster than larger cells. It has been observed that smaller cells precede larger cells in phytoplankton succession in temperate seas (Cushing, 1989; Taylor et al., 1993) and some lakes (Sommer, 1985), and this effect has been often been attributed to the size-dependence in μ^{max}. Some of these so-called allometric relationships have been explained by the transport of essential resources through internal cellular networks (West et al., 1997). This size-dependence also allows for representation of the large range of phytoplankton sizes in the absence of complete information regarding their functional traits (e.g., Irwin et al., 2006; Baird and Suthers, 2007; Verdy et al., 2009; Ward et al., 2011). There are also important differences in traits between groups of phytoplankton (Tang, 1995; Litchman et al., 2007). For instance, diatoms have a higher V^{max} and μ^{max} than dinoflagellates ($b_{dia} > b_{dino}$; Fig. 1.5). In other words, a diatom will grow faster than a dinoflagellate of the same size. Thus, size *and* taxonomy play a role in determining phytoplankton traits, and in this thesis I have considered both perspectives.

1.5 Resource Competition Theory and R*

The functional traits described in the previous section ultimately determine the fitness of each species compared with others. In several of the following chapters, particularly Chapters 3 and 4, I discuss the R* concept from resource competition theory, which is the minimum, steady-state nutrient concentration at which growth and loss processes exactly balance were the species growing in isolation (e.g., Tilman, 1981; Dutkiewicz et al., 2009). If we consider a system with a single limiting nutrient and many different species of phyto-

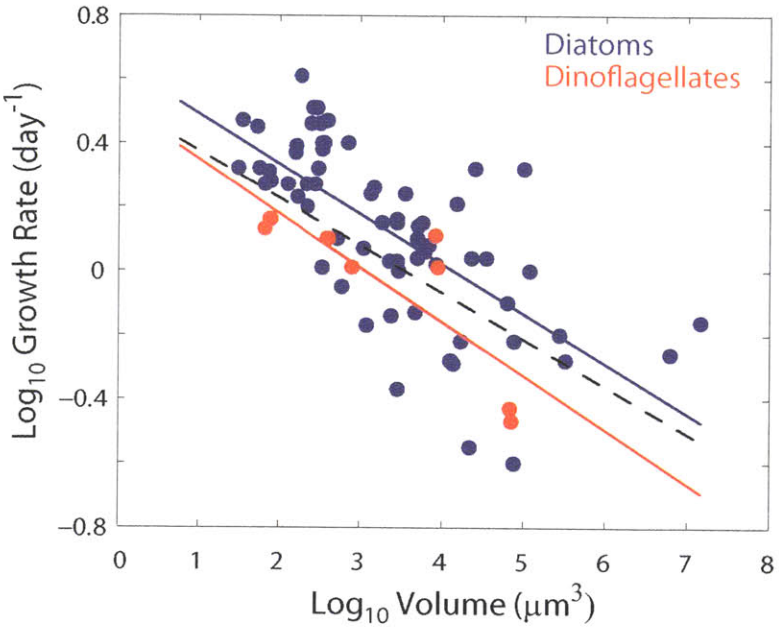

Figure 1.5: Diatom (blue dot) and dinoflagellate (red dot) maximum potential growth rates (μ^{max}, day^{-1}) as a function of cell volume (μm^3). The dashed black line represents a best fit for all phytoplankton, and is $\mu^{max} = 3.49V^{-0.15}$. The blue and red lines are best fits for diatoms and dinoflagellates, respectively, and show that for a given volume, diatoms grow faster than dinoflagellates in laboratory conditions. Data are reproduced from Tang (1995).

plankton of known functional traits, the species with the lowest R* for the limiting nutrient should outcompete the others over time, whereas species with the same or very similar R* should coexist for an extended duration. In the context of the quota model, R* can found by setting $\frac{d}{dt} = 0$ and solving Equations 1.2-1.5 for the steady state number density (X_i^*; the "*" denotes the steady state value), quota (Q_i^*), nutrient levels ($N_i^* = R_i^*$), and growth rate (μ_i^*):

$$X_i(\mu_i - m - D) = 0 \Longrightarrow \mu_i^* = m + D \tag{1.6}$$

$$V_i^{max}\frac{N}{N + k_i^T} - \mu_i Q_i = 0 \Longrightarrow V_i^{max}\frac{R_i^*}{R_i^* + k_i^T} = \mu_i^* Q_i^* \tag{1.7}$$

$$D(N_o - N) - \sum_i V_i^{max}\frac{N}{N + k_i^T}X_i = 0 \Longrightarrow D(N_o - R_i^*) - V_i^{max}\frac{R_i^*}{R_i^* + k_i^T}X_i^* \tag{1.8}$$

$$\mu_i^* = \mu_i^{max}(1 - \frac{Q_i^{min}}{Q_i^*}) \tag{1.9}$$

Rearranging Equation 1.7 and 1.9, solve for R_i^* and Q_i^*:

$$R_i^* = \frac{\mu_i^* Q_i^* k_i^T}{V_i^{max} - \mu_i^* Q_i^*} \tag{1.10}$$

$$Q_i^* = \frac{Q_i^{min}\mu_i^{max}}{\mu_i^{max} - \mu_i^*} \tag{1.11}$$

Combining Equations 1.10 and 1.11 we find R^*:

$$R_i^* = \frac{\mu_i^*\mu_i^{max}Q_i^* k_i^T}{V_i^{max}(\mu_i^{max} - \mu_i^*) - \mu_i^*\mu_i^{max}Q_i^*} \tag{1.12}$$

Studies have shown that the R* concept can be used to predict the results of resource competition among phytoplankton (Tilman, 1981; Dutkiewicz et al., 2009), and I will employ this tool in Chapters 3 and 4 to understand resource competition among phytoplankton and the resulting community structure. In Chapter 3, I consider the Monod, rather than the quota model, and will discuss the Monod form of R* in that chapter.

1.6 An Appreciation for the Role of Predation

Despite the intentional focus on bottom-up processes, a recurring theme throughout the thesis is that both bottom-up and top-down (here, zooplankton grazing) processes jointly regulate the community ecology of phytoplankton. The functional traits of phytoplankton (e.g., size, motility, and palatability) and zooplankton (e.g., prey size preferences and growth and ingestion rates) mediate predator-prey interactions (Hansen et al., 1994; Hansen et al., 1997). There are many possible model representations of zooplankton grazing (Gentleman et al., 2003), though in this thesis I have purposefully adopted simple forms so as to focus on the role of bottom-up processes. Here, I briefly introduce zooplankton grazing as it is considered in each chapter, and explain how the differing model treatments are related.

Zooplankton grazing accounts for much of phytoplankton mortality in the ocean (Calbet and Landry, 2004), and observations show the abundance of predators is typically closely tied to that of their prey (e.g., Colebrook, 1979). There can be temporal lags in the response times of predators to their prey which may result in an increase in phytoplankton abundance

(e.g., Irigoien et al., 2005), but generally the growth rates of prey are nearly balanced by losses to grazing (Lessard and Murrell, 1998; Landry et al., 2000). In Chapter 2, we discuss an analysis of CPR phytoplankton abundance data for many species and diagnose their seasonal cycle of net population growth, which includes both growth and loss processes. Even though a bottom-up perspective suggests that populations of smaller phytoplankton cells might grow faster because of the allometric scaling of maximum growth rate (μ^{max}), we find that net population growth rate does not vary with size or taxonomy. We discuss how this difference may be due top-down zooplankton grazing and refer to existing concepts and studies in the literature rather than explicitly analyzing zooplankton abundance data.

In Chapter 3, we examine patterns of diversity in a global ecosystem model (Follows et al., 2007), and explain these patterns by using a much simplified, 0-D Monod model of phytoplankton growth. In the global model, two classes of zooplankton are explicitly resolved, each with a size-based preference for consumption of phytoplankton, which are themselves classified into two broad size classes. Because grazing rate, which is defined here as the number of phytoplankton consumed per zooplankton per time (phy zoo^{-1} day^{-1}), has been found to generally be a saturating function of prey concentration (Hansen et al., 1997), a Holling II function was used to relate prey density (X; phy m^{-3}) and predation (Holling, 1965). Thus, grazing rate is $gX(X+k)^{-1}$, where k is the half-saturation prey abundance (phy m^{-3}) and g is the maximum possible grazing rate (phy zoo^{-1} day^{-1}). The total loss rate (phy m^{-3} day^{-1}) is found by then multiplying by the grazing rate with zooplankton abundance, or Z (zoo m^{-3}). At low prey densities ($X \ll k$), the grazing rate increases linearly with Xk^{-1}. In the 0-D models by contrast, we simplify the grazing rate such that it does not vary with prey density. As a consequence in the 0-D model, we attribute changes in community structure primarily to the traits of constituent species and environmental variability. In the global model, these same bottom-up mechanisms govern phytoplankton community structure, but with the additional complication of using the Holling II zooplankton grazing. We touch upon this point in Barton et al. (2010a, 2010b).

In Chapter 4, we examine the impact of two different implicit grazing parameterizations on phytoplankton community structure in a size-structured community model where the traits of each species are determined allometrically and uptake rates modified by small-scale fluid turbulence. "Implicit" means that we do not explicitly represent zooplankton abundance (as was done in the global model above), but rather assume that zooplankton and phytoplankton abundance are linked by constant of proportionality. For instance, a given phytoplankton may be 1000 times more abundant than its zooplankton predator. In the first grazing parameterization in this chapter, the grazing rate (day^{-1}) is constant and not a function of prey density (see Eqn. 1.2). This formulation of grazing is similar to what is done in Chapter 3 with 0-D models, but is somewhat unrealistic considering that grazing rate generally increases with prey density. In the second idealized grazing parameterization, the grazing rate increases linearly with prey density, such that the grazing rate (day^{-1}) is $m_z X_i$, where m_z is the implicit form of a zooplankton clearance rate (m^3 phy^{-1} day^{-1}). The loss rate is then $m_z XX$, and because of the X^2 term it is called a "quadratic" loss. Relating the grazing forms used in Chapters 3 and 4, the Holling II and quadratic loss grazing rates are both linear at low prey densities ($k \ll P$).

1.7 "Trait-based" Approach to Marine Microbial Ecology

Bearing in mind the previous discussion, a good deal has been learned about how phytoplankton traits and the environment regulate biogeography, and I give here a few examples of this "trait-based" approach to community ecology. Perhaps the first marine ecologist to link phytoplankton traits to their ecology was Ramon Margalef. He noted that motile phytoplankton were more conspicuous in nutrient-deplete, less turbulent conditions, and that large, fast growing diatoms were most common in nutrient-rich, turbulent conditions, which resulted in his famous "mandala" paradigm (Margalef, 1978). Later, with the discovery of tiny, marine cyanobacteria (Chisholm et al., 1988), distinct *Prochlorococcus* ecotypes with differing traits have been shown to inhabit specific light, nutrient, and temperature niches (Rocap et al., 2003; Johnson et al., 2006). In addition to field- and lab-based studies, trait-based ecosystem models have been illustrative (Follows et al., 2007; Dutkiewicz et al., 2009). For example, Dutkiewicz et al. (2009) found that a model ocean is roughly partitioned between regions dominated by "gleaners" (those species adapted for life with scarce resources) and "opportunists" (those species able to grow quickly to take advantage of abundant resources) in the subtropical and subpolar oceans, respectively. These broad strategies were predicted by MacArthur and Wilson (1967), and are determined by the growth (here, opportunists have high μ^{max}) and uptake (here, gleaners have low k) traits of the model phytoplankton. Despite these and many more advances, there remain many unknowns about what regulates the community ecology of important groups of phytoplankton. In the next section, I pose several unanswered questions that I investigate further in the following thesis chapters.

1.8 Thesis Goals and Outline

The goal of this thesis is to interpret the community ecology of phytoplankton through their functional traits, biotic interactions, and the character of environmental variability in the ocean. Broadly defined, I will examine patterns of ecological succession (changes in community ecology through time), biogeography (changes in community ecology in space), and diversity (the number of species in a community). I briefly outline Chapters 2-4 here, and summarize the major questions and methods used in each chapter.

Chapter 2: Linking phytoplankton functional traits to community ecology in the North Atlantic Ocean

Q1 Can the community ecology observed in the Continuous Plankton Recorder (CPR) survey of diatoms and dinoflagellates be interpreted in terms of phytoplankton functional traits?

Q2 Is the seasonal succession of diatoms and dinoflagellates consistent with regulation by their trophic strategies (e.g., photoautotrophy, mixotrophy, heterotrophy)?

Q3 Is there evidence that the succession of diatoms and dinoflagellates is impacted by the maximum potential growth rate, or μ^{max}?

Q4 Despite the fact that the CPR survey does not sample picoplankton, is there evidence for the existence of gleaners (those adapted to low nutrient levels) and opportunists (those adapted to growing fast in ideal conditions) in the CPR survey?

The CPR database has long been used to assess ecological change through time, such as succession and phenology (Colebrook, 1979; Edwards and Richardson, 2004; Leterme et al., 2005), though these patterns have typically not been well-linked to the traits of survey taxa. In this chapter, I examine the extensive CPR database of observations on diatom and dinoflagellate abundance and relate their successional patterns to a compilation of lab- and field-based data describing two traits: cell size (many other traits scale with cell size) and trophic strategy.

Chapter 3: Patterns of diversity in marine phytoplankton

Q5 What are the patterns of phytoplankton diversity in a global ocean model, and how do they compare to known diversity patterns?

Q6 What regulates the patterns of phytoplankton diversity?

Phytoplankton diversity varies in space. There is equivocal evidence showing greater phytoplankton diversity in lower latitudes, though the causes of this pattern are largely unknown (Pommier et al., 2007; Fuhrman et al., 2008). In this chapter, I use a combination of complex global (Follows et al., 2007) and idealized Monod-type models (e.g., Grover, 1990) to understand the particular combination of traits and environmental conditions that allow for phytoplankton coexistence.

Chapter 4: The impact of turbulence on phytoplankton nutrient uptake rates and community structure

Q7 What impact does small-scale fluid turbulence have on phytoplankton nutrient uptake rates and community structure?

Q8 Where and when in the ocean does the affect of small-scale fluid turbulence on phytoplankton nutrient uptake rates play an important role?

Turbulence at a broad range of spatial and temporal scales plays a role in structuring marine ecosystems by setting the ambient nutrient concentration for which all phytoplankton must compete. In addition, turbulent motion on size scales similar to the cell impacts cellular nutrient uptake rates, though it is not well understood how this effect may influence community structure (defined here as the diversity and relative abundance of species). In this chapter, I use a quota-type model (Droop, 1968) configured in an idealized, zero-dimensional setting to quantify the ecological impact of the additional flux of nutrients toward the cell surface mediated by small-scale fluid turbulence. I investigate how the impact of turbulence is tied to the nature of zooplankton grazing, and discuss where and when this direct impact of turbulence is likely to play an important role.

1.9 References

Aksnes, D., Egge, J., 1991. A theoretical model for nutrient uptake in phytoplankton. Marine Ecology Progress Series 70, 65-72.

Allen, A.P., et al., 2006. Kinetic effects of temperature on rates of genetic divergence and speciation. Proceedings of the National Academy of Sciences 104(24), 9130-9135.

Anderson, L.A., 1995. On the hydrogen and oxygen content of marine phytoplankton. Deep-Sea Research I 42(9), 1675-1690.

Angel, M.V., 1993. Biodiversity of the pelagic ocean. Conservation Biology 7(4), 760-772.

Armbrust, E.V., 2009. The life of diatoms in the worlds oceans. Nature 459, 185-192.

Armstrong, R.A., 1994. Grazing limitation and nutrient limitation in marine ecosystems: Steady state solutions of an ecosystem model with multiple food chains. Limnology and Oceanography 39(3), 597-608.

Baird, M.E., Suthers, I.M., 2007. A size-resolved pelagic ecosystem model. Ecological Modelling 203, 185-203.

Barber, R.T., Hiscock, M.R., 2006. A rising tide lifts all phytoplankton: Growth response of other phytoplankton in diatom-dominated blooms. Global Biogeochemical Cycles 20, GB4S03, doi:10.1029/2006GB002726.

Barton, A.D., et al., 2010a. Patterns of diversity in marine phytoplankton. Science 327, 1509-1511.

Barton, A.D., et al., 2010b. Response to Comment on "Patterns of diversity in marine phytoplankton". Science 329, 512-d.

Calbet, A., Landry, M.R., 2004. Phytoplankton growth, microzooplankton grazing, and carbon cycling in marine systems. Limnology and Oceanography 49(1), 2004, 51-57.

Cermeño, P., et al., 2008a. The role of nutricline depth in regulating the ocean carbon cycle. Proceedings of the National Academy of Sciences 105(51), 20344-20349.

Cermeño, P., et al., 2008b. Resource levels, allometric scaling of population abundance, and marine phytoplankton diversity. Limnology and Oceanography 53(1), 312-318.

Chavez, F.P., Barber, R., 1987. An estimate of new production in the equatorial Pacific. Deep Sea Research I 34(7), 1229-1243.

Chisholm, S.W., et al., 1988. A novel free-living prochlorophyte abundant in the oceanic euphotic zone. Nature 324, 340-343.

Chisholm, S.W., 1992. Phytoplankton size. In Falkowski, P.G., Woodhead, A.D. (eds). Primary Productivity and Biogeochemical Cycles in the Sea. Plenum Press, New York.

Colebrook, J.M., 1979. Continuous Plankton Records: Seasonal cycles of phytoplankton and copepods in the North Atlantic Ocean and North Sea. Marine Biology 51, 23-32.

Colwell, R.K., Hurtt, G.C., 1994. Nonbiological gradients in species richness and a spurious Rapoport effect. American Naturalist 144(4), 570-595.

Cullen, J.J., et al., 2002. Physical influences on marine ecosystem dynamics. In, The Sea, Robinson, A., McCarthy, J.J., Rothschild, B.J., Eds. Wiley, New York, vol. 12, chap. 8.

Cullen, J.J., et al., 2007. Patterns and prediction in microbial oceanography. Oceanography 20(2), 34-46.

Currie, D.J., 1991. Energy and large-scale patterns of animal- and plant-species richness. American Naturalist 137(1), 27-49.

Cushing, D.H., 1989. A difference in structure between ecosystems in strongly stratified waters and in those that are only weakly stratified. Journal of Plankton Research 11(1), 1-13.

Doney, S.C., et al., 2004. From genes to ecosystems: the ocean's new frontier. Frontiers in Ecology and the Environment 2(9), 457-468.

Droop, M.R., 1968. Vitamin B12 and marine ecology, IV. The kinetics of uptake, growth and inhibition in Monochrysis lutheri. Journal of the Marine Biological Association of the United Kingdom 48, 689-733.

Ducklow, H.W., Steinberg, D.K., Buessler, K.O., 2001. Upper ocean carbon export and biological pump. Oceanography 14, 50-58.

Dutkiewicz, S., Follows, M.J., Bragg, J.G., 2009. Modeling the coupling of ocean ecology and biogeochemistry. Global Biogeochemical Cycles 23, GB4017, doi:10.1029/2008GB003405.

Edwards, M., Richardson, A.J., 2004. Impact of climate change on marine pelagic phenology and trophic mismatch. Nature 430, 881-884.

Eppley, R.W., 1972. Temperature and phytoplankton growth in the sea. Fisheries Bulletin 70, 1063-1085.

Falkowski, P.G., Barber, R.T., Smetacek, V., 1998. Biogeochemical Controls and Feedbacks on Ocean Primary Production. Science 281(5374), 200-206.

Falkowski, P.G., et al., 2004. The evolution of modern eukaryotic phytoplankton. Science 305, 354-360.

Field, C.B., et al., 1998. Primary production of the biosphere: integrating terrestrial and oceanic components. Science 281, 237-240.

Finlay, B.J., 2002. Global dispersal of free-living microbial eukaryote species. Science 296, 1061-1064.

Follows, M.J, et al., 2007. Emergent biogeography of microbial communities in a model ocean. Science 315, 1843-1846.

Follows, M.J., Dutkiewicz, S., 2011. Modeling diverse communities of marine microbes. Annual Reviews in Marine Science 3, 427-451.

Fuhrman, J.A., 1999. Marine viruses and their biogeochemical and ecological effects. Nature 399, 541-548.

Fuhrman, J.A., et al., 2008. A latitudinal diversity gradient in planktonic marine bacteria. Proceedings of the National Academy of Sciences 105(22), 7774-7778.

Geisen, M., 2011. Image of coccolithophore. http://earthguide.ucsd.edu

Gentleman, W., et al., 2003. Functional responses for zooplankton feeding on multiple resources: a review of assumptions and biological dynamics. Deep-Sea Research II 50, 2847-2875.

Grover, J.P., 1990. Resource competition in a variable environment: Phytoplankton growing according to Monod's model. American Naturalist 136(6), 771-789.

Hansen, P.J., Bjørnsen, P.K., Hansen, B.W., 1994. The size ratio between planktonic predators and their prey. Limnology and Oceanography 39(2), 395-403.

Hansen, P.J., Bjørnsen, P.K., Hansen, B.W., 1997. Zooplankton grazing and growth: Scaling within the 2-2,000um body size range. Limnology and Oceanography 42(4), 687-704.

Hillebrand, H., 2004. On the generality of the latitudinal diversity gradient. The American Naturalist 163(2), 192-211.

Holling, C.S., 1965. The functional response of predators to prey density and its role in mimicry and population regulation. Memoirs of the Entomological Society of Canada, 45.

Honjo, S., Okada, H., 1974. Community structure of Coccolithophores in the photic layer of the mid-Pacific. Micropaleontology 20, 209-230.

Hughes Martiny, J.B., et al., 2006. Microbial biogeography: putting microorganisms on the map. Nature Reviews Microbiology 4, 102-112.

Huisman, J., Weissing, R.J., 1999. Biodiversity of plankton by species oscillations and chaos. Nature 402, 407-410.

Huisman, J., et al., 2006. Reduced mixing generates oscillations and chaos in the oceanic deep chlorophyll maximum. Nature 439, 322-325.

Hutchinson, G.E., 1959. Homage to Santa Rosalia or Why are there so many kinds of animals? American Naturalist 93, 145-159.

Hutchinson, G.E., 1961. The paradox of the plankton. American Naturalist 95, 137-145.

Irigoien, X., Huisman, J., Harris R.P., 2004. Global biodiversity patterns of marine phytoplankton and zooplankton. Nature 429, 863-867.

Irigoien, X., Flynn, K.J., Harris, R.P., 2005. Phytoplankton blooms: a loophole in microzooplankton grazing impact? Journal of Plankton Research 27(4), 313-321.

Irwin, A.J., et al., 2006. Scaling-up from nutrient physiology to the size-structure of phytoplankton communities. Journal of Plankton Research 28(5), 459-471.

Johnson, Z.I., et al., 2006. Niche partitioning among *Prochlorococcus* ecotypes along ocean-scale environmental gradients. Science 311, 1737-1740.

Karp-Boss, L., Boss, E., Jumars, P.A., 1996. Nutrient fluxes to planktonic osmotrophs in the presence of fluid motion. Oceanography and Marine Biology: an Annual Review 34, 71-107.

Kiørboe, T., 2008. A Mechanistic Approach to Plankton Ecology. Princeton University Press.

Landry, M.R. et al, 2000. Biological response to iron fertilization in the eastern equatorial Pacific (IronEx II): III. Dynamics of phytoplankton growth and microzooplankton grazing. Marine Ecology Progress Series 201, 57-72.

Laws, E.A., et al., 2000. Temperature effects on export production in the open ocean. Global Biogeochemical Cycles 14(4), 1231-1246.

Le Quéré, C., et al., 2005. Ecosystem dynamics based on plankton functional types for global ocean biogeochemistry models. Global Change Biology 11, 2016-2040.

Lessard, E.J., Murrell, M.C., 1998. Microzooplankton herbivory and phytoplankton growth in the northwestern Sargasso Sea. Aquatic Microbial Ecology 16, 173-188.

Leterme, S.C., et al., 2005. Decadal basin-scale changes in diatoms, dinoflagellates, and phytoplankton color across the North Atlantic. Limnology and Oceanography 50(4), 1244-1253.

Litchman, E., et al., 2007. The role of functional traits and trade-offs in structuring phytoplankton communities: scaling from cellular to ecosystem level. Ecology Letters 10, 1170-1181.

Litchman, E., Klausmeier, C.A., 2008. Trait-based community ecology of phytoplankton. Annual Reviews of Ecology, Evolution, and Systematics 39, 615-639.

Longhurst, A.R. 1998. Ecological Geography of the Sea. Academic Press, San Diego, CA, USA, 560 pp.

MacArthur, R.H., MacArthur, J.W., 1961. On bird species diversity. Ecology 42(3), 594-598.

MacArthur, R.H., Wilson, E.O., 1967. The Theory of Island Biogeography, Princeton University Press, Princeton, NJ.

Margalef, R., 1978. Life-forms of phytoplankton as survival alternatives in an unstable environment. Oceanologica acta 1(4), 493-509.

Matishov, G., et al., 2000. Biological Atlas of the Arctic Seas 2000: Plankton of the Barents and Kara Seas. Available online:
http://www.nodc.noaa.gov/OC5/BARPLANK/WWW/HTML/bioatlas.html

McGill, B.J., et al., 2006. Rebuilding community ecology from functional traits. Trends in Ecology and Evolution 21(4), 178-185.

McGillicuddy, D.J., et al., 2007. Eddy/Wind interactions stimulate extraordinary mid-ocean plankton blooms. Science 316, 1021-1026.

Mittlebach, G.G., et al., 2007. Evolution and the latitudinal diversity gradient: speciation, extinction and biogeography. Ecology Letters 10, 315-331.

Monod, J., 1950. La technique de culture continue, théorie et applications. Ann. Inst. Pasteur (Paris) 79, 390-410.

Paine, R.T., 1966. Food web complexity and species diversity. American Naturalist 100 (910), 65-75.

Partensky, F., Hess, W.R., Vaulot, D., 1999. *Prochlorococcus*, a marine photosynthetic prokaryote of global significance. Microbiology and Molecular Biology Reviews 63(1), 106-127.

Pedrós-Alió, C., 2006. Marine microbial diversity: can it be determined? Trends in Microbiology 14(6), 257-263.

Pomeroy, L.R., et al., 2007. The microbial loop. Oceanography 20(2), 28-34.

Pommier, T., et al., 2007. Global patterns of diversity and community structure in marine bacterioplankton. Molecular Ecology 16, 867-880.

Ptacnik, R., et al., 2008. Diversity predicts stability and resource use efficiency in natural phytoplankton communities. Proceedings of the National Academy of Sciences 105(13), 5134-5138.

Ryther, J.H., 1969. Photosynthesis and fish production in the sea. Science 166(3901), 72-76.

Rocap, G., et al., 2003. Genome divergence in two *Prochlorococcus* ecotypes reflects oceanic niche differentiation. Nature 424, 1042-1047.

Rohde, K., 1992. Latitudinal gradients in species diversity: the search for the primary cause. Oikos 65(3), 514-527.

Sarmiento, J.L.S, Gruber, N., 2006. Ocean biogeochemical dynamics. Princeton University Press, Princeton, NJ, USA.

Sarthou, G., et al., 2005. Growth physiology and fate of diatoms in the ocean: a review. Journal of Sea Research 53, 25-42.

Scott, F., 2011. Image of Protoperidinium latistriatum.
http://www.antarctica.gov.au/media/news/2010/?a=12389

Sherr, E.B., Sherr, B.F., 1994. Bacterivory and herbivory: key roles of phagotrophic protists in pelagic food webs. Microbial Ecology 28, 223-235.

Sigman, D.M, Boyle, E.A., 2000. Glacial/interglacial variations in atmospheric carbon dioxide. Nature 407, 859-869.

Smayda, T.J., 1997. Harmful algal blooms: Their ecophysiology and general relevance to phytoplankton blooms in the sea. Limnology and Oceanography 42(5), 1137-1153.

Smayda, T.J., Reynolds, C.S., 2001. Community assembly in marine phytoplankton: application of recent models to harmful dinoflagellate blooms. Journal of Plankton Research 23(5), 447-461.

Sommer, U., 1985. Seasonal succession of phytoplankton in Lake Constance. BioScience 35(6), 351-357.

Tang, E.P.Y., 1995. The allometry of algal growth rates. Journal of Plankton Research 17(6), 1325-1335.

Taylor, A.H., et al., 1993. Seasonal succession in the pelagic ecosystem of the North Atlantic and the utilization of nitrogen. Journal of Plankton Research 15(8), 875-891.

Taylor, F.J.R., Hoppenrath, M., Saldarriaga, J.F., 2008. Dinoflagellate diversity and distribution. Biodiversity Conservation 17, 407-418.

Tilman, D., 1981. Tests of resource competition theory using four species of Lake Michigan algae. Ecology 62(3), 802-815.

Tomas, C., et al., 1997. Identifying marine phytoplankton. Academic Press.

Vallina, S.M., LeQuéré, C., 2011. Stability of complex food webs: Resilience, resistance and the average interaction strength. Journal of Theoretical Biology 272, 160-173.

Verdy, A., Follows, M., Flierl, G., 2009. Optimal phytoplankton cell size in an allometric model. Marine Ecology Progress Series 379, 1-12.

Verity, P.G., Villareal, T.A., Smayda, T.J., 1988. Ecological investigations of colonial Phaeocystis pouchetii. II. The role of life cycle phenomena in bloom termination. Journal of Plankton Research 10, 749-766.

Violle, C., et al., 2007. Let the concept of trait be functional! Oikos 116, 882-92.

Wanninkhof, R., 1992. Relationship between gas exchange and wind speed over the ocean. Journal of Geophysical Research 97, 7373-7381.

Ward, B.A., Dutkiewicz, S., Follows, M.J., 2011. Size-structured food webs in the global ocean: theory, model, and observations. Submitted, Marine Ecology Progress Series.

Waterbury, J., 2004. Little things matter a lot. Oceanus 43(2), 1-5.

West, G.B., Brown, J.H., Enquist, B.J., 1997. A general model for the origin of allometric scaling laws in biology. Science 276, 122-126.

Westoby, M., Wright, I.J., 2004. Land-plant ecology on the basis of functional traits. Trends in Ecology and Evolution 2195), 261-268.

Williams, R., Follows, M.J., 2011. Ocean Dynamics and the Carbon Cycle,Cambridgue University Press, Cambridge, U.K.

Worm, B., et al., 2006. Impacts of biodiversity loss on ocean ecosystem services. Science 314, 787-790.

Zubkov, M.V., et al., 1998. Picoplanktonic community structure on an Atlantic transect from 50N to 50S. Deep-Sea Research I 45, 1339-1355.

Zubkov, M.V., Tarran, G.A., 2008. High bacterivory by the smallest phytoplankton in the North Atlantic Ocean. Nature 455, 224-227.

Chapter 2

Linking phytoplankton functional traits to community ecology in the North Atlantic Ocean

The collaborative work in this chapter is based upon the following publication in preparation: Barton, A.D., Finkel, Z.V., Ward, B.A., Johns, D.G., Follows, M.J., *in prep.* Linking phytoplankton functional traits to community ecology in the North Atlantic Ocean.

2.1 Summary

The Continuous Plankton Recorder (CPR) survey provides a unique, long-term ecological record of the diverse diatom and dinoflagellate communities in the North Atlantic Ocean. We have investigated the mechanisms regulating their community ecology by linking the mean annual cycles of abundance for 113 diatom and dinoflagellate taxa to taxon-specific data on two functional traits: trophic strategy (photoautotrophy, mixotrophy, or heterotrophy) and cell size. Diatoms bloom in spring and are followed in succession by mixotrophic and heterotrophic dinoflagellates, with the latter peaking in summer months. Despite the higher expected metabolic costs of maintaining both photoautotrophic and heterotrophic capabilities, we hypothesize that mixotrophic dinoflagellates peak earlier than heterotrophs because of the temporary advantage afforded by photosynthesizing when light and nutrients are available. We found a decrease in the mean cell size of the most abundant diatom and dinoflagellate taxa during typically nutrient-deplete summer conditions, which we hypothesize is driven by smaller cells having higher nutrient affinities than larger cells and the increased availability of smaller prey for smaller dinoflagellates. In contrast to laboratory observations of maximum potential growth rate (μ^{max}) which show that smaller cells should grow faster than larger cells under ideal conditions and diatoms faster than dinoflagellates of the same size, we found that the maximum net growth rate (μ^{net}), as diagnosed from mean annual cycles of abundance for each CPR taxa, is typically much less than μ^{max} and scales neither with cell size nor taxonomic group. This suggests that even though fast-growing phytoplankton (high μ^{max}) may outpace their competitors for a short duration, in general their predators quite rapidly respond and effectively crop down their abundance. Thus, on the ecological timescales measured by the CPR survey ($\sim$1 month), growth and loss processes nearly balance across many phytoplankton taxa.

2.2 Introduction

2.2.1 Background

Diatoms and dinoflagellates are diverse taxonomic groups of phytoplankton, each with thousands of species, spanning a broad range in size, morphology, behavior, and biochemistry (Tomas et al., 1997; Taylor et al., 2008). They play important and dynamic ecological and biogeochemical roles in the ocean on varying spatial and temporal scales. Ephemeral "blooms" of diatoms in turbulent, nutrient-rich periods spur export of organic matter from the ocean surface and effectively transfer organic matter and energy to higher trophic levels (Ryther, 1969). Motile dinoflagellates are typically more abundant in more quiescent, nutrient-deplete periods that are characterized by efficient recycling of organic matter in the surface ocean within the "microbial loop" (Azam et al., 1983). Thus, diatom- and dinoflagellate-dominated marine food webs are quite different in character of mineral export and recycling and play different roles in regulating biogeochemical cycles (Cushing, 1999). Moreover, decadal scale variability in phytoplankton biomass and the relative abundances of diatom and dinoflagellates has been observed in the North Atlantic Ocean (e.g., Reid, 1998; Barton et al., 2003; Leterme et al., 2005), highlighting the importance of understanding the mechanisms regulating their community ecology and biogeochemical roles.

The dynamics of ecological communities are regulated by the interplay of constituent species traits, biotic interactions, and the environment (McGill et al., 2006; Litchman and Klausmeier, 2008). Margalef (1978), Smayda (1997), and others first applied this trait-based approach to the study of the community ecology of diatoms and dinoflagellates. Recently, progress has been made toward uncovering the crucial traits and trade-offs that regulate community dynamics by analyzing compilations of laboratory data from many taxa (Litchman et al., 2007; Bruggeman, 2009). Increasingly, this view of ecological communities guides mechanistic plankton community models that move beyond resolving several broad plankton functional types with generic traits (e.g., Baird and Suthers, 2007; Follows et al., 2007; Ward et al., 2011a,b). Despite these advances, there remains a need to connect extensive field observations of diverse communities to the traits of each constituent species in order to better identify the mechanisms governing their community ecology. Here, we examine the community ecology of diatoms and dinoflagellates, as seen in the Continuous Plankton Recorder (CPR) survey, in relation to two quite fundamental phytoplankton traits: cell size and trophic strategy. Cell size is a fundamental trait because it determines many important physiological rates and interactions (Kiørboe, 2008; Litchman and Klausmeier, 2008), while trophic strategy describes the degree to which phytoplankton gain their nutrients and energy by photoautotrophy, heterotrophy, or some combination of both (mixotrophy).

The CPR survey of plankton abundance, with its broad spatial, temporal, and taxonomic coverage and consistent methodology, provides a unique record of ecological dynamics in the subarctic and northern subtropical North Atlantic Ocean (Fig. 2.1). The survey does not cover all phytoplankton (picoplankton are notably absent) and data collection frequency and density varies through time. For example, the number of samples taken per month in each survey area varies from as little as 0 to as many as 70, with a mean of nearly 7. Quite often, no samples were taken in a given area and month (see Richardson et al., 2006 for more discussion on density of sampling). Nevertheless, it is an excellent record of ecologically and biogeochemically important diatom and dinoflagellate taxa (Barnard et al., 2004). We analyzed time series of monthly mean abundance across the entire North Atlantic basin for each of 51 dinoflagellate and 62 diatom taxa available during the period of

1958-2006 and differentiated the patterns of abundance among taxa with differing traits, as inferred from the literature (see Methods). Using this analysis of trait and taxa abundance data, we address three primary questions regarding the mechanistic controls of diatom and dinoflagellate community ecology: What role does trophic strategy play in the community ecology of diatoms and dinoflagellates? Does the maximum potential growth rate (μ^{max}, day^{-1}), which is a key trait used in many ecosystem model formulations (e.g., Barton et al., 2010), play a role in regulating diatom and dinoflagellate community ecology? And lastly, what evidence is there for opportunist- ("r") and gleaner-like ("k") strategies in the observed CPR communities?

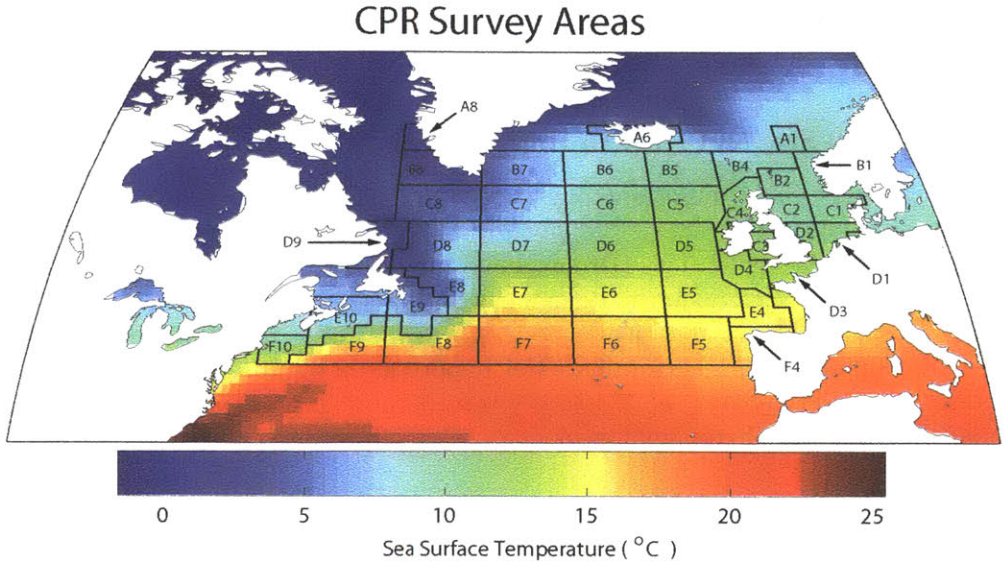

Figure 2.1: Map of CPR Standard Survey Areas, superimposed upon the annual mean sea surface temperature climatology for 1971-2000 (Smith and Reynolds, 2003), indicating that the survey straddles the subpolar and northern subtropical gyres.

2.2.2 Hypotheses

Trophic Strategies

Trophic strategy, or the means by which an organism acquires nutrients and energy, is a fundamental trait, and we hypothesize that this trait plays a key role in regulating phytoplankton community dynamics. With the exception of perhaps a few heterotrophic, benthic taxa (Lewin, 1953), marine diatoms are considered to be primarily oxygenic photoautotrophs that must take up inorganic forms of essential nutrients from their environment. Diatoms typically dominate oceanic blooms of phytoplankton found in turbulent, nutrient-rich periods (Chisholm, 1992; Barber and Hiscock, 2006), and become nutrient-limited when resources, including silica, are scarce (Martin-Jézéquel et al., 2000). In contrast, dinoflagellate

trophic strategies range from near-pure autotrophy to pure heterotrophy (Hansen, 2011). Heterotrophic dinoflagellates, such as *Protoperidinium* spp. (Hansen, 1991), consume prey and/or particulate matter and act as herbivores in the marine food web. Mixotrophic dinoflagellates, such as *Prorocentrum* spp., combine photoautotrophic and heterotrophic capabilities and are extremely common in a range of habitats and conditions (Stoecker, 1999; Hansen, 2011). Unlike many phytoplankton grazers–such as copepods, that eat prey significantly smaller than themselves–dinoflagellate prey includes, but is not limited to, diatoms and other dinoflagellates of similar size (prey may also be somewhat larger than the predator; Hansen et al., 1994). Put simply, photoautotrophic diatoms may bloom in response to abundant light and nutrients, heterotrophic dinoflagellates thrive in response to abundant prey, and mixotrophic dinoflagellates grow with a combination of light, nutrients, and prey. In the context of the CPR survey, we examine the abundance patterns of photoautotrophs, mixotrophs, and heterotrophs and relate them to the availability of their key resources, light and nutrients, prey, or both.

The Role of Cell Size and Growth Rate

Cell size constrains many important physiological rates in phytoplankton, including the maximum potential growth rate (μ^{max}, day^{-1}), which is defined as the greatest achievable growth rate under ideal conditions (Droop, 1968; Irwin et al., 2006; Litchman et al., 2007). In both observational (e.g., Sommer, 1985; Smayda, 1997) and modeling (Taylor et al, 1993; Baird and Suthers, 2007) studies, it has been argued that μ^{max} plays an important role in ecological dynamics, and here we evaluate this hypothesis in the context of the CPR survey of diatoms and dinoflagellates. μ^{max} is a key trait because, in the following simple model, the temporal change in phytoplankton biomass (B, molN m^{-3}) is a balance of growth and loss processes:

$$\frac{1}{B}\frac{dB}{dt} = \mu^{max}\gamma(T, I, N) - \lambda(B, Z) \tag{2.1}$$

where $\gamma(T, I, N)$ is a growth-modifying function of temperature (T), light (I), and nutrients (N) with a maximum of 1 and minimum of 0. Loss processes (λ) may be a function of phytoplankton and zooplankton (Z) biomass, representing losses to predation, mortality, sinking, viral lysis, and respiration. With ideal growth conditions ($\gamma = 1$; perhaps representative of the spring bloom), losses are small compared with growth ($\lambda \ll \mu^{max}$) and the per capita population growth is $\frac{1}{B}\frac{dB}{dt} \approx \mu^{max}$. In this limit, the net growth rate, or $\mu^{net} = \mu^{max}\gamma - \lambda$, approaches μ^{max}. Even with increasing losses ($\lambda \approx \mu^{max}\gamma$), μ^{max} remains important in determining whether net population growth is positive or negative.

Laboratory studies reveal that μ^{max} scales with cell mass (m, μgC cell^{-1}) such that $\mu^{max} = bm^a$, where b is a taxonomic group-specific constant and a is approximately -0.25 (Tang, 1995; Finkel, 2007). In this context, smaller cells grow faster than larger cells, and diatoms grow faster than dinoflagellates of the same size ($b_{dia} > b_{dino}$). It has been observed that smaller cells precede larger cells in phytoplankton succession in temperate seas (Cushing, 1989; Taylor et al., 1993) and some lakes (Sommer, 1985), and this effect has been captured in size-structured plankton community models (e.g., Baird and Suthers, 2007). This early dominance in the bloom of smaller cells should be somewhat short-lived because the smaller phytoplankton tend to have smaller predators, who themselves have faster generation times and are able to effectively crop their prey abundance (Hansen et al., 1997; Landry et al., 2000; Kiørboe, 2008; Ward et al., 2011a). Whether or not diatom and dinoflagellate successional patterns relate to their different, characteristic μ^{max} values is

unclear (Smayda, 1997). Considering these arguments, our approach is to look at seasonal cycles of abundance for phytoplankton of different cell size and taxonomic group and relate these patterns to μ^{max}, as predicted by cell size and taxonomy (e.g., Tang, 1995; Litchman et al., 2007).

Gleaners and Opportunists

Phytoplankton communities are often characterized by either the dominance of gleaner (those adapted to low resource levels) or opportunist species (those able to grow quickly with ample resources), and this distinction underpins our conceptual picture of phytoplankton biogeography and seasonal succession (Stewart and Levin, 1973; Cullen et al., 2002; Dutkiewicz et al., 2009). With respect to the differences between diatom and dinoflagellate communities, Margalef (1978) and others have argued that the spring-summer succession from diatoms to dinoflagellates reflects a shift from opportunists to gleaners. Diatoms are considered to be the classic opportunists, or "r" strategists, with their ability to grow relatively quickly compared with other taxonomic groups (Tang, 1995; Litchman et al., 2007). However, dinoflagellates do not, as a group, have the high affinity for inorganic nutrients expected of gleaners (Smayda, 1997; Litchman et al., 2007). What alternative strategies might dinoflagellates employ to be considered gleaners? Flagella allow dinoflagellates to take advantage of light, access nutrients, and avoid predation by swimming through the water column (Klausmeier and Litchman, 2001). Many dinoflagellates are known also to produce toxins that mediate competition for resources and limit predation in their favor (Smayda, 1997). Mixotrophic dinoflagellates may also exploit multiple resources (nutrients and prey), making them competitive in comparison to photoautotrophic and heterotrophic specialists when resources are scarce (Ward et al., 2011b).

Thus, the division between gleaners and opportunists is apparent between taxonomic groups, but we hypothesize that this division also exists within groups and is primarily connected to cell size. Because of their high nutrient affinities and specific uptake rates of nutrients (molN m^{-3} day^{-1}), smaller phytoplankton cells tend to be more competitive in oligotrophic conditions than larger cells (Raven, 1998; Litchman et al., 2007). Observations confirm the numerical dominance of smaller phytoplankton, such as *Prochlorococcus*, in oligotrophic seas (Irigoien et al., 2004; Johnson et al., 2006). In the language of resource competition theory, these cells have lower values of R^* (Dutkiewicz et al., 2009). We hypothesize that within each taxonomic group a shift toward smaller taxa is likely in resource-scare conditions. Using the CPR data, we evaluate changes in the size structure of diatoms and dinoflagellates throughout the year.

2.3 Materials and Methods

2.3.1 Cell Size Database

We mined the literature for cell size (cell volume and cell carbon content) estimates for diatom and dinoflagellate taxa that occur in the CPR database (Table 2.1; Appendix 1). The goal was to increase the number of taxa with a robust size estimate. Cell size of the individual taxon is expected to vary (from 2-fold to ~1 order of magnitude) due to several factors, including: changes in cell size over the cell cycle, decreases in average diatom cell size associated with asexual reproduction, and environmental and biological selection for specific cell size (Round et al., 1990; Armbrust and Chisholm, 1992; Finkel et al., 2010).

A limited set of size measurements have been previously compiled for the CPR database from the Biological Atlas of the Arctic Seas 2000: Plankton of the Barents and Kara Seas (2000). Cell size estimates for the Atlas were calculated from tables of average cell volumes and weights compiled for the Barents Sea (Solovieva, 1976; Makarevich et al., 1991; Makarevich et al., 1993). From this source, size estimates are available for 38 diatoms and 18 dinoflagellates. Our updated database includes size estimates for 62 diatoms and 51 dinoflagellates identified as part of the CPR survey used in this study (Table 2.1). Linear cellular dimensions, cell volume and cell carbon estimates were compiled. If only linear dimensions were provided, volume was estimated from standard formulas for the closest geometric shapes (Hillebrand et al., 1999; Olenina et al., 2006). For any single source if both cellular carbon and cell volume estimates were provided, cell volume was used and converted to cell carbon with standard allometric conversion factors (Menden-Deuer and Lessard, 2000). We chose to convert from cell volume to carbon in order to maximize the consistency within the database. When provided, every individual size measurement is used in the calculation of average cell size (Olenina et al., 2006), but most studies only provided estimates of the average size of each taxa. In cases where one of the observations for a taxa differs in excess of an order of magnitude from other observations it was not included in the estimate of average cell size. For the aggregated generic CPR categories, each species or spp. sized from each individual study was treated as an individual sample in the computation of the weighted mean to prevent any one species or location from excessively dominating the estimate of size. In the case of taxa that produce chains or mats, we have attempted to quantify the size of individual cells.

2.3.2 Trophic Strategy Database

Based upon published reports, we categorized each of the CPR taxa simply as a photoautotroph, mixotroph, or heterotroph using the criteria described below (Table 2.1; Appendix 2). Those taxa, notably the diatoms, containing plastids and photosynthetic pigments, but with no evidence for consumption of organic particles or prey, are considered to be photoautotrophic. Because of the ubiquity of mixotrophy among dinoflagellates and the difficulty of ruling out heterotrophic behaviors in dinoflagellate taxa (Stoecker, 1999), we assume for this analysis that there are no purely photoautotrophic dinoflagellates. Dinoflagellates in this classification scheme are, therefore, mixotrophs or heterotrophs. Mixotrophic dinoflagellates contain plastids and photosynthetic pigments, and show evidence for the consumption of organic particles or prey, such as the presence of food vacuoles or direct observation of feeding (Hansen and Calado, 1999). We did not quantify the relative importance of photoautotrophy or heterotrophy to mixotrophic dinoflagellates, and have not distinguished between native plastids or pigments and kleptochloroplasts (Skovgaard, 1998) or algal symbionts (Tarangkoon et al., 2010). Pure heterotrophic dinoflagellates contain no functioning plastids or photosynthetic pigments, and show evidence for consumption of organic particles or prey. For those *Ceratium* taxa with no published accounts regarding their trophic strategy, we have assumed they are mixotrophic. While this partitioning simplifies a great array of behaviors (Hansen, 2011), it allows us to compare patterns of seasonal succession among differing, broadly-grouped trophic strategies.

Diatoms			Dinoflagellates			
CPR ID	Taxon	Log Cell Mass (μgC cell^{-1})	CPR ID	Taxon	Log Cell Mass (μgC cell^{-1})	Trophic Strategy
101	Paralia sulcata	-3.85	121	Ceratium fusus	-2.28	M
102	Skeletonema costatum	-4.32	122	Ceratium furca	-2.26	M
103	Thalassiosira spp.	-2.78	123	Ceratium lineatum	-2.74	M
104	Dactyliosolen antarcticus	-2.23	124	Ceratium tripos	-2.04	M
105	Dactyliosolen mediterraneus	-3.10	125	Ceratium macroceros	-2.18	M
106	Rhizosolenia imbrica. shrubsolei	-2.81	126	Ceratium horridum	-1.87	M
107	Rhizosolenia styliformis	-1.93	127	Ceratium longipes	-2.30	M
108	Rhizosolenia hebetata semispina	-2.62	128	Ceratium arcticum	-1.13	M
109	Rhizosolenia alata indica	-2.32	129	Protoceratium reticulatum	-2.73	M
110	Rhizosolenia alata alata	-2.42	131	Ceratium kofoidii	-3.78	M
111	Rhizosolenia alata inermis	-2.65	132	Pyrophacus spp.	-2.03	M
112	Chaetoceros (Hyalochaete) spp.	-2.55	217	Ceratium falcatum	-2.10	M
113	Chaetoceros (Phaeoceros) spp.	-1.86	220	Amphisolenia spp.	-1.00	H
114	Odontella sinensis	-1.69	221	Ceratium arietinum	-1.08	M
115	Asterionella glacialis	-4.08	222	Ceratium azoricum	-2.20	M
116	Thalassiothrix longissima	-3.24	223	Ceratium belone	-2.54	M
117	Thalassionema nitzschioides	-4.16	224	Ceratium bucephalum	-0.80	M
118	Nitzschia seriata	-3.94	225	Ceratium buceros	-2.60	M
119	Nitzschia delicatissima	-4.40	226	Ceratium candelabrum	-2.00	M
151	Actinoptychus spp.	-2.95	227	Ceratium carriense	-1.72	M
152	Asteromphalus spp.	-3.43	228	Ceratium compressum	-1.28	M
153	Bacillaria paxillifer	-3.64	229	Ceratium declinatum	-2.38	M
154	Bacteriastrum spp.	-3.53	230	Ceratium extensum	-2.29	M
155	Bellerochea malleus	-2.48	231	Ceratium gibberum	-1.78	M
156	Biddulphia alternans	-2.86	232	Ceratium hexacanthum	-1.20	M
157	Odontella aurita	-3.16	233	Ceratium inflatum	-1.79	M
158	Odontella granulata	-1.72	234	Ceratium karstenii	-1.74	M
160	Odontella regia	-1.94	235	Ceratium lamellicorne	-1.28	M
161	Odontella rhombus	-1.85	237	Ceratium massiliense	-2.00	M
162	Cerataulina pelagica	-2.94	238	Ceratium minutum	-2.23	M
163	Climacodium frauenfeldianum	-3.43	240	Ceratium pentagonum	-2.18	M
164	Corethron criophilum	-2.79	241	Ceratium petersii	-2.32	M
165	Coscinodiscus concinnus	-1.04	242	Ceratium platycorne	-2.61	M
166	Coscinodiscus spp.	-0.75	243	Ceratium praelongum	-2.01	M
167	Detonula confervacea	-3.94	244	Ceratium pulchellum	-2.02	M
168	Ditylum brightwellii	-2.58	245	Ceratium setaceum	-2.46	M
169	Eucampia zodiacus	-3.06	246	Ceratium teres	-2.35	M
170	Fragilaria spp.	-3.73	247	Ceratium trichoceros	-2.63	M
171	Guinardia flaccida	-2.38	248	Ceratium vultur	-2.17	M
172	Gyrosigma spp.	-2.11	249	Ceratocorys spp.	-1.97	M
173	Hemiaulus spp.	-3.12	250	Cladopyxis spp.	-3.00	H
174	Lauderia borealis	-2.75	251	Dinophysis spp.	-2.88	H
175	Leptocylindrus danicus	-3.89	252	Exuviaella spp.	-2.84	M
176	Navicula spp.	-3.18	253	Gonyaulax spp.	-2.27	M
177	Cylindrotheca closterium	-4.42	254	Oxytoxum spp.	-2.76	H
178	Rhaphoneis amphiceros	-3.89	255	Protoperidinium spp.	-1.94	H
179	Planktoniella sol	-3.19	257	Podolampas spp.	-2.50	H
180	Rhizosolenia acuminata	-0.74	258	Pronoctiluca pelagica	-2.78	H
182	Rhizosolenia bergonii	-1.96	259	Prorocentrum spp.	-3.10	M
183	Rhizosolenia calcar-avis	-2.07	262	Ceratium falcatiforme	-2.39	M
185	Rhizosolenia delicatula	-3.40	263	Ceratium longirostrum	-1.86	M
186	Rhizosolenia fragilissima	-3.15				
187	Rhizosolenia setigera	-2.09				
188	Rhizosolenia stolterfothii	-2.77				
189	Schroederella delicatula	-3.10				
190	Stephanopyxis spp.	-2.40				
191	Streptotheca tamesis	-2.71				
192	Surirella spp.	-2.41				
199	Nitzschia spp.	-3.85				
200	Odontella mobiliensis	-2.19				
202	Asterionella kariana	-4.40				
205	Stauroneis membranacea	-2.99				

Table 2.1: Log_{10} of cell mass (μgC cell^{-1}) and trophic strategy (M=mixotroph, H=Heterotroph) of CPR survey diatoms (62) and dinoflagellates (51). All diatoms are considered to be photoautotrophic. See Appendix 1 and 2 for sources.

2.3.3 Analysis of Continuous Plankton Recorder Data

The Sir Alister Hardy Foundation for Ocean Science (SAHFOS) has operated the CPR survey in the North Atlantic Ocean since 1931, with consistent phytoplankton measuring techniques since 1958 (Richardson et al., 2006). Ships of opportunity tow the plankton recorder at roughly 7-9 meters depth on quasi-regular routes, and plankton caught on the spooling filtering mesh are enumerated microscopically upon return to the laboratory. The microscopic analysis of the filtering meshes is converted empirically to a semi-quantitative measure of cell number density (cells vol^{-1}), which we term "abundance". Throughout, we purposefully leave the generic volume units (vol) in the description of abundance because the exact volume filtered varies with ship towing speed and plankton density (Jonas et al., 2004). The size of the filtering mesh (270 μm on a side) and the differential preservation of survey taxa (e.g., armored vs. unarmored dinoflagellates) imply that sampling biases may exist. We describe these biases by plotting the maximum observed monthly mean abundance (Fig. 2.2A) and biomass (B; μgC vol^{-1}; Fig. 2.2B) for each diatom (62) and dinoflagellate (51) taxa. There is no significant relationship between the log of maximum abundance and cell mass (m), though other observations suggest the slope should range from -2/3 to -5/3 (Finkel, 2007). There is a significant positive relationship between the log of cell mass and maximum biomass ($B = 1.51m^{0.77}$, $n = 113$, $r^2 = 0.23$, $p < 0.0001$), though other observations suggest that this exponent should be closer to 0 (Chisholm, 1992). It is clear that small cells are under-sampled relative to larger ones (Richardson et al., 2006). Nevertheless, the survey's consistent methodology allows for diagnosis of population changes through time (longer than monthly timescales), and multiple taxa can be considered together with care. Though we calculate an estimate of phytoplankton biomass (μgC vol^{-1}) by multiplying the abundance (cells vol^{-1}) and cell mass (μgC $cell^{-1}$) in Fig. 2.2, we present only the abundance in other figures as this is the quantity measured by the survey.

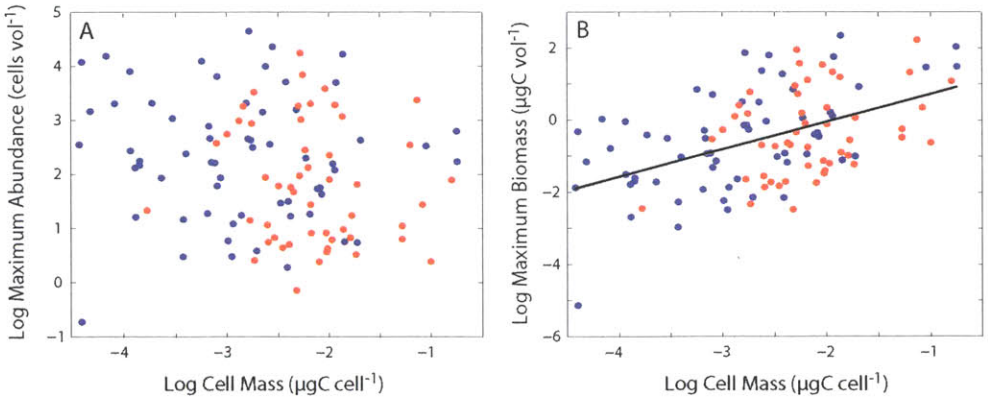

Figure 2.2: Relationship between the log of cell mass (m, μgC $cell^{-1}$) and maximum CPR abundance (A; cells vol^{-1}) and biomass (B; μgC vol^{-1}) for 62 diatom taxa (blue dots) and 51 dinoflagellate taxa (red dots). There is no significant relationship between the log of abundance and cell mass, though other observations suggest a significant slope ranging from -2/3 to -5/3 (Finkel, 2007). There is a positive relationship (black line) between the log of cell mass and maximum biomass ($B = 1.51m^{0.77}$, $n = 113$, $r^2 = 0.23$, $p < 0.0001$), though other observations suggest that this exponent should be close to 0 (Chisholm, 1992).

Monthly mean abundance data for all phytoplankton taxa across the 41 standard survey areas in the North Atlantic Ocean (Fig. 2.1) during 1958-2006 were provided by SAHFOS. In addition, they provided data indicating the number of distinct observations taken within each year, month, and survey area. From the broader list of phytoplankton surveyed, we considered only the 62 diatom and 51 dinoflagellate taxa that were routinely monitored across all zones and years (Table 2.1). Here, we describe the methods by which we averaged the CPR database over multiple years, areas, and taxa and provide estimates of the associated uncertainty. For each of the 113 taxa within each of 41 survey areas, we calculated a mean annual cycle of abundance, weighting the mean by the number of observations taken of each taxon in a zone and a given year and month. We then calculated a basin-wide mean annual cycle for each taxon, this time weighting the average by the geographic area (km^2) of each of the zones. We then determined an unweighted average over multiple taxa (e.g., Figs. 2.3-2.5). We considered only areas, months, and years with greater than two samples and have not attempted to interpolate for missing data. When averaging over multiple taxa to find composite seasonal cycles of abundance, we use only those diatoms (59) and dinoflagellates (36) with detectable data in more than 6 months of the year. The 6-month threshold is intended to reduce the impact of poorly-sampled taxa in the mean statistics. The averaging, as we have done here, is inherently a trade-off between having enough data for robust statistics and retaining taxa- and area-specific patterns.

Given the natural spatial and temporal variability of ocean ecosystems and the relatively sparse CPR sampling, the monthly mean abundance data provided by SAHFOS cannot capture the "true" mean abundance for a given taxa in a particular month, area, and year. We assume this representation error is equal in all the years ($l = 1958, \ldots, 2006$), and estimate it by calculating the standard error ($\delta^{est}_{i,j,k,l}$) for all the year data for each taxon ($i = 1, \ldots, 113$), area ($j = 1, \ldots, 41$), and month of the year ($k = 1, \ldots, 12$):

$$\delta^{est}_{i,j,k,l} = \frac{\sigma_{i,j,k}}{\sqrt{l'_{i,j,k} - 1}} \tag{2.2}$$

where $l'_{i,j,k}$ is the number of years with data in the temporal range ($l = 1958, \ldots, 2006$) and $\sigma_{i,j,k}$ is the standard deviation of all available data. If the errors from year-to-year are random and uncorrelated, the error associated with calculating the mean annual cycle for each taxon and area is, after Taylor (1997):

$$\delta_{i,j,k} = [\sum_{l} (\frac{w_{i,j,k,l}}{\sum_{l} w_{i,j,k,l}})^2 (\delta^{est}_{i,j,k,l})^2]^{\frac{1}{2}} \tag{2.3}$$

where the weights, $w_{i,j,k,l}$, are the number of CPR observations in each taxon, area, month, and year. When calculating the error associated with averaging over the basin, we also assume that area-to-area errors are uncorrelated and random, such that:

$$\delta_{i,j} = [\sum_{k} (\frac{w_{i,j,k}}{\sum_{k} w_{i,j,k}})^2 (\delta_{i,j,k})^2]^{\frac{1}{2}} \tag{2.4}$$

where the weights, $w_{i,j,k}$, are the geographic area (km^2) of each survey area. Unlike when averaging over multiple years and zones, when averaging over multiple taxa observed at the

same place and time, we assume the errors are correlated, such that:

$$\delta_j = \frac{\sum_i \delta_{i,j}}{i'} \tag{2.5}$$

where i' is the number of taxa averaged. The assumption of uncorrelated errors on interannual and basin scales, but correlated errors for species measured in the same place and time, is reasonable considering the characteristic time and space scales of coordinated variability in marine ecosystems at this latitude ($\sim$ 100km; Doney et al., 2003).

2.4 Results

Here we report the basin-wide mean seasonal succession patterns of abundance for all diatoms and dinoflagellates (Fig. 2.3), differing trophic strategies (Fig. 2.4), and four size classes of diatoms and dinoflagellates (Fig. 2.5).

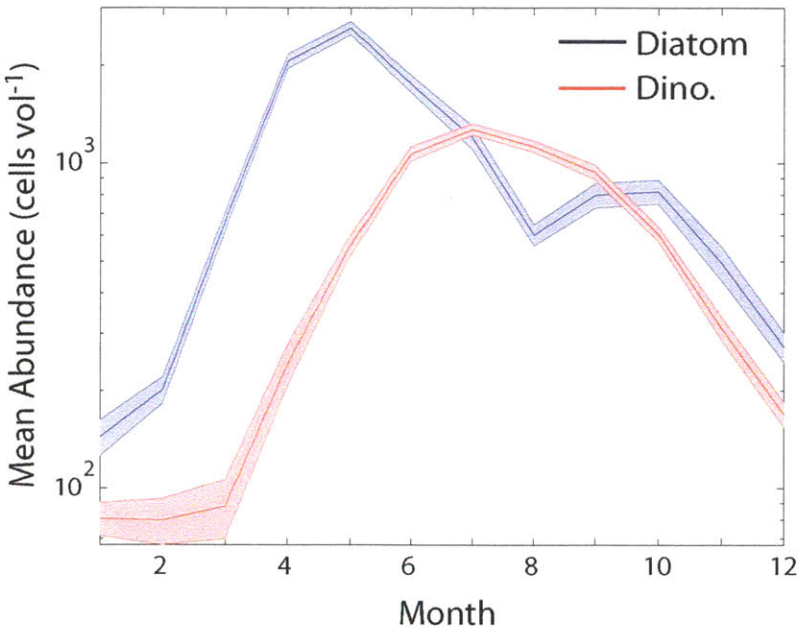

Figure 2.3: Monthly mean abundance (cells vol^{-1}) for diatoms (blue) and dinoflagellates (red), averaged over all CPR survey areas. Only those taxa with detectable abundances in more than 6 months during the year are included (59 diatoms, 36 dinoflagellates). Shaded error bars indicate two standard errors ($\pm 2\sigma$).

Diatoms (59 taxa considered) reach a maximum abundance in spring (February-May) and decline through the summer (June-August; Fig. 2.3). The diatom spring maximum is followed by a peak in dinoflagellate abundance in summer (36 taxa considered), which is in turn followed by a fall diatom bloom. This successional pattern is broadly consistent across latitudes (see Appendix 3) and in coastal vs. open ocean locations (data not shown) within the CPR survey area, and has been observed widely enough such that it has become

a paradigm in temperate seas (e.g., Margalef, 1978; Cushing, 1989; Taylor et al., 1993). This pattern has also been observed in previous analyses of the CPR survey data (Leterme et al., 2005; McQuatters-Gollop et al., 2007).

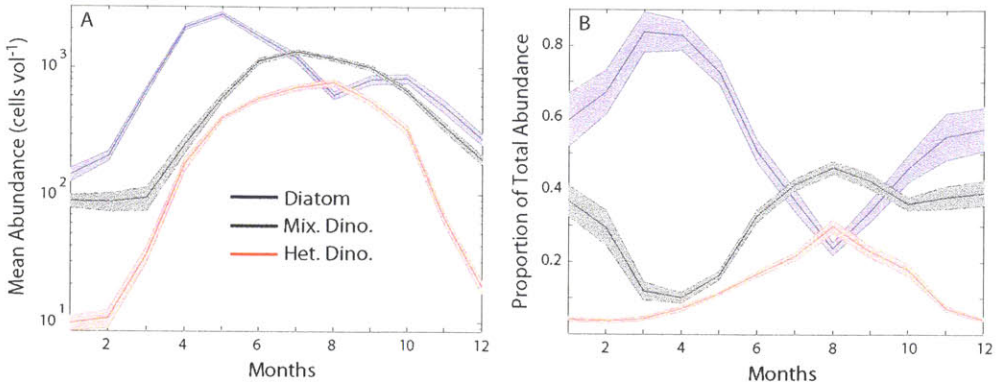

Figure 2.4: A) Monthly mean abundance (cells vol^{-1}), averaged across all areas, years, and taxa within taxonomic groups, for photoautotrophic diatoms and heterotrophic and mixotrophic dinoflagellates. Only those taxa with detectable abundances in more than 6 months during the year are included (59 diatoms, 32 mixotrophs, 4 heterotrophs). The shaded error bars indicate two standard errors ($\pm 2\sigma$). B) Same data as for A), but normalized by the sum of all three curves.

When differentiating abundance patterns according to trophic strategy, we find that an early bloom in photoautotrophic diatoms (59 taxa) is followed, in sequence, by mixotrophic (32 taxa) and heterotrophic dinoflagellates (4 taxa; Fig. 2.4A). The peak in heterotrophic abundance coincides with the summer diatom minimum. In terms of timing of the seasonal cycles, photoautotrophs and heterotrophs are out of phase (Fig. 2.4B). Relative to heterotrophs, mixotrophic dinoflagellates remain more abundant during winter. When looking over a range of latitudes (see Appendix 3), we find that mixotrophic and heterotrophic dinoflagellates tend to peak at roughly the same time in northern latitudes, whereas the mixotrophic peak precedes that of heterotrophs by up to two months in more southern latitudes.

Lastly, we differentiate the seasonal cycles of abundance between equal, logarithmically-spaced size classes of diatoms and dinoflagellates, averaged across all areas and years (Fig. 2.5). The size classes are as follows (Cell mass units are μgC $cell^{-1}$): i) m$> 10^{-2}$ (10 diatoms, 12 dinoflagellates), ii) $10^{-2} >$m$> 10^{-3}$ (24 diatoms, 23 dinoflagellates), iii) $10^{-3} >$m$> 10^{-4}$ (20 diatoms, 1 dinoflagellate), and iv) m$< 10^{-4}$ (5 diatoms, 0 dinoflagellates). In Fig. 2.5B, we normalize by the maximum abundance observed within each size bin, such that the normalized mean abundance scales from a minimum possible of 0 to a maximum of 1. There appears to be little differentiation in bloom timing among the different size classes of diatoms. The data suggest, however, that the largest diatoms continue to increase in abundance for approximately one month beyond the smaller size classes in both spring and fall blooms. Among dinoflagellates, the largest group appears to peak earlier than the smallest two groups by approximately one month. Additionally, the abundance of the largest dinoflagellates remain relatively constant, while the smallest taxa show a seasonal

change.

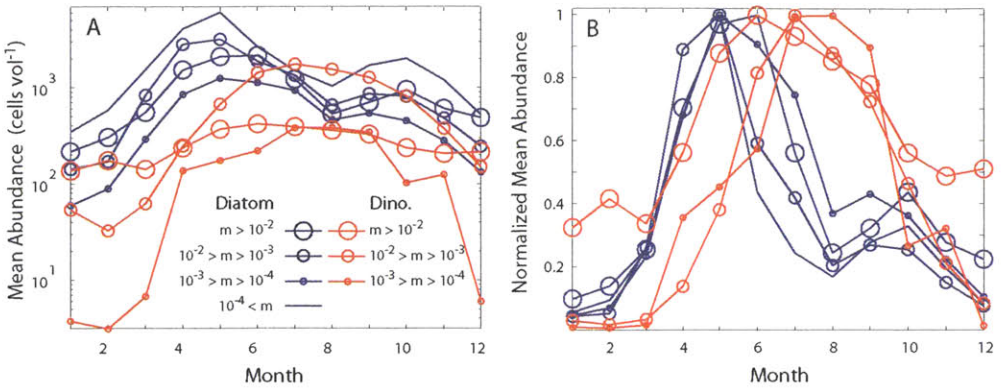

Figure 2.5: A) Monthly mean abundance (cells vol^{-1}) for equal, logarithmically-spaced size classes of diatoms (blue) and dinoflagellates (red), averaged across all areas and years, and in B), the same data, but normalized by the maximum of each curve to fall from 0 to 1. The size classes are as follows (Cell mass units are μgC cell^{-1}): i) m> 10^{-2} (10 diatoms, 12 dinoflagellates), ii) 10^{-2} >m> 10^{-3} (24 diatoms, 23 dinoflagellates), iii) 10^{-3} >m> 10^{-4} (20 diatoms, 1 dinoflagellate), and iv) m< 10^{-4} (5 diatoms, 0 dinoflagellates). Error bars, as in Figures 3 and 4, are omitted for clarity.

2.5 Discussion

The results (Figs. 2.3-2.5) depict mean, basin wide ecological patterns among diatoms and dinoflagellates of a range of trophic strategies and cell sizes. In the following section, we discuss these results in the context of the three initial hypotheses.

2.5.1 Trophic Strategies

Here we discuss the hypothesis that trophic strategy plays a key role in the ecological dynamics observed in the CPR data. Each winter in the CPR survey latitudes, ocean mixed layers deepen and entrain nutrients to the surface, readying the ocean surface for phytoplankton growth. With the exception of overwintering predators (Wesche et al., 2007), grazers are relatively sparse in the spring, and with the plentiful light and nutrients, photosynthesis may exceed respiration and allow photoautotrophic phytoplankton to rapidly bloom (Figs. 2.3-2.5). Heterotrophic dinoflagellates, by contrast, peak during the summer minimum of diatoms. In spring, they begin to increase their abundance somewhat more slowly than diatoms (but in concert with other dinoflagellates), and ultimately their rate of increase slows as the diatom abundance is greatly diminished in summer. While the diatoms certainly have other predators, such as copepods, and the heterotrophic dinoflagellates other prey, it is known that the dinoflagellates consume diatoms of similar size (Hansen et al., 1994; Hansen and Calado, 1999). Thus, the successional patterns of diatoms and dinoflagellates in Fig. 2.4 are consistent with heterotrophic dinoflagellates increasing their abundance in

response to increased diatom and dinoflagellate prey abundance, though from these data alone it is impossible to directly confirm the predation.

While there are exceptions (the largest dinoflagellates peak soon after the diatoms; Fig. 2.5), dinoflagellate abundance tends to peak in oligotrophic, summer conditions (Figs. 2.4-2.5). It is perhaps surprising that there are only minor differences in the timing of the mean seasonal cycles of mixotrophic and heterotrophic dinoflagellates. Nevertheless, mixotrophs reach their maximum slightly earlier than do heterotrophs (Fig. 2.4). Why might mixotrophs follow photoautotrophs but precede heterotrophs? During nutrient-replete bloom conditions, diatoms can take up nutrients and grow faster than can dinoflagellates (Tang, 1995; Litchman et al., 2007). With abundant prey, pure heterotrophs tend to have higher growth and grazing rates than mixotrophs (Pérez et al., 1997; Zubkov and Tarran, 2008). In these two extremes of abundant nutrients or prey, the mixotrophs should be outcompeted by specialist photoautotrophs and heterotrophs, respectively, and it is believed that this outcome results from the cost to mixotrophs of maintaining both autotrophic and heterotrophic capabilities (Ward et al., 2011b). However, in between these extremes mixotrophs enjoy the "bet-hedging" mechanism of being able to consume multiple resources, meaning they can persist in varying conditions (Li et al., 2000; Litchman, 2007). Mixotrophs gain an advantage compared with heterotrophs from being able to photosynthesize when nutrients are present, and this may explain, in part, their earlier peak. This ability to exploit multiple resources may also explain why mixotroph abundance does not decline nearly as much in relative terms during winter as it does for heterotrophs (Fig. 2.4). Mixotrophs may also eat their nutrient competitors (diatoms, dinoflagellates) and in some cases their predators (other dinoflagellates), liberating resources, either nutrients or prey, for their own use (Thingstad et al., 1996). The conceptual picture is that the diatom and dinoflagellate succession evident in the CPR survey can be understood in terms of a succession of trophic strategies, from photoautotrophy to heterotrophy. This is consistent with the interpretation of trophic strategies given in previous observational (Chang et al., 2003) and modeling studies (Bruggeman, 2009).

2.5.2 The Role of Cell Size and Growth Rate

Taken together, field observations of phytoplankton communities (e.g., Sommer, 1985; Cushing, 1989), compilations of laboratory data describing μ^{max} (Tang, 1995; Litchman et al., 2007), and plankton community modeling studies (Taylor et al., 1993; Baird and Suthers, 2007) support the hypothesis that μ^{max} plays a role in regulating ecological dynamics. Faster growing taxa–which are often smaller cells or taxonomic groups such as diatoms–should dominate more slowly growing taxa in nutrient-replete periods. Is evidence for this mechanism found in the CPR data?

Perhaps the most straight-forward way to address this question is to compare patterns of seasonal succession between different size classes of diatoms and dinoflagellates (Fig. 2.5). Recall that in the limit of ideal conditions ($\gamma = 1$) and small losses ($\mu^{max} \gg \lambda$), Equation 2.1 simplifies to $\frac{1}{B}\frac{dB}{dt} \approx \mu^{max}$. Were μ^{max} a critical trait in this context, we might expect to see smaller phytoplankton blooming soonest and strongest in the spring in the CPR data. However, this does not appear to be the case for diatoms, where different size classes show similar successional patterns. For dinoflagellates, larger cells peak well in advance of smaller cells, though this is possibly linked to their flexible trophic strategies (see above) and the fact that they have a higher initial abundance in spring. Though not shown here, this pattern over size classes holds true when looking over the different latitude bands of

CPR survey areas (e.g., Zones A, B, etc. from Fig. 2.1). There are at least two related interpretations of why μ^{max} does not seem to be important here: a) the CPR survey, as compiled, cannot resolve the timescales on which μ^{max} plays a key role and b) growth and loss processes (λ) are roughly balanced on the survey timescales.

First, we consider the possibility that the importance of μ^{max} may be obscured by the monthly timescales in the CPR survey. A brief discussion of field observations from the 1989 North Atlantic Bloom Experiment (NABE; Taylor et al., 1993) is illustrative here. In the NABE spring bloom, the onset of the bloom was dominated by the smallest phytoplankton with the fastest growth rates (1-5μm in size), and they were followed closely by larger, more slowly-growing phytoplankton ($> 5\mu$m). It is thought that the abundance of the smaller phytoplankton is rapidly controlled by their smaller, quickly-growing grazers ($\sim$1 week), while the predators of the larger phytoplankton are somewhat slower to respond and crop down their prey. These transient dynamics, characterized by smaller cells being replaced by larger cells as the dominant bloom taxa (Chisholm, 1992; Irigoien et al., 2004; Schartau et al, 2010), play out on a timescale of days to weeks. Therefore, it is possible that the CPR survey, as analyzed here (Figs. 2.3-2.5), simply cannot resolve the narrow timescale on which μ^{max} is important.

A second and related possibility is that growth and loss processes are roughly in balance for a given taxa on the timescales of the CPR survey, thereby obscuring the size-dependence in μ^{max}. This alternative suggests that population growth should be governed by small imbalances between growth and loss and generally be quite slow compared to the μ^{max} limit. Consider again Equation 2.1, where the net population growth, or μ^{net}, is the balance of growth and loss processes, $\mu^{net} \approx \mu^{max} - \lambda$. An imbalance between growth and loss (or $\mu^{max} \gg \lambda$ and $\mu^{net} \approx \mu^{max}$) leads to a bloom because of the grazing "loophole" (Irigoien et al., 2005). However, grazers typically respond rapidly to increases in their prey, such that $\mu^{max} \approx \lambda$ and $\mu^{net} \approx 0$ (Lessard and Murrell, 1998; Landry et al., 2000). Which of these two limits appear to be reflected in the CPR data? Using the mean annual cycles of abundance (P_k, *cells vol*$^{-1}$) for each CPR taxa and survey area with greater than 6 months of data available, we diagnosed μ^{net} in each of k months of the year, defined as $\mu^{net} = \frac{dP_k}{dt}\frac{1}{P_k}$. In Fig. 2.6, we show the maximum μ^{net} for each taxa and area and find that μ^{net} is typically lower than laboratory-based predictions for μ^{max} (black dashed line; Tang, 1995), mostly likely because of losses ($\lambda > 0$), non-ideal growth conditions ($\gamma < 1$), and the averaging in the CPR data. We also found no significant relationship between cell mass and maximum μ^{net} rate among diatoms or dinoflagellates. Additionally, there are no apparent, coherent differences in maximum μ^{net} between diatoms and dinoflagellates, despite the observation that diatoms grow faster, on average, than dinoflagellates in laboratory conditions (e.g., Tang, 1995). When looking at maximum μ^{net} over multiple CPR survey areas for spatial patterns, there does not appear to be any spatially-coherent variation between μ^{net} and cell mass or taxonomic group (data compiled in Fig. 2.6). Based upon this analysis, it appears that growth and loss processes roughly balance on the CPR timescales ($\sim$ 1 month) across a range of cells sizes and taxonomic groupings, meaning that μ^{net} is typically much less than μ^{max}. Regardless of transient dynamics, which suggest that smaller phytoplankton may initially outgrow larger phytoplankton, we argue that predator populations (Landry et al., 2000; Kiørboe, 2008) or declining nutrient concentrations (Martin-Jézéquel et al., 2000) slow prey population increases on timescales that are rapid relative to the CPR survey's resolution.

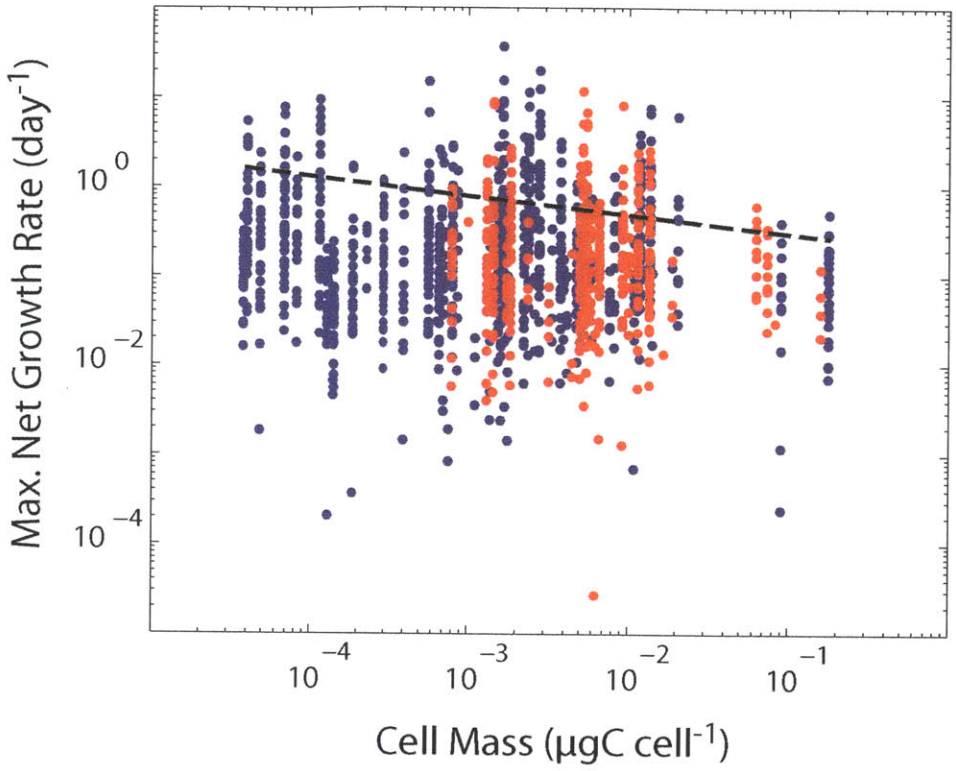

Figure 2.6: Maximum net growth rate (μ^{net}; day^{-1}) plotted against cell mass (m; $\mu gC\ cell^{-1}$) for diatoms (blue dots) and dinoflagellates (red dots), as diagnosed from seasonal cycles of abundance within each of the 41 CPR survey areas. Only those diatom (54) and dinoflagellate taxa (29) with greater than 6 months of data and a maximum $\mu^{net} > 0$ were considered. There is no significant relationship between the maximum net growth rate and cell mass for either diatoms or dinoflagellates. The dashed black line is the laboratory-based relationship between μ^{max} and cell mass for all phytoplankton types ($\mu^{max} = 3.45m^{-0.21}$; Tang, 1995). Because this line is an empirical prediction gleaned from data on many species, it is unsurprising that maximum μ^{net} can exceed the lab-based prediction for μ^{max}.

2.5.3 Gleaners and Opportunists

Here, we discuss evidence for the existence of gleaners and opportunists in the CPR data. We do not consider the very smallest phytoplankton cells in the ocean–such as picoeukaryotes, cyanobacteria, and coccolithophores–that are often described as gleaners, as they are not sampled by the CPR survey. First, we discuss how the taxonomic transition from diatoms to dinoflagellates can be considered a shift from opportunists to gleaners (Margalef, 1978). Rather than being a difference in ability to acquire scarce inorganic nutrients related to size differences, it is likely that this shift is largely defined by behavioral differences between taxonomic groups. Dinoflagellates use mixotrophy, toxin production, and swimming to compensate for their generally poor nutrient affinity (Litchman et al., 2007), and thus tend to do relatively well compared with diatoms in nutrient-deplete summer conditions. By contrast, it is thought that diatoms use their relatively fast growth and uptake rates, coupled with temporary escape from predation (Kiørboe, 2008), to benefit in bloom conditions.

However, we argue that a shift between gleaners and opportunists occurs within taxonomic groups, primarily through a shift in cell size. We calculated the mean cell mass of the most abundant diatom and dinoflagellate taxa (those taxa comprising greater than 95% of the cumulative abundance in each month) and found a shift towards smaller diatoms during summer, with a somewhat weaker shift apparent for dinoflagellates (Fig. 2.7). This size shift was most pronounced in "D" and "E" CPR zones that straddle the boundary between subpolar and subtropical gyres (see Appendix 3, Fig. 2.1). A similar seasonal size shift has been observed in temperate coastal waters and is consistent with theoretical predictions about how maximum cell size should change as a function of ambient nutrient concentration (Kiørboe, 2008). While we do not have nutrient data co-located with CPR observations, summer at this latitude is characterized by a strong depletion in nutrients (Conkright et al., 2000). Why do smaller diatoms dominate during the nutrient-deplete summer months? We hypothesize that during quiescent, nutrient-deplete conditions, phytoplankton growth tends to be limited by the diffusion of nutrients towards the cell surface and smaller cells are more competitive than their larger peers because of their higher nutrient affinities. We hypothesize that this size constraint is eased when greater ambient inorganic nutrient levels are available in the spring and fall, and larger cells may grow. While the total amount of available inorganic nutrients determines the range of cells sizes that may survive, the abundance of each size class is tightly cropped by their attendant grazers (Armstrong, 1994; Ward et al., 2011a). This process is thought to explain the positive correlation between inorganic nutrients and cell size (e.g., Irigoien et al., 2004; Schartau et al., 2010) and variations in plankton size spectra (e.g., San Martin et al., 2006).

The size shift within dinoflagellates is less pronounced, though still apparent. There are two principal explanations for why the shift may be smaller for dinoflagellates. Firstly, mixotrophy tends to alleviate nutrient limitation through phagotrophy when nutrients are scarce (Ward et al., 2001b). Secondly, it may be that the prey of summer dinoflagellates-either diatoms, dinoflagellates, or unresolved taxa such as picoeukaryotes–are quite small themselves. Fig. 2.5 suggests that the larger dinoflagellates follow the diatom bloom most closely, but the smaller dinoflagellates peak in summer with smaller prey. This sequence would be consistent with the notion that dinoflagellates may consume similar-sized prey, and that the abundant summer prey should be smaller cells (Fig. 2.7).

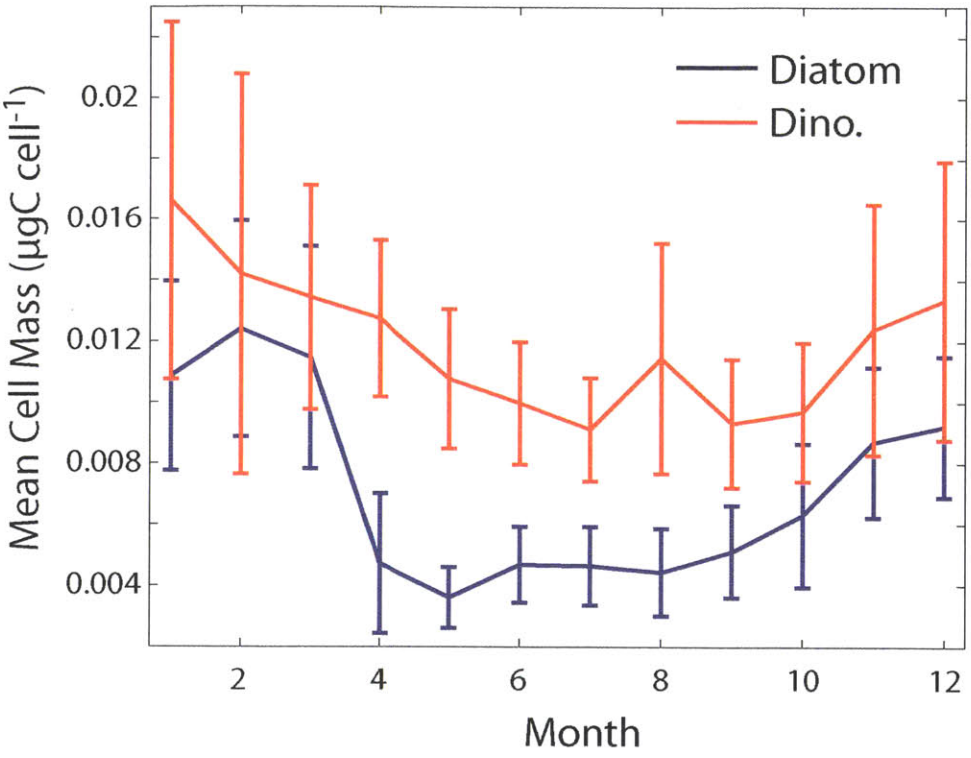

Figure 2.7: Mean cell mass ($\mu gC\ cell^{-1}$) of diatom and dinoflagellate taxa accounting for 95% of the cumulative abundance within each group and month. Only those taxa with detectable abundances in more than 6 months during the year are included (59 diatoms, 36 dinoflagellates). Error bars indicate two standard errors ($\pm\ 2\sigma$).

2.6 Conclusions

Diatoms and dinoflagellates are ecologically and biogeochemically important phytoplankton taxonomic groups, and here we have interpreted their observed community dynamics through two functional traits, trophic strategy and cell size. The databases on cell size and trophic strategy are substantial improvements upon existing, similar resources, and could prove to be valuable resources beyond this study.

While there are other important differences between diatom and dinoflagellates (e.g., motility, growth rates), the temporal succession in trophic strategy from photoautotrophs, to mixotrophs, and then to heterotrophs may be driven by the seasonal availability of relevant resources, light and nutrients, prey, or both. To our knowledge, this study is the first attempt to differentiate the ecological patterns of dinoflagellates according to their trophic strategy, and we suggest that this perspective may be crucial for interpreting the ecology of organisms beyond diatoms and dinoflagellates. For instance, recent evidence suggests that as much as 40-95% of total bacterivory is carried out by small ($\sim 5\mu m$), mixotrophic algae in the temperature North Atlantic Ocean (Zubkov and Tarran, 2008). Many harmful algal blooms are also attributed to mixotrophic dinoflagellates (Smayda, 1997). Clearly, mixotrophs play a key role in marine ecology and the regulation of marine biogeochemical cycles. However, most models of marine ecosystems do not explicitly consider dinoflagellates and typically represent only photoautotrophy. Future marine ecosystem models would benefit from viewing trophic strategy as a flexible, continuous trait, rather than an either-or designation (e.g., Ward et al., 2011b).

We have also found evidence that cell size plays a structuring role in the community dynamics of diatom and dinoflagellates. While there appears to be a shift toward the dominance of smaller cells within each taxonomic group in summer conditions that are typically nutrient-deplete in this region, we find little evidence for differentiation of taxa according to their laboratory-measured, size-linked maximum potential growth rates (μ^{max}). In both inferences, size-regulated zooplankton grazing is likely to play a key role. We hypothesize that during nutrient-deplete, summer conditions, smaller cells are able to grow and dominate the ecosystem because of their high nutrient affinity, but are tightly cropped down by their small, relatively quickly-growing grazers. Previous observations have shown that in the nutrient-replete growth phase in spring, the same small cells take off first but are soon corralled by their predators, consistent with previous observations (Taylor et al., 1993; Landry et al., 2000). Larger cells may have slower growth rates, but also a slower grazing response. In support of this idea that growth and loss processes tend to balance across many taxa on CPR analysis timescales ($\sim$ 1 month), we found that the maximum net population growth (μ^{net}) is roughly equal across a range of cell sizes and taxa. Thus, a high μ^{max} is, at best, a temporary advantage in the presence of size-regulated grazing.

There are, of course, many other relevant traits for marine phytoplankton that we have not considered (see Litchman and Klausmeier, 2008). In our view, however, these two traits–cell size and trophic strategy–in combination with zooplankton grazing, are fundamental and essential. Additional studies should identify further crucial traits and quantify their roles in regulating phytoplankton community ecology. Lastly, we argue that models used for prediction and assessment of marine ecosystems and biogeochemical cycles should capture, at a minimum, some measure of the range of trophic strategies and phytoplankton cell sizes present in the ocean, as well and the size-dependence of interactions among phytoplankton and their predators.

2.7 References

Armbrust, E.V., Chisholm, S.W., 1992. Patterns of cell size change in a marine centric diatom: variability evolving from clonal isolates. Journal of Phycology 28, 146-156.

Armstrong, R.A., 1994. Grazing limitation and nutrient limitation in marine ecosystems: Steady state solutions of an ecosystem model with multiple food chains. Limnology and Oceanography 39(3), 597-608.

Azam, F., et al., 1983. The ecological role of water-column microbes in the sea. Marine Ecology Progress Series 10, 257-263.

Baird, M.E., Suthers, I.M., 2007. A size-resolved pelagic ecosystem model. Ecological Modelling 203, 185-203.

Barber, R.T., Hiscock, M.R., 2006. A rising tide lifts all phytoplankton: Growth response of other phytoplankton in diatom-dominated blooms. Global Biogeochemical Cycles 20, GB4S03, doi:10.1029/2006GB002726.

Barnard, R., et al., 2004. Continuous Plankton Records: Plankton Atlas of the North Atlantic Ocean (1958-1999). II. Biogeographical charts. Marine Ecology Progress Series Supp., 11-75.

Barton, A.D., et al., 2003. The Continuous Plankton Recorder survey and the North Atlantic Oscillation: Interannual- to Multidecadal-scale patterns of phytoplankton variability in the North Atlantic Ocean. Progress in Oceanography 58, 337-358.

Barton, A.D., et al., 2010. Patterns of Diversity in Marine Phytoplankton. Science 327, 1509-1511.

Bruggeman, J., 2009. Succession in plankton communities: A trait-based perspective. Ph.D. thesis, Vrije Universiteit, Amsterdam.

Chang, F. H., et al., 2003. Seasonal and spatial variation of phytoplankton assemblages, biomass and cell size from spring to summer across the north-eastern New Zealand continental shelf. Journal of Plankton Research 25, 737-758.

Chisholm, S.W., 1992. Phytoplankton size. In Falkowski, P.G., Woodhead, A.D. (eds). Primary Productivity and Biogeochemical Cycles in the Sea. Plenum Press, New York.

Conkright, M.E., Gregg, W.W., Levitus, S., 2000. Seasonal cycle of phosphate in the open ocean. Deap-Sea Research I 47, 159-175.

Cullen, J.J., et al., 2002. Physical influences on marine ecosystem dynamics. In The Sea, Robinson, A., McCarthy, J.J., Rothschild, B.J., Eds. Wiley, New York, vol. 12, chap. 8.

Cushing, D.H., 1989. A difference in structure between ecosystems in strongly stratified waters and in those that are only weakly stratified. Journal of Plankton Research 11(1), 1-13.

Doney, S.C., et al., 2003. Mesoscale variability of Sea-viewing Wide Field-of-view Sensor (SeaWiFS) satellite ocean color: Global patterns and spatial scales. Journal of Geophysical Research Oceans 108 (C2), 3024, DOI 10.1029/2001JC000843.

Droop, M.R., 1968. Vitamin B12 and marine ecology, IV. The kinetics of uptake, growth and inhibition in Monochrysis lutheri. Journal of the Marine Biological Association of the United Kingdom 48, 689-733.

Dutkiewicz, S., Follows, M.J., Bragg, J.G., 2009. Modeling the coupling of ocean ecology and biogeochemistry. Global Biogeochemical Cycles 23, GB4017, doi:10.1029/2008GB003405.

Finkel, Z.V., 2007. Does size matter? The evolution of modern marine food webs. In: The evolution of aquatic photoautotrophs. Eds. Falkowski, P.G., Knoll, A.H.. Academic Press. Chapter 15, 333-350.

Finkel, Z.V., et al., 2010. Phytoplankton in a changing world: cell size and elemental stoichiometry: Journal of Plankton Research 32, 119-137.

Follows, M.J., Dutkiewicz, S., Grant, S., Chisholm, S.W., 2007. Emergent biogeography of microbial communities in a model ocean. Science 315, 1843-1846.

Hansen, P.J., 1991. Quantitative importance and trophic role of heterotrophic dinoflagellates in a coastal food web. Marine Ecology Progress Series 73, 253-261.

Hansen, P.J., Bjørnsen, P.K., Hansen, B.W., 1994. The size ratio between planktonic predators and their prey. Limnology and Oceanography 39(2), 395-403.

Hansen, P.J., Bjørnsen, P.K., Hansen, B.W., 1997. Zooplankton grazing and growth: Scaling within the 2-2,000um body size range. Limnology and Oceanography 42(4), 687-704.

Hansen, P.J., Calado, A.J., 1999. Phagotrophic mechanisms and prey selection in free-living dinoflagellates. Journal of Eukaryotic Microbiology, 46(4), 382-389.

Hansen, P.J., 2011. The role of photosynthesis and food uptake for the growth of marine mixotrophic dinoflagellates. Journal of Eukaryotic Microbiology 1-12.

Hillebrand, H., et al., 1999. Biovolume calculation for pelagic and benthic microalgae. Journal of Phycology 35, 403-426.

Irigoien, X., Huisman, J., Harris R.P., 2004. Global biodiversity patterns of marine phytoplankton and zooplankton. Nature 429, 863-867.

Irigoien, X., Flynn, K.J., Harris, R.P., 2005. Phytoplankton blooms: a loophole in microzooplankton grazing impact? Journal of Plankton Research 27(4), 313-321.

Irwin, A.J., et al., 2006. Scaling-up from nutrient physiology to the size-structure of phytoplankton communities. Journal of Plankton Research 28(5), 459-471.

Jonas, T.D., et al., 2004. The volume of water filtered by a Continuous Plankton Recorder sample: the effect of ship speed. Journal of Plankton Research 26(12), 1499-1506.

Johnson, Z.I., et al., 2006. Niche partitioning among Prochlorococcus ecotypes along ocean-scale environmentla gradients. Science 311, 1737-1740.

Kiørboe, T., 2008. A Mechanistic Approach to Plankton Ecology. Princeton University Press.

Klausmeier, C.A., Litchman, E., 2001. Algal games: The vertical distribution of phytoplankton in poorly mixed water columns. Limnology and Oceanography 46(8), 1998-2007.

Landry, M.R. et al, 2000. Biological response to iron fertilization in the eastern equatorial Pacific (IronEx II): III. Dynamics of phytoplankton growth and microzooplankton grazing. Marine Ecology Progress Series 201, 57-72.

Lessard, E.J., Murrell, M.C., 1998. Microzooplankton herbivory and phytoplankton growth in the northwestern Sargasso Sea. Aquatic Microbial Ecology 16, 173-188.

Leterme, S.C., et al., 2005. Decadal basin-scale changes in diatoms, dinoflagellates, and phytoplankton color across the North Atlantic. Limnology and Oceanography 50(4), 1244-1253.

Lewin, J.C., 1953. Heterotrophy in diatoms. Journal of General Microbiology, 9, 305-313.

Li, A., Stoecker, D. K., Coats, D. W., 2000. Spatial and temporal aspects of Gyrodinium galatheanum in Chesapeake Bay: distribution and mixotrophy. Journal of Plankton Research 22 (11), 2105-2124.

Litchman, E., 2007. Evolution of Primary Producers in the Sea. Elsevier, Ch. Resource competition and the ecological success of phytoplankton, pp. 351-375.

Litchman, E., et al., 2007. The role of functional traits and trade-offs in structuring phytoplankton communities: scaling from cellular to ecosystem level. Ecology Letters 10, 1170-1181.

Litchman, E., Klausmeier, C.A., 2008. Trait-based community ecology of phytoplankton. Annual Reviews of Ecology, Evolution, and Systematics 39, 615-639.

Makarevich, P.R., Larionov, V.V., Druzhkov, N.V., 1991. The average cell weights of the dominant phytoplankton species of the Barents Sea, Kola Scientific Center AN SSSR: Apatity, Kola Scientific Center, p. 12.

Makarevich, P.R., Larionov, V.V., Druzhkov, N.V., 1993. The average weights of the dominant phytoplankton of the Barents Sea. Algologiya 13, 103-106.

Margalef, R., 1978. Life-forms of phytoplankton as survival alternatives in an unstable environment. Oceanologica acta 1(4), 493-509.

Martin-Jézéquel, V., Hidebrand, M., Brzezinski, M.A., 2000. Silcon metabolism in diatoms: implications for growth. Journal of Physcology 36, 821-840.

Matishov, G., et al., 2000. Biological Atlas of the Arctic Seas 2000: Plankton of the Barents and Kara Seas. Available online:
http://www.nodc.noaa.gov/OC5/BARPLANK/WWW/HTML/bioatlas.html)

McGill, B.J., et al., 2006. Rebuilding community ecology from functional traits. Trends in Ecology and Evolution 21(4), 178-185.

McQuatters-Gollop, A., et al., 2007. Spatial patterns of diatom and dinoflagellate seasonal cycles in the NE Atlantic Ocean. Marine Ecology Progress Series 339, 301-306.

Menden-Deuer, S., Lessard, E.J., 2000. Carbon to volume relationships for dinoflagellates, diatoms, and other protist plankton. Limnology and Oceanography 45, 569-579.

Olenina, I., et al., 2006. Biovolumes and size-classes of phytoplankton in the Baltic Sea. HELCOM Baltic Sea Environmental Proceedings, 144.

Pérez, M.T., Dolan, J.R., Fukai, E., 1997. Planktonic oligotrich ciliates in the NW Mediterranean: growth rates and consumption by copepods. Marine Ecology Progress Series 155, 89-101.

Raven, J.A., 1998. The Twelfth Tansley Lecture, Small is Beautiful: The Picophytoplankton. Functional Ecology 12(4), 503-513.

Reid, P.C., 1998. Phytoplankton change in the North Atlantic. Nature, 391, 546.

Richardson, A.J., et al., 2006. Using continuous plankton recorder data. Progress in Oceanography 68, 27-74.

Round, F.E., Crawford, R.M., Mann, D.G., 1990. The Diatoms: biology and morphology of the genera. Cambridge, Cambridge University Press.

Ryther, J.H., 1969. Photosynthesis and fish production in the sea. Science 166(3901), 72-76.

San Martin, E., Harris, R.P., Irigoien, X., 2006. Latitudinal variation in plankton size spectra in the Atlantic Ocean. Deep-Sea Research II 53, 1560-1572.

Schartau, M., Landry, M.R., Armstrong, R.A., 2010. Density estimation of plankton size spectra: a reanalysis of IronEx II data. Journal of Plankton Research 32(8), 1167-1184.

Skovgaard, A., 1998. Role of chloroplast retention in a marine dinoflagellate. Aquatic Microbial Ecology, 15, 293-301.

Smayda, T.J., 1997. Harmful algal blooms: Their ecophysiology and general relevance to phytoplankton blooms in the sea. Limnology and Oceanography 42(5), 1137-1153.

Smith, T.M., Reynolds, R.W., 2003. Extended Reconstruction of Global Sea Surface Temperatures Based on COADS Data (1854-1997). Journal of Climate 16, 1495-1510.

Solovieva, A.A., 1976. Primary production and phytoplankton in the coastal waters of the Barents Sea, Biology of the Barents and White Seas: Apatity, Kola Scientific Center AN SSSR, 25-32.

Sommer, U., 1985. Seasonal succession of phytoplankton in Lake Constance. BioScience 35(6), 351-357.

Stewart. F.M., Levin, B.R., 1973. Partitioning of resources and the outcome of interspecific competition: A model and some general considerations. The American Naturalist 107, 171-198.

Stoecker, D. K., 1999. Mixotrophy among dinoagellates. Journal of Eukaryotic Microbiology 46 (4), 397-401.

Tang, E.P.Y., 1995. The allometry of algal growth rates. Journal of Plankton Research 17 (6), 1325-1335.

Tarangkoon, W., Hansen, G., Hansen, P.J., 2010. Spatial distribution of symbiont-bearing dinoflagellates in the Indian Ocean in relation to oceanographic regimes. Aquatic Microbial Ecology, 58: 197-213.

Taylor, A.H., et al., 1993. Seasonal succession in the pelagic ecosystem of the North Atlantic and the utilization of nitrogen. Journal of Plankton Research 15(8), 875-891.

Taylor, F.J.R., Hoppenrath, M., Saldarriaga, J.F., 2008. Dinoflagellate diversity and distribution. Biodiversity Conservation 17, 407-418.

Taylor, J.R., 1997. An Introduction to Error Analysis: The Study of Uncertainties in Physical Measurements. University Science Books, Sausalito, CA, USA.

Thingstad, T.F., et al., 1996. On the strategy of "eating your competitor": A mathematical analysis of algal mixotrophy. Ecology 77 (7), 2108-2118.

Tomas, C., et al., 1997. Identifying marine phytoplankton. Academic Press.

Ward, B.A., Dutkiewicz, S., Follows, M.J., 2011a. Size-structured food webs in the global ocean: theory, model, and observations. Submitted, Marine Ecology Progress Series.

Ward, B.A., et al., 2011b. Biophysical aspects of mixotrophic resource acquisition and competition. Accepted, The American Naturalist.

Wesche, A., Wiltshire, K.H., Hirche, H.J., 2007. Overwintering strategies of dominant calanoid copepods in the German Bight, southern North Sea. Marine Biology 151, 1309-1320.

Zubkov, M.V., Tarran, G.A., 2008. High bacterivory by the smallest phytoplankton in the North Atlantic Ocean. Nature 455, 224-227.

2A Appendices

2A.1 Cell Size Database

Table 2A.1: Diatom and dinoflagellate $\log_{10}$ mean cell size and standard deviation of cell size for n available estimates from the literature. Zoe Finkel (Mt. Allison University) led the development of the following database, as described in the Methods section above.

CPR ID	Taxon	Log Mean Cell Mass (μgC cell^{-1})	Log SD Cell Mass (μgC cell^{-1})	Number of Size Estimates	Sources
101	Paralia sulcata	-3.85	-4.02	7	1,2,7,37,47,53
102	Skeletonema costatum	-4.32	-4.18	44	1,2,5,6,7,9,27,28,29,35,37,47,50,51,53
103	Thalassiosira spp.	-2.78	-2.46	19	13,18,19,20,30,35,37,47,50,53
104	Dactyliosolen antarcticus	-2.23	-2.13	2	4,19
105	Dactyliosolen mediterraneus	-3.10	-3.06	5	6,18,50,51,53
106	Rhizosolenia imbrica. shrubsolei	-2.81	-3.09	9	1,5,6,18,35,47
107	Rhizosolenia styliformis	-1.93	-2.03	9	1,20,47,50,51,53
108	Rhizosolenia hebetata semispina	-2.62	-2.55	11	1,7,50,51,53
109	Rhizosolenia alata indica	-2.32	-2.50	3	6,18,50
110	Rhizosolenia alata alata	-2.42	-2.12	22	1,5,7,9,13,19,20,28,31,35,47,50,51,53
111	Rhizosolenia alata inermis	-2.65	-2.84	2	13,19
112	Chaetoceros (Hyalochaete) spp.	-2.55	-2.32	3	9,19
113	Chaetoceros (Phaeoceros) spp.	-1.86	-1.76	1	9
114	Odontella sinensis	-1.69	-2.15	5	1,2,5,18,47
115	Asterionella glacialis	-4.08	-4.33	8	1,2,28,37,47,53
116	Thalassiothrix longissima	-3.24	-3.58	4	1,31,51,53
117	Thalassionema nitzschioides	-4.16	-4.39	19	1,2,6,7,18,28,37,47,50,51
118	Nitzschia seriata	-3.94	-3.89	8	5,6,9,18,31,47,51,53
119	Nitzschia delicatissima	-4.40	-4.40	5	5,6,9,18,47
121	Ceratium fusus	-2.28	-2.37	14	1,5,6,32,37,41,45,47,49,51,53
122	Ceratium furca	-2.26	-2.47	12	1,2,32,37,46,47,49,50,53
123	Ceratium lineatum	-2.74	-3.02	12	1,2,35,46,47,50,53
124	Ceratium tripos	-2.04	-2.27	13	1,5,6,46,47,50,51
125	Ceratium macroceros	-2.18	-2.48	8	1,6,46,49,50,53
126	Ceratium horridum	-1.87	-1.68	6	1,5,37,47
127	Ceratium longipes	-2.30	-2.60	6	1,5,35,46,53
128	Ceratium arcticum	-1.13		1	9
129	Protoceratium reticulatum	-2.73	-3.04	4	1,37
131	Ceratium kofoidii	-3.78		1	40
132	Pyrophacus spp.	-2.03	-1.98	3	1,2,53
151	Actinoptychus spp.	-2.95	-3.59	5	1,2,47,50
152	Asteromphalus spp.	-3.43	-3.44	2	51,53
153	Bacillaria paxillifer	-3.64	-3.68		5,7,50
154	Bacteriastrum spp.	-3.53	-3.81	9	1,6,18,28,35,50,53
155	Bellerochea malleus	-2.48	-2.57	4	5,13,47
156	Biddulphia alternans	-2.86	-2.83	3	2,5,47
157	Odontella aurita	-3.16	-3.61	5	1,7,47,53
158	Odontella granulata	-1.72	-1.70	2	9,47
160	Odontella regia	-1.94	-2.80	2	5,47
161	Odontella rhombus	-1.85	-1.90	4	2,5,9,47
162	Cerataulina pelagica	-2.94	-3.57	6	2,6,7,27,47,53
163	Climacodium frauenfeldianum	-3.43	-4.41	4	18,49,50,51
164	Corethron criophilum	-2.79	-2.72	9	13,18,20,26,28,31,37,50
165	Coscinodiscus concinnus	-1.04	-1.05	3	1,16,47
166	Coscinodiscus spp.	-0.75		2	1,7,16,26,47
167	Detonula confervacea	-3.94	-4.20	6	1,5,47,53
168	Ditylum brightwellii	-2.58	-2.55	18	1,2,7,18, 27,29,32,47,50,53
169	Eucampia zodiacus	-3.06	-2.93	14	1,2,18,31,47,49,50,53
170	Fragilaria spp.	-3.73	-3.73	10	1,2,37,47,53
171	Guinardia flaccida	-2.38	-2.68	16	1,6,7,18,47,50,51
172	Gyrosigma spp.	-2.11	-3.55	2	1,5,9,35,37,47,49,53
173	Hemiaulus spp.	-3.12	-3.20	4	6,18,49,50,51,53
174	Lauderia borealis	-2.75	-2.58	12	1,2,5,9,18,28,47,50,53
175	Leptocylindrus danicus	-3.89	-4.15	21	1,2,5,7,18,19,28,47,49,53
176	Navicula spp.	-3.18	-2.72	18	1,5,9,13,19,20,35,37,47,49,53
177	Cylindrotheca closterium	-4.42	-4.35	14	2,7,13,18,19,20,36,47,49,51,53
178	Rhaphoneis amphiceros	-3.89		1	5
179	Planktoniella sol	-3.19	-3.41	5	15,18,50,51,53

Continued on next page

CPR ID	Taxon	Log Mean Cell Mass (μgC cell^{-1})	Log SD Cell Mass (μgC cell^{-1})	Number of Size Estimates	Sources
180	Rhizosolenia acuminata	-0.74	-1.07	3	17,18,51
182	Rhizosolenia bergonii	-1.96	-2.03	2	18,50
183	Rhizosolenia calcar-avis	-2.07	-2.47	5	2,6,18,50,53
185	Rhizosolenia delicatula	-3.40	-3.28	9	1,5,7
186	Rhizosolenia fragilissima	-3.15	-3.06	20	1,2,6,7,18,27,35,53
187	Rhizosolenia setigera	-2.09	-1.96	14	1,5,7,9,18,47
188	Rhizosolenia stolterfothii	-2.77	-2.80	11	1,2,5,6,18,45,47,50,51
189	Schroederella delicatula	-3.10	-3.26	7	1,4,5,18,37,47,53
190	Stephanopyxis spp.	-2.40	-2.61	3	1,2,18,32,35,47
191	Streptotheca tamesis	-2.71	-3.45	2	5,47
192	Surirella spp.	-2.41	-2.10	6	1,28,47
199	Nitzschia spp.	-3.85	-3.65	20	1,9,18,47,50,53
200	Odontella mobiliensis	-2.19	-2.09	7	1,2,5,18,37,47
202	Asterionella kariana	-4.40	-4.70	4	1,47
205	Stauroneis membranacea	-2.99	-3.77	2	5,9
217	Ceratium falcatum	-2.10		1	40
220	Amphisolenia spp.	-1.00	-0.84	11	23,49,50
221	Ceratium arietinum	-1.08	-0.97	2	9,50
222	Ceratium azoricum	-2.20	-3.04	2	37,40
223	Ceratium belone	-2.54		1	51
224	Ceratium bucephalum	-0.80		1	9
225	Ceratium buceros	-2.60	-2.72	2	6,51
226	Ceratium candelabrum	-2.00	-2.35	2	6,51
227	Ceratium carriense	-1.72		1	6
228	Ceratium compressum	-1.28		1	40
229	Ceratium declinatum	-2.38	-2.42	2	49,51
230	Ceratium extensum	-2.29	-2.38	3	50,51,53
231	Ceratium gibberum	-1.78		1	51
232	Ceratium hexacanthum	-1.20	-1.15	2	6,53
233	Ceratium inflatum	-1.79		1	57
234	Ceratium karstenii	-1.74	-1.88	2	6,51
235	Ceratium lamellicorne	-1.28		1	40
237	Ceratium massiliense	-2.00	-2.18	2	50,53
238	Ceratium minutum	-2.23	-2.26	2	9,47
240	Ceratium pentagonum	-2.18	-2.35	5	6,49,50,51,53
241	Ceratium petersii	-2.32		1	40
242	Ceratium platycorne	-2.61		1	51
243	Ceratium praelongum	-2.01		1	51
244	Ceratium pulchellum	-2.02	-2.29	3	50,51,53
245	Ceratium setaceum	-2.46		1	51
246	Ceratium teres	-2.35	-2.42	3	6,49,51
247	Ceratium trichoceros	-2.63	-4.24	2	6,51
248	Ceratium vultur	-2.17		1	51
249	Ceratocorys spp.	-1.97	-2.09	4	32,51,53
250	Cladopyxis spp.	-3.00	-3.59	3	1,9,53
251	Dinophysis spp.	-2.88	-2.96	11	1,20,35,47,53
252	Exuviaella spp.	-2.84	-2.76	8	1,9,47,53
253	Gonyaulax spp.	-2.27	-1.96	24	1,9,37,47,49,50,53
254	Oxytoxum spp.	-2.76	-3.04	9	1,9,37,49,50,53
255	Protoperidinium spp.	-1.94	-1.75	71	1,5,20,41,42,47,50,53
257	Podolampas spp.	-2.50	-2.97	3	37,50,53
258	Pronoctiluca pelagica	-2.78	-2.64	3	1,9,53
259	Prorocentrum spp.	-3.10	-3.10	19	1,2,32,35,37,46,47,49,50,53
262	Ceratium falcatiforme	-2.39		1	40
263	Ceratium longirostrum	-1.86		1	40

Cell Size Database References

1. Olenina, I., et al., 2006. Biovolumes and size-classes of phytoplankton in the Baltic Sea. HELCOM Baltic Sea Environmental Proceedings 106, 144.
2. Gallegos, C.L., 2011. Phytoplankton guide to the Chesapeake Bay and other regions, Phytoplankton Lab of the Smithsonian Environmental Research Center. Online database accessed April 2011: http://serc.si.edu/labs/phytoplankton/guide/index.aspx
3. Scott, F.J. and Marchant, J., Eds., 2005. Antarctic marine protists. Australian Biological Resources Study. Hobart.
4. Tomas, C.R., 1997. Identifying marine phytoplankton. San Diego, Academic Press.
5. Wiltshire, K.H. Durselen, C.-D., 2004. Revision and quality analyses of the Helgoland Reede long-term phytoplankton data archive. Helgoland Marine Research 58, 252-268.
6. Vilicic, D., 1985. An examination fo cell volume in dominant phytoplankton species of the central and southern Adriatic Sea. Internationale revue der Gesamten Hydrobiologie 70(6), 829-843.

7. Snoeijs, P., et al., 2002. The importance of diatom cell size in community analysis. Journal of Phycology 38, 265-272.
8. Kuylenstierna, M. Karlson, B., 2011. Checklist of phytoplankton in the Skagerrak-Kattegat, Swedish Meteorological and Hydrological Institute. Online database accessed April 2011:
http://www.smhi.se/oceanografi/oce_info_data/plankton_checklist/ssshome.htm
9. Matishov, G., et al., 2000. Biological Atlas of the Arctic Seas 2000: Plankton of the Barents and Kara Seas.
Available online:
http://www.nodc.noaa.gov/OC5/BARPLANK/WWW/HTML/bioatlas.html)
10. Hasle, G.R., et al., 1983. Cymatosiraceae, a new diatom family. Bacillaria 6, 9-156.
11. Aziz, A., 2005.. Brackish water algae from Bangladesh. I. Biddulphia spp. Bangladesh Journal of Botany 34(2), 109-113.
12. Carpenter, E.J., Janson, S., 2000. Intracellular cyanobacterial symbionts in the marine diatom Climacodium frauenfeldianum (Bacillariophyceae). Journal of Phycology 36(3), 540-544.
13. Kang, S.-H., et al., 2001. Antarctic phytoplankton assemblages in the marginal ice zone of the northwestern Weddell Sea. Journal of Plankton Research 23(4), 333-352
14. Williams, R.B. (1964). Division rates of salt marsh diaoms in relation to salintiy and cell size. Ecology 45(4), 877-880.
15. Finkel, Z.V., 2001. Light absorption and size scaling of light-limited metabolism in marine diatoms. Limnology and Oceanography 46(1), 86-94.
16. kaloud, P., 2008. Images from the North Sea, kaloud, P. Personal pages. Department of Botany, Faculty of Science, Charles University in Prague Czech Republic. Online database accessed April 2011,
http://botany.natur.cuni.cz/skaloud/index_NorthSea.htm
17. Moore, J.K., Villareal, T.A., 1996. Size-ascent rate relationships in positively buoyant marine diatoms. Limnology and Oceanography 41(7), 1514-1520.
18. Smayda, T.J., 1965. A quantitative analysis of the phytoplankton of the Gulf of Panama. II. On the relationship between C^{14} assimilation and the diatom standing crop. Inter-American Tropical Tuna Commission 9(7), 467-531.
19. Cornet-Barthaux, V., et al., 2007. Biovolume and biomass estimates of key diatoms in teh Southern Ocean. Aquatic Microbial Ecology 48, 295-308.
20. Moro, I., et al., 2000. Microalgal communities of hte sea ice, ice-covered and ice-free waters of Wood Bay (Ross Sea, Antarctica) during the austral summer 1993-94. Marine Ecology 21(3-4), 233-245.
21. Burns, D.A., Mitchell, J.S., 1982. Further examples of the dinoflagellate genus Ceratium from New Zealand coastal waters. New Zealand Journal of Marine and Freshwater Research 16, 57-67.
22. Faust, M.A., Gulledge, R.A., 2002. Identifying harmful marine dinoflagellates. Smithsonian Institution Contributions from the United States National Herbarium, Smithsonian National Museum of Natural History 42, 1-144.
23. Carbonell-Moore, M.C., 2004. On the taxonomical positon of Lessardia Salarriaga et Taylor within the family Podoplampadaceae Lindemann (Dinophyceae). Phycological Research 52, 340-345.
24. Hernandez-Becerril, D.U., et al., 2008. Marine Planktonic dinoflagellates of the order Dinophysiales (Dinophyta) from coasts of the tropical Mexican Pacific, including two new

species fo the genus Amphisolenia. Journal of the Marine Biological Associatiom of the United Kingdom 88(1), 1-15.
25. Caroppo, C., 2001. Autoecology and morphological variability of Dinophysis sacculus (Dinophyceae: Dinophysiaceae) in a Mediterranean lagoon. Journal of the Marine Biological Association of the United Kingdom 81, 11-21.
26. Hitchcock, G.L. (1982). A comparative study of the size-dependent organic composition of marine diatoms and dinoflagellates. Journal of Plankton Research 4(2), 363-377.
27. Conley, D.J., et al., 1989. Differences in silca content between marine and freshwater diatoms. Limnology and Oceanography 34(1), 205-213.
28. Brzezinski, M.A., 1985. The Si:C:N ratio of marine diatoms: Interspecific variability and the effect of some environmental variables. Journal of Phycology 21, 347-357.
29. Montagnes, D.J.S., et al., 1994. Estimating carbon, nitrogen, protein, and chlophyll a from volume in marine phytoplankton. Limnology and Oceanography 39(5), 1044-1060.
30. Montagnes, D.J.S., Franklin, D.J., 2001. Effect of temperature on diatom volume, growth rate, and carbon and nitrogen content: Reconsidering some paradigms. Limnology and Oceanography 46(8), 2008-2018.
31. Sommer, U., 1989. Maximal growth rates of Antarctic phytoplankton: Only weak dependence on cell size. Limnology and Oceanography 34(6), 1109-1112.
32. Menden-Deuer, S., Lessard, E.J., 2000. Carbon to volume relationships for dinoflagellates, diatoms, and other protist plankton. Limnology and Oceanography 45, 569-579.
33. Shimada, C., et al., 2006. Seasonal variation in skeletal silicification of Neodenticula seminae, a marine planktonic diatom: sediment trap experiments in the NW Pacific Ocean (1997-2001). Marine Micropaleontology 60, 130-144.
34. Shimada, C., Tanimura, Y., 2006. Spatial variability in valve morphology of Neodenticula seminae, an oceanic diatoms in the subarctic North Pacific and Bering Sea. Paleontological research 10(1), 79-89.
35. Katechakis, A., et al., 2004. Feeding selectivities and food niche separation of Acartia clausi, Penilia avidostris (Crustacea) and Doliolum denticulatum (Thaliacea) in Blanes Bay (Catalan Sea, NW Mediterranean). Journal of Plankton Research 26(6), 589-603.
36. Shuter, B.G. 1978. Size dependence of phophorus and nitrogen subsistence quotas in unicellular microrganisms. Limnology and Oceanography 23(6), 1248-1255.
37. Guisande, C., et al., 2002. Estimation of copepod trophic niche in the field using amino acids and marker pigments. Marine Ecology Progress Series 147(156), 147-156.
38. Gomez, F., 2007. Gymnodiniod dnoflagelates (Gymnodiniales, Dinophyceae) in the Open Pacific Ocean. Algae 22(4), 273-286.
39. Tas, S., et al., 2006. New record of a dinoflagellate species Corythodinium tesselatum (Stein) Loeblich Jr. Loeblich III from Turkish coastal waters of the north-eastern Mediterranean Sea. Turk Journal of Botany 30, 55-57.
40. Huisman, J.M., 1989. The genus Ceratium (Dinophyceae) in Bass Strait and adjoining waters, southern Australia. Australian Journal of Botany 2, 425-454.
41. Jensen, F., Hansen, B.W., 2000. Ciliates and heterotrophic dinoflagellates in the marginal ice zone of the central Barents Sea during summer. Journal of the Marine Biological Association of the United Kingdom 80, 45-54.
42. Hansen, B.W., Jensen, F., 2000. Specific growth rates of protozooplankton in the marginal ice zone of the central Barents Sea during spring. Journal of the Marine Biological Association of the United Kingdom 80, 37-44.

43. Okamoto, T., Takahashi, E., 1984. Taxonomy and distribution of some Ceratium species in the Antarctic Ocean. Memoirs of National Institute of Polar Research. Special issue 32, Symposium on Polar Biology 6, 14-23.
44. Nakamura, Y., 1998. Growth and grazing of a large heterotrophic dinoflagellate, Noctiluca scintillans, in laboratory cultures. Journal of Plankton Research 20(9), 1711-1720.
45. Jeong, H.-J., et al., 2002. Growth and grazing rates of the prostomatid ciliate Tiarina fusus on red-tide and toxic algae. Aquatic Microbial Ecology 28, 289-297.
46. Belgrano, A., et al., 2002. Allometric scaling of maximum population density: a common rule for marine phytoplankton and terrestrial plants. Ecology Letters 5, 611-613.
47. Hoppenrath, M. (2011). Alfred Wegener Institute Sylt Island time series. http://starcentral.mbl.edu/microscope/portal.php
48. Price, L.L., et al., 1998. Influence of continuous light and L:D cycles on the growth and chemical composition of Prymnesiophyceae including coccolithophores. Journal of Experimental Marine Biology and Ecology 223(2), 223-234.
49. Takahashi, M.T., Bienfang, P.K., 1983. Size structure of phytoplankton biomass and photosynthesis in subtropical Hawaiian waters. Marine Biology 76(2), 203-211.
50. Yamamoto, T., 1995. Contribution of Micro- and Nanophytoplankton cell carbon to particulate organic carbon in the East China Sea during May 1980. Journal Fac Applied Biological Science 34, 147-160.
51. Beers, J. R., et al., 1975. Microplankton of the North Pacific central gyre. Population structure and abundance, June 1973. Internationale Revue der Gesamten Hydrobiologie 60(5), 607-638.
52. Plankton net, 2011. Alfred Wegener Institute for Polar and Marine Research. http://planktonnet.awi.de
53. Mikaelyan, A.S., et al., 2011. Cell volumes of phytoplankton of the Black Sea. http://phyto.bss.ibss.org
54. Fernandez, C.E., Garcia, C.B., 1998. The dinoflagellates of the genera Ceratium and Ornithocercus collected in the Golfo de Salamanca, Colombian Caribbean Sea. Revista Academica de Colombia Ciencia 22(85), 539-559.
55. Druzhkov, N.V., et al., 2001. The sea-ice algal community of seasonal pack ice in the southwestern Kara Sea in late winter. Polar Biology 24(1), 70-72.
56. Druzhkov, N.V., et al., 2001. Phytoplankton in the south-western Kara Sea: composition and distribution. Polar Biology 20(1), 95-108.
57. Sournia, A., 1967. Le genre Ceratium (Peridinien planctonique) dans le Canal de Mozambique. Contribution a une revision mondiale. Vie et Milieu Ser. A. 18, 375-499.
58. Schmidt, C.J.B., et al., 2008. Influence of phytoplankton diets on the ingestion rate and egg production of Acartia clausi and A. Lilljeborgii (Copepoda: Calanoida) from Bahia del La Pax, Gulf of California. Hidrobiologia 18(Supplement), 133-140.
59. Fanuko, N., Valck, M., 2009. Phytoplankton composition and biomass of the northern Adriatic lagoon of Stella Maris, Croatia. Acta Bot. Croatia 68(1), 29-44.

2A.2 Trophic Strategy Database

Trophic Strategy References

1. Arndt, H., Hausmann, K., Wolf, M., 2003. Deep-sea heterotrophic nanoflagellates of the Eastern Mediterranean Sea: qualitative and quantitative aspects of their pelagic and

CPR ID	Taxon	Trophic Strategy	References
121	Ceratium fusus	M	2,14,25
122	Ceratium furca	M	31,32,34
123	Ceratium lineatum	M	25,27,30
124	Ceratium tripos	M	11,25
125	Ceratium macroceros	M	25
126	Ceratium horridum	M	19
127	Ceratium longipes	M	14
128	Ceratium arcticum	M	6,33
129	Protoceratium reticulatum	M	13,35
131	Ceratium kofoidii	M	10
132	Pyrophacus spp.	M	7,13
217	Ceratium falcatum	M	
220	Amphisolenia spp.	H	10,36
221	Ceratium arietinum	M	
222	Ceratium azoricum	M	8
223	Ceratium belone	M	
224	Ceratium bucephalum	M	
225	Ceratium buceros	M	
226	Ceratium candelabrum	M	8,10
227	Ceratium carriense	M	10
228	Ceratium compressum	M	
229	Ceratium declinatum	M	
230	Ceratium extensum	M	10
231	Ceratium gibberum	M	10
232	Ceratium hexacanthum	M	
233	Ceratium inflatum	M	
234	Ceratium karstenii	M	
235	Ceratium lamellicorne	M	
237	Ceratium massiliense	M	8,10
238	Ceratium minutum	M	
240	Ceratium pentagonum	M	10
241	Ceratium petersii	M	
242	Ceratium platycorne	M	10
243	Ceratium praelongum	M	10
244	Ceratium pulchellum	M	
245	Ceratium setaceum	M	
246	Ceratium teres	M	10
247	Ceratium trichoceros	M	24
248	Ceratium vultur	M	10
249	Ceratocorys spp.	M	10,20,23
250	Cladopyxis spp.	H	13
251	Dinophysis spp.	H	3,5,12,15,25,26
252	Exuviaella spp.	M	13
253	Gonyaulax spp.	M	15,16,34
254	Oxytoxum spp.	H	8,10,13
255	Protoperidinium spp.	H	9,21,22
257	Podolampas spp.	H	10,18,21,29
258	Pronoctiluca pelagica	H	1,10,13
259	Prorocentrum spp.	M	4,13,17,25,34,35
262	Ceratium falcatiforme	M	28
263	Ceratium longirostrum	M	

Table 2A.2: Trophic strategy (M=Mixotroph, H=Heterotroph) and associated references for CPR survey dinoflagellates.

benthic occurrence. Marine Ecology Progress Series, 256: 45-56.
2. Baek, S.H., Shimode, S., Kikuchi, T., 2007. Reproductive ecology of the dominant dinoflagellate, Ceratium fusus, in coastal area of Sagami Bay, Japan. Journal of Oceanography, 63: 35-45.
3. Berland, B.R., et al., 1995. Recent aspects of nutrition in the dinoflagellate Dinophysis cf. acuminate. Aquatic Microbial Ecology, 9: 191-198.
4. Bralewska, J.M., Witek, Z., 1995. Heterotrophic dinoflagellates in the ecosystem of the Gulf of Gdansk. Marine Ecology Progress Series, 117: 241-248.
5. Carvalho, W.F., Minnhagen, S., Graneli, E., 2008. Dinophysis norvegica (Dinophyceae), more a predator than a producer? Harmful Algae, 7: 174-183.
6. Druzhkov, N.V., Makarevich, P.R., Druzhkova, E.I., 2001. Phytoplankton in the south-western Kara Sea: composition and distribution. Polar Research, 20(1): 95-108.
7. Faust, M.A., 1998. Morphology and life cycle events in Pyrophacus steinii (schiller) wall et dale (dinophyceae). Journal of Phycology, 34:173-179.
8. Gomez, H., Raimbault, R., Souissa, S., 2007. Two high-nutrient low-chlorophyll phytoplankton assemblages: the tropical central Pacific and the offshore Peru-Chile Current. Biogeosciences, 4: 1101-1113.
9 Gribble, K.E., Anderson, D.M., 2006. Molecular phylogeny of the heterotrophic dinoflagellates Protoperidinium, Diplopsalis and Preperidinium (Dinophyceae), inferred from large subunit rDNA. Journal of Phycology, 42: 1081-1095.
10. Hallegraeff, G.M., Jeffrey, S.W., 1984. Tropical phytoplankton species and pigments of continental shelf waters of North and North-West Australia. Marine Ecology Progress Series, 20: 59-74.
11. Hansen, P.J., Nielsen, T.G., 1997. Mixotrophic feeding of Fragilidium subglobosum (Dinophyceae) on three species of Ceratium: effects of prey concentration, prey species and light intensity. Marine Ecology Progress Series, 147: 187-196.
12. Hansen, P.J., 1991. Dinophysis - a planktonic dinoflagellate genus which can act both as a prey and a predator of a ciliate. Marine Ecology Progress Series, 69: 201-204.
13. Hansen, P.J., 2011. Personal communication.
14. Jacobsen, D.M., Andersen, D.M., 1996. Widespread phagocytosis of ciliates and other protists by marine mixotrophic and heterotrophic thecate dinoflagellates. Journal of Phycology, 32: 279-285.
15. Jacobson, D.M., Andersen, R., 1994. The discovery of mixotrophy in photosynthetic species of Dinophysis (Dinophyceae): light and electron microscopal observations of food vacuoles in Dinophysis acuminata, D. norvegica, and two heterotrophic dinophysoid dinoflagellates. Phycologia, 33(2): 97-110.
16. Jeong, HJ, et al., 2005a. Feeding by red-tide dinoflagellates on the cyanobacterium Synechococcus. Aquatic Microbial Ecology, 41:131-143.
17. Jeong, H.J., et al., 2005b. Feeding by the mixotrophic red-tide dinoflagellate Gonyaulax polygramma: mechanisms, prey species, effects of prey concentration, and grazing impact. Aquatic Microbial Ecology, 38: 249-257.
18. Jeong, H.J., 1999. The ecological roles of heterotrophic dinoflagellates in marine planktonic community. Journal of Eukaryotic Microbiology, 46(4): 390-396.
19. Laatsch, T., et al., 2004. Plastid-derived single gene minicircles of the dinoflagellates Ceratium horridum are localized in the nucleus. Molecular Biology and Evolution, 21(7):1318-1322.
20. Latz, M.I., Lee, A.O., 1995. Spontaneous and simulated bioluminescence of the dinoflagellate Ceratocorys horrida (peridiniales). Journal of Phycology, 31(1): 120-132.

21. Latz, M.I., Jeong, H.J., 1996. Effect of red tide dinoflagellate diet and cannibalism on the bioluminescence of the heterotrophic dinoflagellates Protoperidinium spp. Marine Ecology Progress Series, 132: 275-285.
22. Lessard, E.J., Swift, E., 1985. Species-specific grazing rates of heterotrophic dinoflagellates in oceanic waters, measured with a dual-label radioisotope technique. Marine Biology, 87: 289-296.
23. Menden-Deuer, S., Lessard, E.J., 2000. Carbon to volume relationships for dinoflagellates, diatoms, and other protist plankton. Limnology and Oceanography, 45(3): 569-579.
24. Morton, S.L., 2000. Phytoplankton ecology and distribution at Manatee Cay, Pelican Cays, Belize. Atoll Research Bulletin, 472: 125-132.
25. Mouritsen, L.T., Richardson, K., 2003. Vertical microscale patchiness in nano- and microplankton distributions in a stratified estuary. Journal of Plankton Research, 25(7): 783-797.
26. Riisgaard, K., Hansen, P.J., 2009. Role of food uptake for photosynthesis, growth, and survival of the mixotrophic dinoflagellate Dinophysis acuminata. Marine Ecology Progress Series, 381: 51-62.
27. Rost, B., Richter, K.-W., Riebesell, U., Hansen, P.J., 2006. Inorganic carbon acquisition in red tide dinoflagellates. Plant, Cell and Environment, 29: 810-822.
28. Salomon, P.S., et al., 2009. Infection by Amoebophrya spp. parasitoids of dinoflagellates in a tropical marine coastal area. Aquatic Microbial Ecology, 55: 143-153.
29. Schweikert, M., Elbrachter, M., 2004. First ultrastructural investigations of the consortium between phototrophic eukaryotic endocytobiont and Podolampas bipes (Dinophyceae). Phycologia, 43(5): 614-623.
30. Skovgaard, A., Hansen, P.J., Stoecker, D.K., 2000. Physiology of the mixotrophic dinoflagellate Fragilidium subglobosum. I. Effects of phagotrophy and irradiance on photosynthesis and carbon content. Marine Ecology Progress Series, 201: 129-136.
31. Smalley, G.W., Coats, D.W., 2002. Ecology of the red-tide dinoflagellate Ceratium furca: Distribution, mixotrophy, and grazing impact on ciliate populations of Chesapeake Bay. Journal of Eukaryotic Microbiology, 49(1): 63-73.
32. Smalley, G.W., Coats, D.W., Stoecker, D.K., 2003. Feeding in the mixotrophic dinoflagellate Ceratium furca is influenced by intracellular nutrient concentrations. Marine Ecology Progress Series, 262: 137-151.
33. Stein, R., MacDonald, R.W., Eds. (2003) The Organic Carbon Cycle in the Arctic Ocean. Springer.
34. Stoecker, D.K., 1999. Mixotrophy among dinoflagellates. Journal of Eukaryotic Microbiology, 46(4): 397-401.
35. Stoecker, D.K., Tillman U., Granéli, E., 2006. Phagotrophy in harmful algae. Ecological Studies, 189:177-187.
36. Tarangkoon, W., Hansen, G., Hansen, P.J., 2010). Spatial distribution of symbiont-bearing dinoflagellates in the Indian Ocean in relation to oceanographic regimes. Aquatic Microbial Ecology, 58: 197-213.

2A.3 Latitudinal Variations in Ecological Patterns

Though the focus of this chapter has been the mean, basin-scale ecological patterns seen in the CPR survey, there are regional variations underlying these patterns that warrant mention here. Using the same methodologies as for the mean, basin-scale results presented

in the text above, we show a latitudinal breakdown of the same data presented in Figs. 2.3-2.4 and Fig. 2.7. The 41 CPR survey areas are distributed in roughly zonal bands, from "A" (farthest north) to "F" (farthest south; Fig. 2.1). These bands include both coastal (far eastern and western zones) and pelagic habitats, and span subpolar (north) to subtropical (south) gyre locations. Where possible, we comment on the mechanisms that may generate the latitudinal differences, but emphasize that these variations are the subject of ongoing research (see the Conclusion).

The seasonal succession from diatoms to dinoflagellates appears at all CPR survey latitudes, but the month of peak diatom and dinoflagellate abundance is typically later at higher latitudes (Fig. 2A.1). This effect is thought to be driven by latitudinal variations in light, temperature, and restratification (e.g., Colebrook, 1979; Taylor et al., 1993). The difference in timing between diatom and dinoflagellates peak abundance is generally about 2 months, though this varies somewhat with latitude. Additionally, the magnitude of diatom and dinoflagellate "blooms" increases from south to north, which is likely due to the greater seasonal availability of inorganic nutrients at higher latitudes (e.g., Taylor et al., 1993).

The seasonal succession from diatoms to mixotrophic and heterotrophic dinoflagellates (Fig. 2.4) also shows latitudinal variations (Fig. 2A.2). While the photoautotrophic peak (diatoms) precedes that of dinoflagellates at all latitudes, mixotrophic dinoflagellates precede heterotrophic dinoflagellates by up to two months at southern latitudes ("E" and "F" Areas), but not at all at higher latitudes (Areas "A"-"D"). We speculate that this increased temporal differentiation between heterotrophs and mixotrophs at lower, typically more nutrient-deplete latitudes could be linked to the hypothesis that mixotrophs have a competitive advantage over specialist grazers and photoautotrophs when resources are scarce (Ward et al., 2011b), though additional effort will be needed to confirm or reject this hypothesis.

When averaged over the basin, the mean size of the dominant diatom and dinoflagellate taxa (defined as those contributing 95% of total abundance) declines during summer months (Fig. 2.7). When viewed in zonal bands, however, the size shift at higher latitudes (Areas "A"-"C") is less pronounced when compared with lower latitudes (Areas "D"-"F"). Size-structured community modeling efforts (e.g., Ward et al., 2011a) with a global or basin-scale configuration will allow for greater understanding of the bottom-up and top-down ecological processes underlying these spatial variations in plankton size structure (see also the Conclusion).

Appendix References

Colebrook, J.M., 1979. Continuous Plankton Records: Seasonal cycles of phytoplankton and copepods in the North Atlantic Ocean and the North Sea. Marine Biology 51, 23-32.

Taylor, A.H., et al., 1993. Seasonal succession in the pelagic ecosystem of the North Atlantic and the utilization of nitrogen. Journal of Plankton Research 15(8), 875-891.

Ward, B.A., Dutkiewicz, S., Follows, M.J., 2011a. Size-structured food webs in the global ocean: theory, model, and observations. Submitted, Marine Ecology Progress Series.

Ward, B.A., et al., 2011b. Biophysical aspects of mixotrophic resource acquisition and competition. Accepted, The American Naturalist.

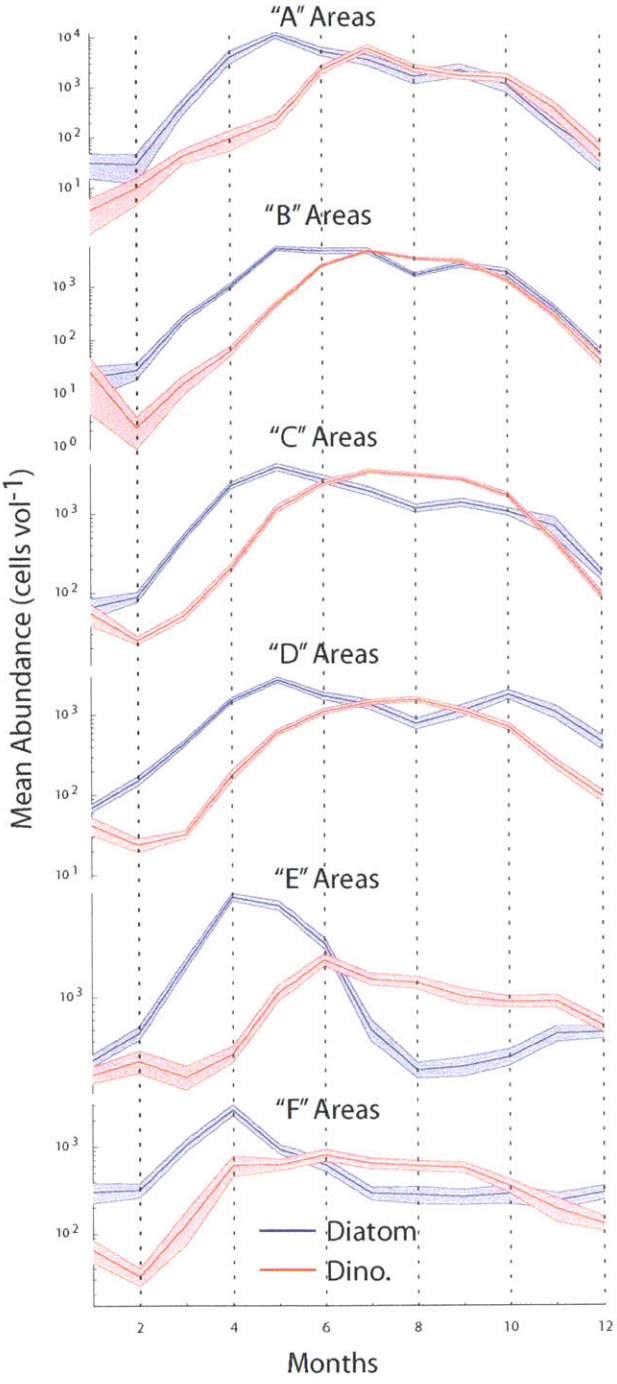

Figure 2A.1: Monthly mean abundance (cells vol^{-1}) for diatoms (blue) and dinoflagellates (red), averaged over all CPR survey areas within each latitude band, from "A" (farthest north) to "F" (farthest south). For a map showing locations of CPR survey areas, see Fig. 2.1. Only those taxa with detectable abundances in more than 6 months during the year are included (59 diatoms, 36 dinoflagellates). Shaded error bars indicate two standard errors ($\pm 2\sigma$).

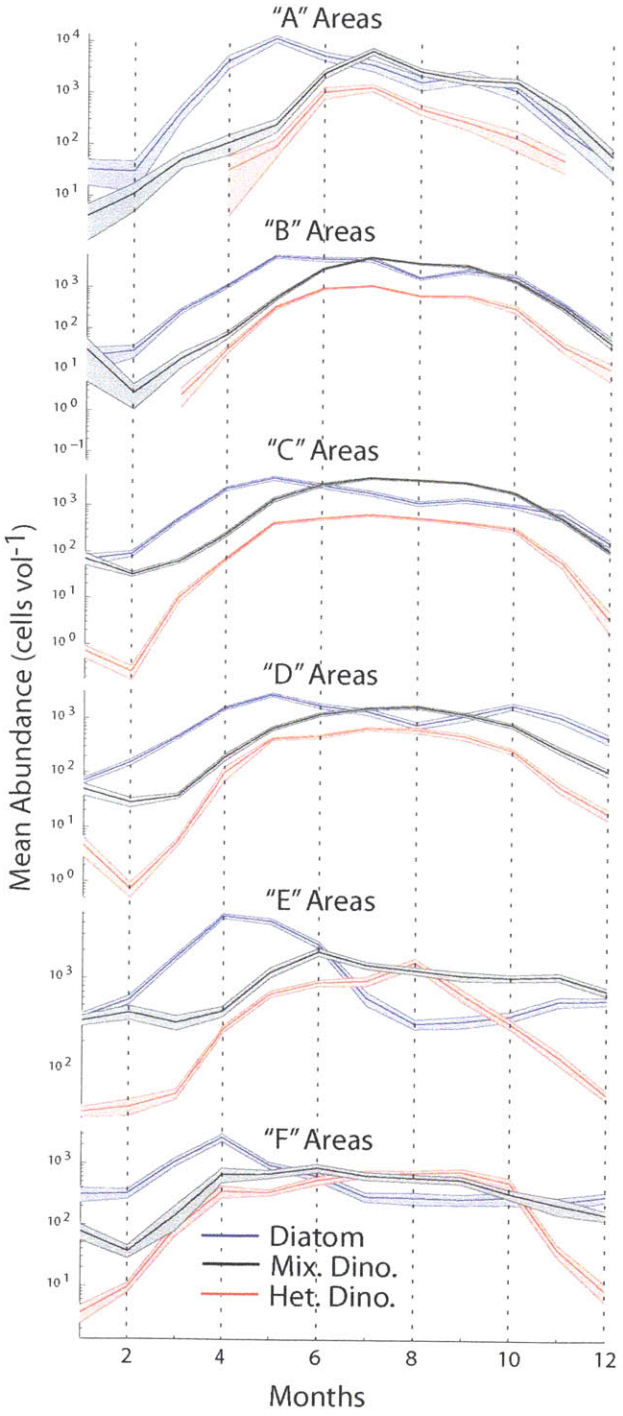

Figure 2A.2: Monthly mean abundance (cells vol^{-1}), averaged across all areas within each latitude band, years, and taxa within taxonomic groups, for photoautotrophic diatoms (blue) and heterotrophic (red) and mixotrophic (black) dinoflagellates. For a map showing locations of CPR survey areas, see Fig. 2.1. "A" areas are the farthest north and "F" the farthest south. Only those taxa with detectable abundances in more than 6 months during the year are included (59 diatoms, 32 mixotrophs, 4 heterotrophs). The shaded error bars indicate two standard errors ($\pm 2\sigma$).

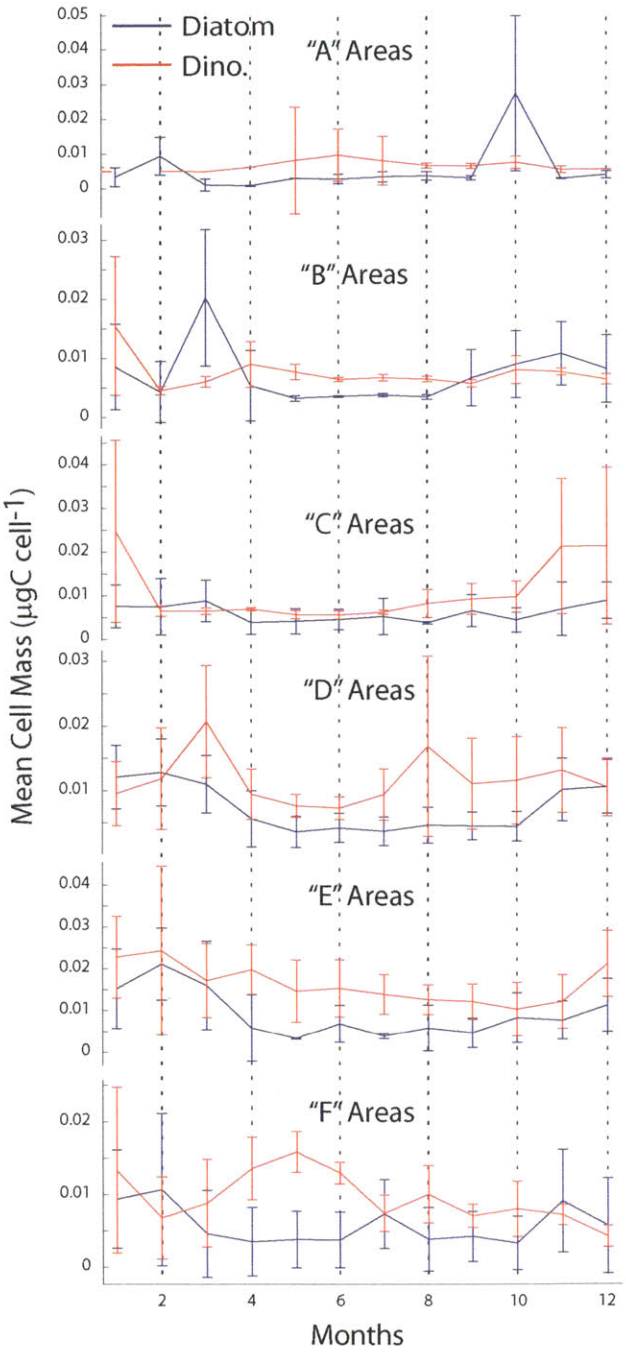

Figure 2A.3: Mean cell mass ($\mu gC\ cell^{-1}$) of diatom (blue) and dinoflagellate (red) taxa accounting for 95% of the cumulative abundance within each group and month within each latitude band of CPR survey areas. For a map showing locations of CPR survey areas, see Fig. 2.1. "A" areas are the farthest north and "F" the farthest south. Only those taxa with detectable abundances in more than 6 months during the year are included (59 diatoms, 36 dinoflagellates). Error bars indicate two standard errors ($\pm\ 2\sigma$).

Chapter 3

Patterns of Diversity in Marine Phytoplankton

The collaborative work in this chapter is based upon the following publication: *Barton, A.D., Dutkiewicz, S., Flierl, G., Bragg, J., Follows, M.J., 2010a. Patterns of diversity in marine phytoplankton. Science 327, 1509-1511.* The paper elicited a technical comment from Jef Huisman (*Huisman, J., 2010. Comment on "Patterns of diversity in marine phytoplankton." Science 329, 512-c*), which we responded to in the following reference: *Barton, A.D., Dutkiewicz, S., Flierl, G., Bragg, J., Follows, M.J., 2010b. Response to Comment on "Patterns of diversity in marine phytoplankton". Science 329, 512-d.* I only briefly describe the comment and our response here.

3.1 Summary

Spatial diversity gradients are a pervasive feature of life on Earth. We examined a global ocean circulation, biogeochemistry, and ecosystem model that indicated a decrease in phytoplankton diversity with increasing latitude, consistent with observations of many marine and terrestrial taxa. In the modeled subpolar oceans, strong seasonal variability of the environment led to the competitive exclusion of phytoplankton with slower growth rates and consequently to lower diversity. The relatively weak seasonality of the stable subtropical and tropical oceans in the global model enabled long exclusion timescales and prolonged coexistence of multiple phytoplankton with comparable fitness. Superimposed on this equator-to-pole diversity decrease were "hot spots" of enhanced diversity in some regions of energetic ocean circulation which reflected a strong influence of lateral dispersal.

3.2 Introduction

In both marine and terrestrial environments, many taxa exhibit a decline in species diversity with increasing latitude (Currie, 1991; Hillebrand, 2004), and this pattern has important implications for ecosystem structure and function (Ptacnik et al., 2008). The extent to which and why marine phytoplankton may follow such patterns is not yet clear, although it has been argued that the biogeography of microbes is governed by a similar set of processes as for macroorganisms (Hughes Martiny et al., 2006). There is some evidence of latitudinal diversity gradients among certain taxa of marine microbes, including bacterioplankton (Pommier et al., 2007; Fuhrman et al., 2008) and coccolithophorids (Honjo and Okada,

1974; Cermeño et al., 2008a), though the generality of these patterns, particularly in the open ocean, is, as yet, equivocal (Cermeño et al., 2008b).

In a recent study, a three-dimensional and time-varying global ocean circulation, biogeochemistry, and ecosystem model was initialized with a relatively large number (78) of virtual phytoplankton types whose traits were assigned stochastically from plausible ranges of possibilities (Follows et al., 2007; Dutkiewicz et al., 2009). Each phytoplankton type was represented by a prognostic equation which determines the rate of change due to light, nutrient and temperature dependent growth, grazing, sinking, non-specific mortality, and transport processes. In addition to the 78 phytoplankton types and 2 zooplankton classes, the global model explicitly represented spatiotemporal patterns of ocean circulation and mixing, the transport and biological transformations of inorganic and organic phosphorus, nitrogen, iron, and silica. The modeled phytoplankton communities "self assembled" according to the relative fitness of the phytoplankton types in the regionally and seasonally varying resource and predatory environment. The emergent phytoplankton populations captured the observed large-scale oceanic patterns in the distribution of phytoplankton biomass and community structure, including the observed niche differentiation among ecotypes of the cyanobacterium *Prochlorococcus* in the Atlantic Ocean (Follows et al., 2007).

3.3 Global Model Diversity

Here, we have studied an ensemble of 10 integrations of the global model, each member having a different, stochastically-seeded selection of phytoplankton types, to examine and interpret the emergent patterns of phytoplankton diversity. In each of the solutions, after a decade of integration, a dozen or so phytoplankton types account for more than 99% of the total global phytoplankton biomass. Others persist at low abundance or with limited geographic distribution, and some decline toward virtual extinction. Fast-growing "opportunist" phytoplankton tend to dominate the biomass of the variable high latitudes while "gleaners" (those best able to survive on minimal resources) dominate the stable, low latitude seas (Grover, 1990; Dutkiewicz et al., 2009). There is also a degree of local coexistence among phytoplankton types. On an annual, vertically-averaged basis, the phytoplankton diversity in the euphotic zone (here assumed to be 0-260m depth) is lower in the polar and subpolar oceans and higher in tropical and subtropical latitudes (Fig. 3.1A). This meridional gradient is clearly seen in the zonally averaged view (Fig. 3.1B) and is consistent with numerous observations of marine and terrestrial ecosystems (Currie, 1991; Hillebrand, 2004), including the sparse observations of marine microbial diversity (Honjo and Okada, 1974; Pommier et al., 2007; Cermeño et al., 2008a; Fuhrman et al., 2008). Superimposed on the model's meridional gradient are "hot spots" of highest diversity, which are generally associated with regions of energetic circulation such as the western boundary currents. The Atlantic Ocean "hot spots" appear to be consistent with observations of increased diatom diversity near to the North African and South American coasts (Cermeño et al., 2008a).

3.4 Explanations for Diversity Patterns

The mechanisms for maintaining the diversity of life on Earth have long interested ecologists (Hutchinson, 1959; Hutchinson, 1961), and the explanations for the meridional diversity gradient have been classified as historical, evolutionary, or ecological in nature (Mittelbach, 2007; Fuhrman et al., 2008). Historical explanations invoke events and changes in Earth

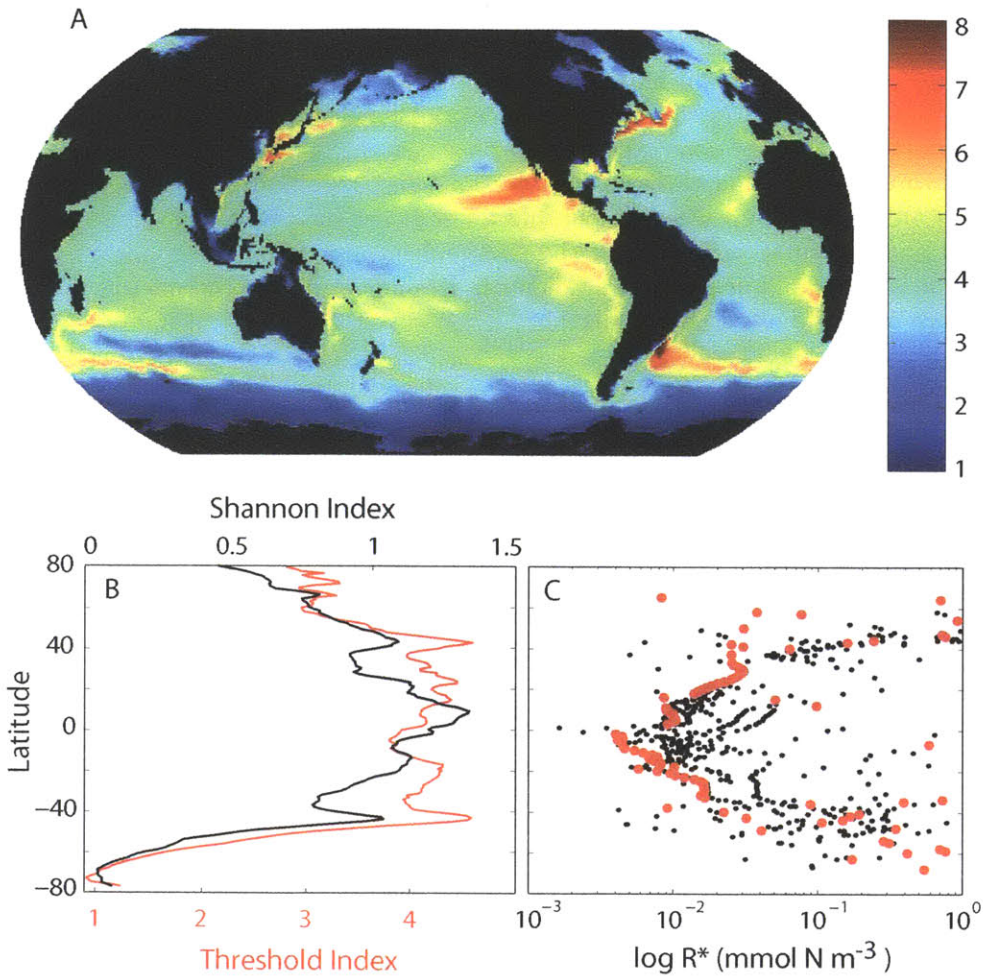

Figure 3.1: A) Diversity of modeled phytoplankton types in the uppermost 260 meters, averaged annually across ten ensemble members. Diversity is defined as the number of phytoplankton types comprising greater than 0.1% of the total biomass. (B) Zonal mean diversity, as well as the Shannon Index, for the map shown in (A). The Shannon Index (H) is calculated as $H = -\sum_j^n p_j ln p_j$, where p_j is the biomass of species j divided by the total biomass. (C) Annual mean R* (small black dots) of all phytoplankton types with a concentration above 10^{-12} mmolN m^{-3} along a meridional transect through the Atlantic Ocean at 20°W in an idealized global model with a single limiting nutrient (Dutkiewicz et al., 2009). The large red dots show the R* for only the most abundant type in each latitude.

history, such as Milankovitch cycles, in setting current species diversity. Evolutionary explanations examine the rates of speciation and extinction and their balance through time (MacArthur and Wilson, 1967; Allen et al., 2006). These processes are not resolved in this model, yet diversity gradients are still apparent. Thus we seek ecological explanations for the model diversity gradients, acknowledging that some real-world processes are not being considered. Niche differentiation, including seasonal succession, plays a role in determining the regional and seasonal habitats of phytoplankton types, adding to, but not fully explaining, the spatial diversity patterns. For example, when we consider one global model run, the total diversity present over the year is somewhat higher than the annual mean of instantaneous diversity due to seasonal succession (Fig. 3.2). However, large-scale diversity gradients are present even when accounting for seasonal succession. We hypothesize that dispersal and temporal variability of the environment are the most significant ecological controls on phytoplankton diversity gradients in this model, while other factors are of lesser importance or not resolved (Appendix 1).

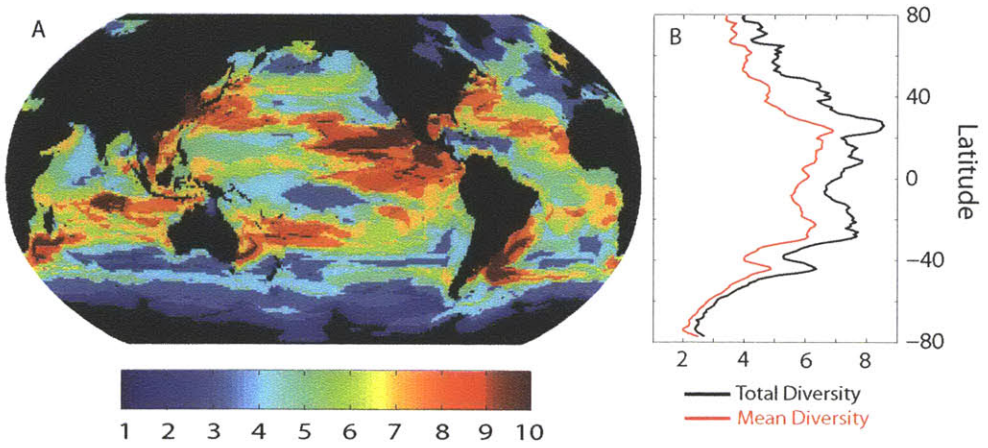

Figure 3.2: (A) Annual total diversity of modeled phytoplankton types in the uppermost 260 meters. The total diversity is defined here as the total number of phytoplankton types comprising greater than 0.1% of the total biomass at that location at any time during the year. (B) Zonal, annual mean diversity (red line; similar to Fig. 3.1B), as well as the zonal mean of total diversity (black line), for the map shown in (A).

3.5 Resource Competition Theory

Resource competition theory (Stewart and Levin, 1973; Tilman, 1981; Grover, 1990; Falkowski and Oliver, 2007; Dutkiewicz et al., 2009) provides a useful framework for illustrating the role of temporal variability in the global model. Consider an idealized system with a single limiting nutrient N (molN m^{-3}) which regulates the growth of phytoplankton, where P_j (molN m^{-3}) is the biomass of the j^{th} phytoplankton type. The rate of change of biomass is determined by the balance between growth and mortality. The rate of change of the nutrient is determined by consumption by phytoplankton and its environmental resupply,

$S_N(t)$ (molN m^{-3} s^{-1}):

$$\frac{dP_j}{dt} = \mu_j P_j \frac{N}{N + k_j} - m_j P_j \tag{3.1}$$

$$\frac{dN}{dt} = -\sum_j [\mu_j P_j \frac{N}{N + k_j}] + S_N(t) \tag{3.2}$$

Here μ_j (s^{-1}), m_j (s^{-1}), and k_j (molN m^{-3}) are the specific growth and mortality rates and half-saturation nutrient concentration for phytoplankton j, respectively. At equilibrium in this system, the phytoplankton type with the lowest environmental nutrient concentration at which the growth and mortality are in balance, also called R^*, is expected to outcompete other phytoplankton types over time (Tilman, 1981; Dutkiewicz et al., 2009):

$$R_j^* = \frac{m_j k_j}{\mu_j - m_j} \tag{3.3}$$

This limit is relevant to the subtropical oceans, which are characterized by a relatively weak seasonal cycle, and a strongly stratified, oligotrophic surface ocean. An emergent feature of the global model solutions was the coexistence of multiple physiologically distinct phytoplankton types with similarly low R^* in the tropical and subtropical regions (Fig. 3.1C, Dutkiewicz et al., 2009), at least for timescale of the model integrations. Since the R^* for each phytoplankton type depends upon imposed physiological characteristics and mortality, there are, in theory, many possible combinations which can achieve the same maximal fitness (lowest R^*). Moreover, the emergent, coexisting community of physiologically distinct but R^*-equivalent organisms is consistent with studies of laboratory populations of manipulated bacteria (Hansen and Hubbell, 1980) and the hypothesis that such a mechanism may be important in maintaining the diversity of marine phytoplankton (Falkowski and Oliver, 2007). This model outcome itself points to a possible explanation for enhanced phytoplankton diversity at lower latitudes and echoes the neutral theory of ecology and the hypothesis of ecological equivalence (Hubbell, 2001).

We analyzed the diversity dynamics within the idealized resource competition framework for the special case where all phytoplankton types have identical R^* (Appendix 2). In support of the emergent pattern in the global model, the idealized simulations indicate that the relatively steady environmental conditions in the tropical and subtropical oceans enable the prolonged coexistence of many phytoplankton with equivalent fitness (equal R^*), which results in enhanced diversity (Fig. 3.3A). However, the oceans are constantly perturbed by atmospheric forcing and internal physical phenomena across a vast range of spatial and temporal scales. Introducing a time-varying, periodic nutrient source to the idealized simulations eventually leads to competitive exclusion of all but the single phytoplankton type which grows fastest under optimal conditions (Fig. 3.3B; Appendix 2), even if the equivalence of R^* is imposed. The slower growing phytoplankton types need a higher time-averaged nutrient concentration to compete with the faster growers and are excluded over time (Appendix 3). Environmental variability creates a competitive structure such that the number of extant phytoplankton types can be reduced through competitive exclusion. Indeed, in the higher latitude, strongly seasonal marine environments where the global model solution exhibits lower diversity (Fig. 3.1), high growth rate and not low R^* is the most appropriate measure of organismal fitness (Dutkiewicz et al., 2009). It is worth noting here that the equilibrium biomass distribution among the discrete model species and the time taken until competitive exclusion is a function of how many species are initialized.

However, simple example here with five phytoplankton types is useful for interpreting the global model, which also has discrete phytoplankton types (78).

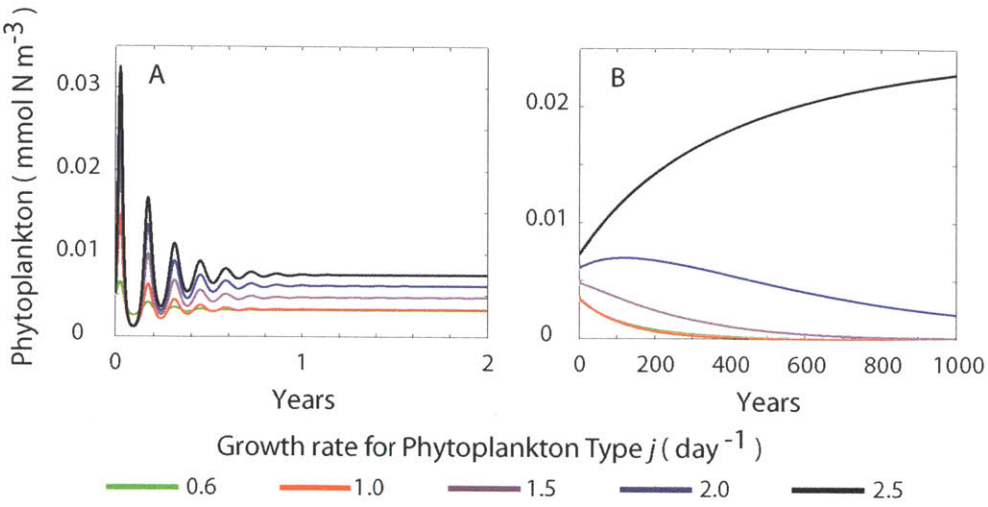

Figure 3.3: Abundances for five hypothetical phytoplankton types with a constant (A) and periodically varying (B) nutrient source ($\omega^{-1} = 365$ days and the amplitude is 0.5). Colors represent phytoplankton with different maximum growth rates (μ). Data in (B) were annually averaged.

3.6 Environmental Variability and Competitive Exclusion

Using the idealized experimental system, we investigated a range of natural frequencies and amplitudes of variability in nutrient supply, and defined the time taken until one phytoplankton type accounts for more than 90% of the total biomass as the timescale of competitive exclusion, or τ_{CE}. This timescale can exceed a thousand years when the environmental variability has either short (hours to days) or long (annual and longer) periodicity (Fig. 3.4). In contrast, when the environment varies with a period of months, competitive exclusion occurs within a few years or less. Large amplitude variations promote rapid exclusion, while small amplitude variations allow for extended coexistence (Appendix 4). Therefore, in the subtropical and tropical oceans, where seasonality is relatively weak, we expect the timescale of competitive exclusion to be long (centuries or more, which is long relative to the length of model integrations) for phytoplankton types with equivalent R^* (Fig. 3.3A). In contrast, the subpolar and polar oceans are subject to strong seasonal variations, including changes in the mixed layer depth which regulate light and nutrient availability. Here, opportunism is favored and the exclusionary pressure by the fastest growing phytoplankton on those with lesser growth rates rates is strong (Fig. 3.4). The exclusion timescale here may be as short as several years, and the long-term coexistence of many phytoplankton types is not sustained. Variability in growth rate, which is sensitive to changes in temperature and light, led to similar results (Appendix 2).

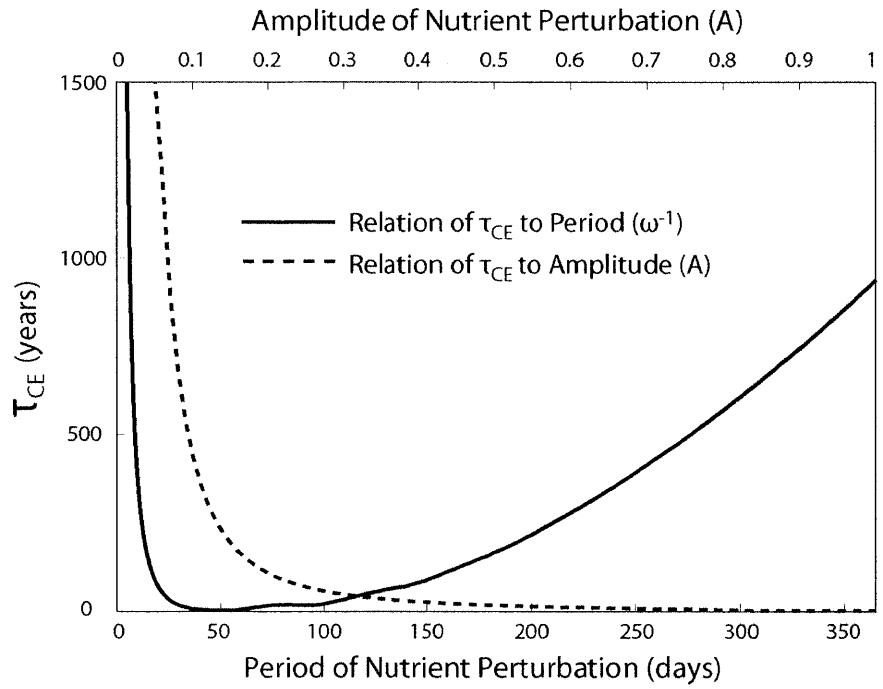

Figure 3.4: The relationship between exclusion timescale (τ_{CE}) and the period (ω^{-1}, solid line) and amplitude (A, dashed line) of the external nutrient source in the idealized model (Appendix 2). We considered a system to be in a state of competitive exclusion when one species comprises greater than 90% of the total biomass.

The timescale of competitive exclusion is set by the character of environmental variability, but local diversity in the global model is ultimately a balance between the removal of species via exclusion and the replenishment of phytoplankton types through physically-mediated dispersal (MacArthur and Wilson, 1967). Here we discuss what these characteristic timescales of dispersal might be in different ocean regimes. If we assume that the time rate of change of phytoplankton is due to dispersal over distance (x) by currents ($\mathbf{u}$), or $\frac{dP}{dt} = \mathbf{u}\frac{dP}{dx}$, we can estimate what the characteristic timescale of dispersal (τ_{disp}) over a distance of 1000km (typical length scale of ecosystem changes in global model) would be for different velocities: $\tau_{disp} \approx \frac{\Delta x}{u}$. In a swift boundary current (~ 1 m s^{-1}) or slow flow within a gyre ($\sim 10^{-2}$ m s^{-1}; Williams and Follows, 2011), τ_{disp} would be 10 days and 3 years, respectively. The rate of long-range dispersal of phytoplankton types between ocean gyres is even slower, taking decades to centuries (Martiny et al., 2009). Thus, in the high latitudes, exclusion is generally rapid relative to dispersal and intergyre exchange ($\tau_{CE} \leq \tau_{disp}$), and diversity is consequently lower. In the tropical and subtropical oceans, the exclusion timescale is typically long relative to the redistribution of phytoplankton by dispersal ($\tau_{CE} \gg \tau_{disp}$). Here, a higher diversity of similar R^* types can be maintained.

3.7 Phytoplankton Diversity "Hot spots"

In the "hot spots" of highest phytoplankton diversity, ocean dynamics, such as lateral advection and stirring due to planetary waves, mix organisms from different habitats. For example, the elevated diversity in the region of the Gulf Stream reflects the rapid polewards and eastwards advection of organisms adapted to tropical and subtropical environments, as has been observed (Cavender-Bares et al., 2001). As the boundary current transports away the subtropical communities and their environments, the transported waters are mixed and their phytoplankton intermingled with locally adapted organisms and eventually outcompeted. The exclusion timescale here is long relative to the advective timescale (see previous section) and the transported population contributes to the local total biomass and diversity (Fig. 3.1A). Similar processes may be responsible for the enhanced diversity in the tropical Eastern Pacific. In contrast, the energetic Antarctic Circumpolar Current region has low diversity because the near-zonal circumpolar flow acts as a barrier to, and not an agent of, communication between marine provinces. This can be understood by assuming that dispersal across this front is mediated by horizontal mixing in the ocean, or $\frac{dP}{dt} = \kappa\frac{d^2P}{dx^2}$, where κ is the horizontal diffusivity ($\kappa \approx 10^3$ m^2 s^{-1}; Williams and Follows, 2011). In this case, the dispersal timescale ($\tau_{disp} \approx \frac{\Delta x^2}{\kappa}$) would be approximately 30 years to mix phytoplankton over 1000km. However, the timescales of competitive exclusion at this latitude are quite rapid by comparison ($\tau_{CE} \ll \tau_{disp}$), and diversity is consequently low.

3.8 Conclusion

While the global model presented here is a simplified system, the emergent patterns of diversity show features generally consistent with the sparse observations of marine microbial diversity. The model's diversity patterns primarily reflect a balance between dispersal and competitive exclusion, with the latter modulated by environmental variability. Both neutral coexistence and niche differentiation play important roles in regulating the diversity and biogeographies of model phytoplankton (Leibold and McPeek, 2006). Such a modeling approach might be extended to explicitly reflect a broader spectrum of marine organisms,

such as heterotrophic microbes and zooplankton, and enable comparison with more observational data sets. The roles of other processes, including speciation and climate change, should also be explored. Further laboratory or mesocosm experiments might be designed to address the potential for coexistence of microbes with equal fitness. New, molecular approaches (Pommier et al., 2007; Fuhrman et al., 2008) will enable efficient, systematic surveys in the near future, and we suggest that a targeted survey of phytoplankton diversity (prokaryotes and eukaryotes), crossing from a subpolar regime, across a boundary current, dispersal-dominated region (the model "hot spots"), and into the interior of a subtropical gyre, could provide a valuable test of the hypothesized patterns and mechanisms which emerge from this study.

3.9 A Brief Summary of Huisman's Comment and Our Response

In his thoughtful comment, Huisman (2010) modeled the competition between two particular phytoplankton with small differences in R^*–one an opportunist (high μ) and the other a gleaner (low k)–and argued that environments of intermediate variability promote their coexistence, apparently contrasting our hypothesis that stability allows for greater diversity of equivalent competitors (equal R^*) in the ocean. Huisman also demonstrated, much as we had, that gleaners dominate in more stable environments and opportunists in more variable conditions.

The root of the difference in interpretation lies in the number of species considered and how their traits (here, μ, k, and m) may vary: in our initial paper (Barton et al., 2010a), we considered a diverse community with a broad range of traits, whereas Huisman considered just two competing species. In our response (Barton et al., 2010b), we developed an analysis that indicated what range of phytoplankton traits would be able to coexist under a given environmental variability, and compared this prediction to a physiologically possible trait space that was, in part, based upon the results from the global model simulations. Using this approach, we argued that our original interpretations of the mechanisms governing model diversity patterns remained valid and that Huisman's results were complementary to our hypotheses. In essence, Huisman's example was a special case of a broader problem that we addressed in Barton et al. (2010a; 2010b).

3.10 References

Allen, A.P., et al., 2006. Kinetic effects of temperature on rates of genetic divergence and speciation. Proceedings of the National Academy of Sciences 104(24), 9130-9135.

Barton, A.D., et al., 2010a. Patterns of diversity in marine phytoplankton. Science 327, 1509-1511.

Barton, A.D., et al., 2010b. Response to Comment on "Patterns of diversity in marine phytoplankton". Science 329, 512-d.

Cavender-Bares, K.K., et al., 2001. Nutrient gradients in the western North Atlantic Ocean: Relationship to microbial community structure and comparison to patterns in the Pacific Ocean. Deep-Sea Research I 48, 2373-2395.

Cermeño, P., et al., 2008a. The role of nutricline depth in regulating the ocean carbon cycle. Proceedings of the National Academy of Sciences 105(51), 20344-20349.

Cermeño, P., et al., 2008b. Resource levels, allometric scaling of population abundance, and marine phytoplankton diversity. Limnology and Oceanography 53(1), 312-318.

Currie, D.J., 1991. Energy and large-scale patterns of animal- and plant-species richness. American Naturalist 137(1), 27-49.

Dutkiewicz, S., Follows, M.J., Bragg, J.G., 2009. Modeling the coupling of ocean ecology and biogeochemistry. Global Biogeochemical Cycles 23, GB4017, doi:10.1029/2008GB003405.

Falkowski, P.G., Oliver, M.J., 2007. Mix and match: how climate selects phytoplankton. Nature Reviews Microbiology 5, 813-819.

Follows, M.J, et al., 2007. Emergent biogeography of microbial communities in a model ocean. Science 315, 1843-1846.

Fuhrman, J.A., et al., 2008. A latitudinal diversity gradient in planktonic marine bacteria. Proceedings of the National Academy of Sciences 105(22), 7774-7778.

Grover, J.P., 1990. Resource competition in a variable environment: Phytoplankton growing according to Monod's model. American Naturalist 136(6), 771-789.

Hansen, S.R., Hubbell, S.P., 1980. Single-nutrient microbial competition: Qualitative agreement between experimental and theoretical outcomes. Science 207, 1491-1493.

Hillebrand, H., 2004. On the generality of the latitudinal diversity gradient. The American Naturalist 163(2), 192-211.

Honjo, S., Okada, H., 1974. Community structure of Coccolithophores in the photic layer of the mid-Pacific. Micropaleontology 20, 209-230.

Hubbell, S.P., 2001. The unified neutral theory of biodiversity and biogeography. Princeton University Press, Princeton, New Jersey, USA.

Hughes Martiny, J.B., et al., 2006. Microbial biogeography: putting microorganisms on the map. Nature Reviews Microbiology 4, 102-112.

Huisman, J., 2010. Comment on "Patterns of diversity in marine phytoplankton." Science 329, 512-c.

Hutchinson, G.E., 1959. Homage to Santa Rosalia or Why are there so many kinds of animals? The American Naturalist 93(870), 145-159.

Hutchinson, G.E., 1961. The paradox of the plankton. American Naturalist 95, 137-145.

Leibold, M.A., McPeek, M.A., 2006. Coexistence of the niche and neutral perspectives in community ecology. Ecology 87(6), 1399-1410.

MacArthur, R.H., Wilson, E.O., 1967. The Theory of Island Biogeography, Princeton University Press, Princeton, NJ.

Martiny, A.C., et al., 2009. Taxonomic resolution, ecotypes and the biogeography of *Prochlorococcus*. Environmental Microbiology 11(4), 823-832.

Mittlebach, G.G., et al., 2007. Evolution and the latitudinal diversity gradient: speciation, extinction and biogeography. Ecology Letters 10, 315-331.

Pommier, T., et al., 2007. Global patterns of diversity and community structure in marine bacterioplankton. Molecular Ecology 16, 867-880.

Ptacnik, R., et al., 2008. Diversity predicts stability and resource use efficiency in natural phytoplankton communities. Proceedings of the National Academy of Sciences 105(13), 5134-5138.

Stewart, F.M., Levin, B.R., 1973. Partitioning of resources and the outcome of interspecific competition: A model and some general considerations. American Naturalist 107(954), 171-198.

Tilman, D., 1981. Tests of resource competition theory using four species of Lake Michigan algae. Ecology 62(3), 802-815.

Williams, R., Follows, M.J., 2011. Ocean Dynamics and the Carbon Cycle,Cambridge University Press, Cambridge, U.K.

3A Appendices

3A.1 Possible Explanations for Diversity Patterns

We analyzed the roles of temporal variability and dispersal in regulating phytoplankton diversity in the global model. Here, we discuss in greater detail a range of mechanisms that have been hypothesized for regulating diversity in other studies. A number of studies have focused on the environmental and biological correlates of diversity, including relationships with primary productivity (Irigoien et al., 2005) and energy or temperature (Currie, 1991). The relationship between biomass and diversity in the global model is not inconsistent with the "hump-shaped" pattern found by Irigoien et al. (2005), but it is unclear how this relationship would act as a causal mechanism in the global model. We borrow from Torsvik et al. (2002) in organizing other mechanisms considered, which include trophic interactions, spatial heterogeneity of habitats, internal oscillations and chaotic interactions among competing species, and the area and geometry of habitats.

First, top-down processes, or trophic interactions, have long been implicated in structuring ecosystems (Paine, 1966). For phytoplankton, zooplankton grazing (Armstrong, 1994) or viral infection (Fuhrman, 1999) may regulate abundances and influence species diversity. In the global model, top-down processes are represented explicitly. Two classes of zooplankton are resolved, each with a size-based preference for consumption of phytoplankton, which are classified into two broad size classes. We do not invoke prey-specific predation and use Holling II saturating functions to relate prey density and predation (Holling, 1965). These grazers provide only two "limiting factors" (Armstrong and McGeehee, 1980) and do not, as parameterized, play a central role in regulating the diversity patterns. Moreover, viral lysis is represented in a simple, linear mortality term. Thus, we do not invoke grazing or viral lysis as primary controls on the meridional diversity gradient in the global model. Second, spatial heterogeneity of habitats has been found to promote increased diversity (MacArthur and MacArthur, 1961). In the ocean, features such as mesoscale vortices may contribute to spatial heterogeneity and diversity (Bracco et al., 2000). However, the spatial resolution of the global model (1^o) is too coarse to resolve heterogeneity of habitats on the mesoscale. Third, internal oscillations and chaotic interactions among competing species can allow for higher diversity in certain circumstances (Huisman and Weissing, 1999). However, we do not find evidence of this in the global model solutions, possibly because the mixing between adjacent ocean areas dampens internal oscillations.

Finally, there are two hypotheses related to habitat geometry–both of which have the potential to make interpreting modeled spatial patterns of phytoplankton diversity difficult–that warrant additional discussion. The first is the mid-domain effect (Colwell and Hurtt, 1994; Colwell and Lees, 2000; Colwell et al., 2004), which states that for species ranges of random size that are randomly distributed in a bounded geographical range, there will be

the greatest number of species in the middle of the domain. There is considerable debate over the design, applicability, and interpretation of mid-domain null models (Zapata et al., 2003). However, because we attribute a mid-domain maximum in phytoplankton diversity to natural processes, we are compelled to argue why the mid-domain null model by itself does not explain the latitudinal gradients in species diversity shown in Fig. 3.1. We generated 1000 realizations of a hypothetical phytoplankton ecosystem along a meridional transect from 80°N to 80°S (note that this is the latitudinal extent of the global model), each with 78 species. Each species range size was chosen at random between a minimum of 0° and a maximum of 160° in extent. The midpoint of the range was placed randomly along the transect such that the range could not exceed the minimum and maximum latitudes. As shown in other studies (Colwell and Hurtt, 1994), the number of species is maximum at the equator (Fig. 3A.1). The dotted and dashed black lines show the maximum possible and mean range, respectively, for all species centered at a given latitude. A consequence of this null model is that the size of species ranges decreases with latitude. However, the biogeography of phytoplankton species in the global model do not generally show smaller ranges at higher latitudes (Dutkiewicz et al., 2007). This apparent contradiction of species range size between the mid-domain null model and the global model suggests that the mid-domain effect is not a primary driver of the equator-to-pole phytoplankton diversity gradient.

The second is the species-area relationship (Rosenzweig, 1995), which states that larger areas tend to have more species. In the case of latitudinal diversity gradients, the hypothesis implies that the greater area (of land or ocean) in the tropics allows for greater diversity. The amount of ocean area, when summed across zonal bands, peaks at lower latitudes (Fig. 3A.2). The same is true of the Atlantic and Pacific Ocean basins. The zonal mean phytoplankton diversity in the global model is also maximum at low latitudes (Fig. 3A.2), suggesting that there may be a role for the species-area relationship. However, we argue that ocean area is not a primary cause of the equator-to-pole phytoplankton diversity gradient for several reasons.

The zonal mean diversity gradient (Fig. 3A.2) is essentially an average of all the possible meridional transects in the global model. The model grid cells are internally homogeneous, so looking at model transect diversity data is size independent in the model context, even if the actual size of the model grid cells varies with latitude.

One primary mechanism linking species diversity to area is the range of habitats contained within the area (Huston, 1994). Generally, larger areas have a greater range of habitats and more species. Fig. 3A.2A shows the sum of ocean model grid cells at each latitude, which peaks in the Southern Ocean. Because this latitude has low phytoplankton diversity, it is unlikely that the number of grid cells plays a role in creating the diversity gradient. We also show that a greater range of habitats within a zonal band (here estimated by the zonal range in global model sea surface temperature) supports a larger number of phytoplankton types in that zonal band (Fig. 3A.2B). However, the range of habitats is more closely tied to ocean dynamics (note the mid-latitude peaks in the SST range associated with the presence of strong western boundary currents) than directly to ocean area (Fig. 3A.2B). In this context, we argue that the total phytoplankton diversity at a given latitude is more closely related to the range of habitats than to total ocean area. Note here that the total number of phytoplankton types within a zonal band is quite different from the mean number of phytoplankton types in each grid cell in a latitude band (Fig. 3.1B), but we suggest that the former shows the relative unimportance of the species-area relationship to marine phytoplankton diversity gradients in the global model.

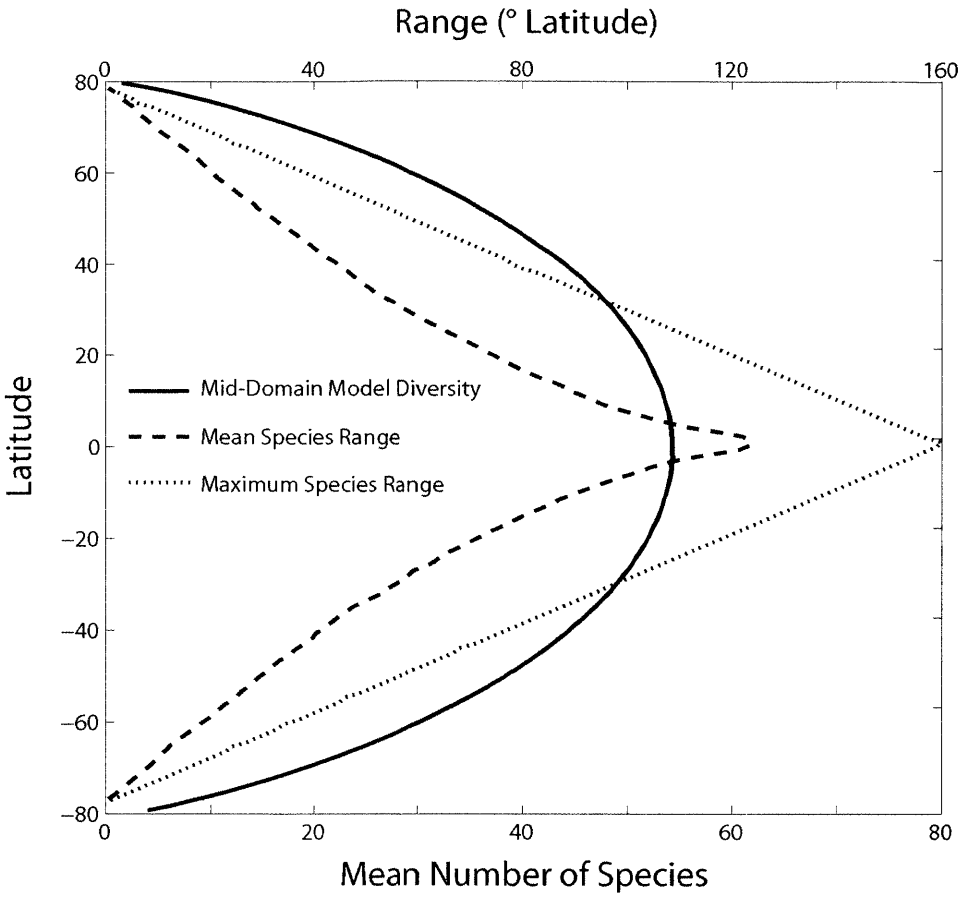

Figure 3A.1: Mean number of species present at each latitude (solid line) resulting from the mid-domain null model alone (averaged over the 1000 realizations). The dotted and dashed black lines show the maximum possible and mean range, respectively, for species with a range centered at a given latitude. The model domain is from 80°N to 80°S.

Lastly, the phytoplankton diversity in the Atlantic and Pacific basins are nearly identical, whereas the area in the Pacific Ocean is larger than the Atlantic Ocean (data not shown).

These arguments taken together suggest that the species-area relationship is not the primary driver of the meridional diversity gradients in the global ocean model.

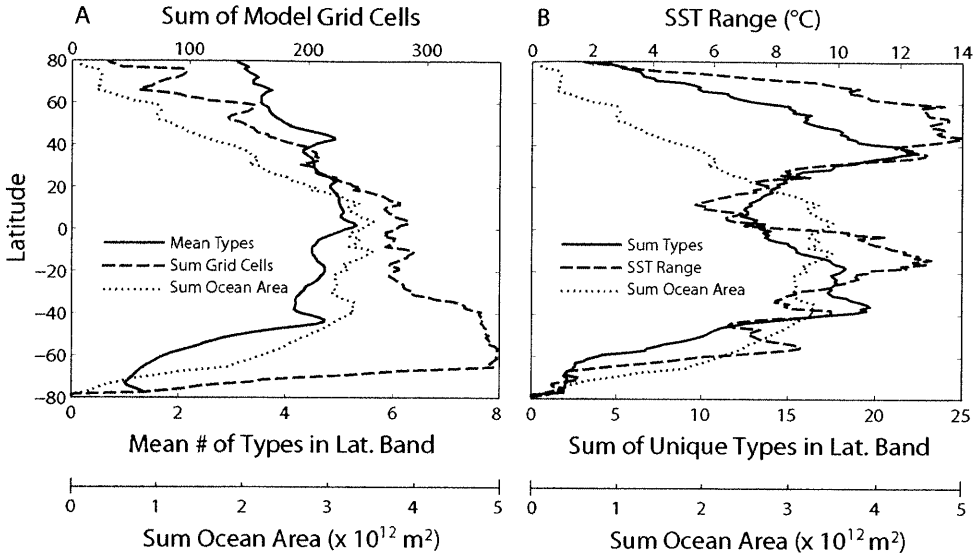

Figure 3A.2: (A) Zonal sum of ocean area (dotted line), zonal sum of model ocean grid cells (dashed line), and zonal mean diversity in the top 260 meters (solid line). (B) Zonal sum of ocean area (dotted line), zonal range of model sea surface temperature (SST; dashed line), and zonal sum of unique phytoplankton types occurring in the top 260 meters (solid line). The zonal range of SST is defined as $max(SST) - min(SST)$ within each latitude band.

3A.2 Numerical Experiments using Resource Competition Theory: Steady and Variable Cases

We have idealized the global model by invoking resource competition theory (Stewart and Levin, 1973; Tilman, 1981; Grover, 1990; Falkowski and Oliver, 2007; Dutkiewicz et al., 2009; Equations 3.1-3.3) and conducting numerical experiments under different characteristic environmental variabilities. Here, we describe the experiments in greater detail, and note that the governing equations are simpler than those used in the global model (Follows et al., 2007; Dutkiewicz et al., 2009). We examined the frequency and amplitude of the resupply of nutrients, or $S_N(t)$, relating the character of variability in $S_N(t)$ to particular ocean habitats and the attendant diversity of phytoplankton. One important difference between the resource competition and global model is that grazing is more realistic in the later (Follows et al., 2007; Dutkiewicz et al., 2009), whereas it is a simple, linear mortality term that is constant for all species in the former. In a steady environment with a single, limiting nutrient, the phytoplankton type with the lowest R^* is expected to outcompete other phytoplankton types over time (Tilman, 1981). Numerically integrating Equations 3.1 and 4.4 for an arbitrary number of phytoplankton types engineered to have identical R^*s but different growth rates and half-saturations (mortality is constant for all types), all

phytoplankton types can coexist (at least for the duration of model runs) in balance with a constant nutrient source, $S_N(t) = S_o$ (Fig. 3.3A). The relative abundance of the phytoplankton types with identical fitness depends on the growth rates and initial conditions, with the fastest grower being the most abundant. We allowed a typical subtropical North Atlantic August nitrogen concentration (0.25 mmolN m^{-3}) to be equivalent to R*. By fixing μ_j to a range from 0.6-2.5 day^{-1} and setting m_j to 0.5 day^{-1}, the half-saturation values, k_j, can be calculated directly from Equation 3.3. The number of phytoplankton types was set to 5, though this choice is arbitrary. We let the delivery of nutrients to the surface, or $S_N(t)$, be constant through time and equal to the consumption by phytoplankton. This form of $S_N(t)$ assumes a tight coupling between the delivery of nutrients and the growth of phytoplankton and is an idealization of subtropical ecosystems which are typically nutrient deplete.

Introducing a time-varying, periodic nutrient source, $S_N(t) = AS_o sin(\omega t) + S_o$, to the idealized system described by Equations 3.1 and 4.4 leads to competitive exclusion of all but the single phytoplankton type which grows fastest under optimal conditions (i.e., highest μ; Fig. 3.3B), even if the equivalence of R^* is imposed. In Fig. 3.3B, the parameters are as described above, and ω^{-1}=365 days and the amplitude A is 0.5.

To describe the dependence of the exclusion timescale on the period of environmental variability, we explored a range of natural periodicities, from a few hours to several years (Fig. 3.4). Similarly, varying A from 0 (steady case) to 1 showed that large amplitude variations promote rapid competitive exclusion, whereas small amplitude variations allow for a longer timescale of exclusion.

Moreover, the variability of other parameters in the system can produce qualitatively similar results. We discuss here an experiment where we allowed the specific growth rate, or μ, in Equations 3.1 and 4.4 to be a periodic function, $\mu_j = \overline{\mu_j} A sin(\omega t) + \overline{\mu_j}$, where A is the amplitude and $\overline{\mu_j}$ is the time-mean specific growth rate for phytoplankton j. This periodic form approximates the impact of changes in temperature, nutrients, and light on the growth rates of phytoplankton. We allow $S_N(t)$ to be constant, set R^* to be equal for all phytoplankton types, and keep all other parameters the same as in previous experiments. As with the experiments with a periodic $S_N(t)$, we find that larger amplitudes (A) and variability timescales of weeks to months in the growth rate led to competitive exclusion, while short (days to a week) and long (months to years) timescales of variability allow for coexistence. In the steady case, or $A = 0$, coexistence occurs.

3A.3 Competitive Exclusion and Growth Rates

Here, we discuss in detail why phytoplankton types with larger growth rates outcompete those with lesser growth rates in a variable environment.

Equation 3.1 can be written as:

$$\frac{1}{P_j}\frac{\partial P_j}{\partial t} = \mu_j \frac{N}{N + k_j} - m_j \equiv G_j \tag{3A.1}$$

where G_j can be considered a combined growth term the includes both cellular division and mortality. If $G_j > 0$, phytoplankton j becomes more abundant; if $G_j = 0$, there is no change to its population. At a steady state and for $N = R^*$, we have (rearranging Equation 3.3):

$$k_j = R^*(u_j - 1) \tag{3A.2}$$

where $u_j = \frac{\mu_j}{m}$. Note that we let mortality be constant across all species, as was done in the numerical experiments. If we substitute this expression for k_j into the expression for G_j, we find an expression for G_j in terms of m and u_j:

$$G_j = m(u_j - 1)\frac{N - R^*}{N + R^*(u_j - 1)} \tag{3A.3}$$

We now let the nutrient concentration vary periodically about a mean value:

$$N = N_o + N_1 sin(\omega t) \tag{3A.4}$$

This is a form similar to the way we idealized the nutrient source term, or $S_N(t)$. If we normalize by R^* such that $n_o = \frac{N_o}{R^*}$ and $n_1 = \frac{N_1}{R^*}$, Equation 3A.3 can be written as:

$$G_j = m(u_j - 1)\frac{n_o - n_1 sin(\omega t) - 1}{n_o - n_1 sin(\omega t) + u_j - 1} \tag{3A.5}$$

We are interested in how well each phytoplankton type survives, or their time averaged value of G_j relative to other types. Taking the time average of Equation 3A.5:

$$\langle G_j \rangle = m(u_j - 1)\left(1 - \frac{u_j}{\sqrt{(n_o + u_j - 1)^2 - n_1^2}}\right) \tag{3A.6}$$

In the steady case where $N = R^*$, $n_o = 1$ and $n_1 = 0$. This is analogous to the numerical example presented in Fig. 3.3A. In this case, $\langle G_j \rangle = 0$, meaning that all species can coexist together.

However, when $n_1 \neq 0$, the ambient nutrient concentration varies from R^*, and as we showed in Fig. 3.3B, the species with the highest growth rate excluded the others. We can calculate the mean concentration, or n_o, required for each species to survive by forcing $\langle G_j \rangle$ to be zero. This gives:

$$n_o = \sqrt{u_j^2 + n_1^2} - u_j + 1 \tag{3A.7}$$

This n_o term is an effective R^*, or the time averaged concentration of nutrient that a species with a particular u needs to coexist and survive in the variable environment represented by n_1. As with the numerical experiments for a varying nutrient source, we let $n_1 = 0.5$. In the case that u is large, n_o approaches 1, implying $N_o = R^*$. For small u, N_o is appreciably larger than R^*, meaning slower growing species would need higher time-averaged nutrient concentrations to coexist with faster growing species. Instead, as was shown in Fig. 3.3B, the slower growers are excluded over time by the faster growing phytoplankton. This analysis shows that environmental variability introduces an effective R^* (which is greater than R^*), and that this quantity decreases with increasing u. In other words, the largest u will outcompete all the others in a temporally varying system.

We note that by fixing R^* and allowing u_j to vary for phytoplankton types, we are analyzing one particular mechanism for achieving equivalent n_o and coexistence. While other combinations of parameters are technically possible, the global model results in lower latitudes indicated that the equivalence of R^* is an important constraint.

3A.4 Dependence of Timescale of Competitive Exclusion on Environmental Variability

Fig. 3.4 shows the dependence of the timescale of competitive exclusion (τ_{CE}) on the period of variability in nutrient supply. The shape of the curve can be explained in terms of the magnitude of departures in the ambient nutrient concentration from R^*. Larger magnitude departures from R^* allow for faster growing species to outcompete slower growing species. Here, we formalize this argument.

Equations 3.1 and 4.4 can be rewritten as:

$$\frac{\partial N}{\partial t} = -\sum_j [P_j g(s_j, N)] + S_N(t) \tag{3A.8}$$

$$\frac{1}{P_j}\frac{\partial P_j}{\partial t} = g(s_j, N) - m \tag{3A.9}$$

where mortality is constant for all species and the growth term for species j has been generalized as:

$$\frac{\mu_j N}{N + k_j} = g(s_j, N) \tag{3A.10}$$

The generalized $g(s_j, N)$ term implies that growth is a function of the nutrient concentration (N) and species-specific traits (μ and k). The nutrient source, $S_N(t)$, can be written as:

$$S_N(t) = S_o + \epsilon S_1(t) \tag{3A.11}$$

such that $S_N(t)$ is composed of a long-term mean source (S_o) and a smaller ($\epsilon \ll 1$) time-varying component ($S_1(t)$). The approximate solutions to N and P in Equations 3A.8 and 3A.9 can be written as:

$$N(t) \approx N_o + \epsilon N_1(t) \tag{3A.12}$$

$$P(t) \approx P_o + \epsilon P_1(t) \tag{3A.13}$$

where $N_o = R^*$. Additionally, we have dropped the species subnotation (j) from P for brevity. Rewriting Equations 3A.8 and 3A.9 in terms of the approximations for N and P gives:

$$\frac{\partial(N_o + \epsilon N_1)}{\partial t} = -\sum_j [(P_o + \epsilon P_1) g(s_j, N_o + \epsilon N_1)] + (S_0 + \epsilon S_1) \tag{3A.14}$$

$$\frac{1}{(P_o + \epsilon P_1)}\frac{\partial(P_o + \epsilon P_1)}{\partial t} = g(s_j, N_o + \epsilon N_1) - m \tag{3A.15}$$

where the time-dependent notation in P, N, and S (e.g., $P(t)$) has been dropped for brevity. Expanding each equation and equating terms of order 1 and ϵ, respectively, we find:

$$\frac{1}{P_o}\frac{\partial P_o}{\partial t} = g(s_j, N_o) - m \tag{3A.16}$$

$$\frac{\partial N_o}{\partial t} = -\sum_j P_o g(s_j, N_o) + S_o \tag{3A.17}$$

$$\frac{1}{P_o}\frac{\partial P_1}{\partial t} = N_1 g'(s_j, N_o) \tag{3A.18}$$

$$\frac{\partial N_1}{\partial t} = -\sum_j g'(s_j, N_o) N_1 P_o - \sum_j g(s_j, N_o) P_1 + S_1 \tag{3A.19}$$

where:

$$g'(s_j, N_o) = \frac{\partial g}{\partial N}(s_j, N_o) = \frac{\mu_j N_o}{(N_o + k_j)^2} \tag{3A.20}$$

and:

$$g(s_j, N_o) = g(s_j, R^*) = m \tag{3A.21}$$

Of interest is the dependence of N_1, or the departures in N from R*, on the timescale of environmental variation in S_1. Taking the time derivative of Equation 3A.19 gives:

$$\frac{\partial^2 N_1}{\partial t^2} + \frac{\partial N_1}{\partial t} I + mnI = \frac{\partial S_1}{\partial t} \tag{3A.22}$$

where:

$$I = \sum_j g'(s_j, N_o) P_o = \sum_j \frac{\mu_j N_o}{(N_o + k_j)^2} P_o \tag{3A.23}$$

If we allow the nutrient source to vary as $S_1 = Re[\hat{S} e^{i\omega t}]$, then N_1 has solutions in the form of $N_1 = Re[\hat{N} e^{i\omega t}]$. Substituting the solution for N_1 into Equation 3A.22 gives an expression for $\hat{N}$ in terms of ω:

$$\hat{N} = \frac{\hat{S} i\omega}{Im - \omega^2 + Ii\omega} \tag{3A.24}$$

the magnitude of which is:

$$|\hat{N}| = \frac{|\hat{S}||\omega|}{\sqrt{(Im - \omega^2)^2 + (I\omega)^2}} \tag{3A.25}$$

Equation 3A.25 describes the relationship between the frequency of environmental variability and the magnitude of departures from R*, or $|\hat{N}|$. Fig. 3.4 shows the relationship between the timescale of competitive exclusion and the period of nutrient source ($S_N(t)$) variability in the environment. In Fig. 3A.3, we plot the same Fig. 3.4, but now with $|\hat{N}|$ overlaid. For large departures in N from R*, fast growing species are able to outcompete the rest, leading more quickly to a state of competitive exclusion. The departure is greatest when the period of variability in the forcing is one to three months, coincident with the regime associated with rapid competitive exclusion (Fig. 3.4). At these frequencies, the balance between growth and loss is broken intermittently and opportunism (high μ) is favored. When experiencing high frequency variability (hours to days), the organisms integrate over the changes in resource resupply, effectively experiencing a time-averaged source. With lower frequency variability (annual or longer), the short-lived organisms essentially experience near-steady state conditions. In both limits, the ambient nutrient concentration, N, does not vary strongly from R^* and long-term coexistence is possible among phytoplankton with equivalent R^*.

3A.5 Appendix References

Armstrong, R.A., McGehee, R., 1980. Competitive Exclusion. American Naturalist 115(2), 151-170.

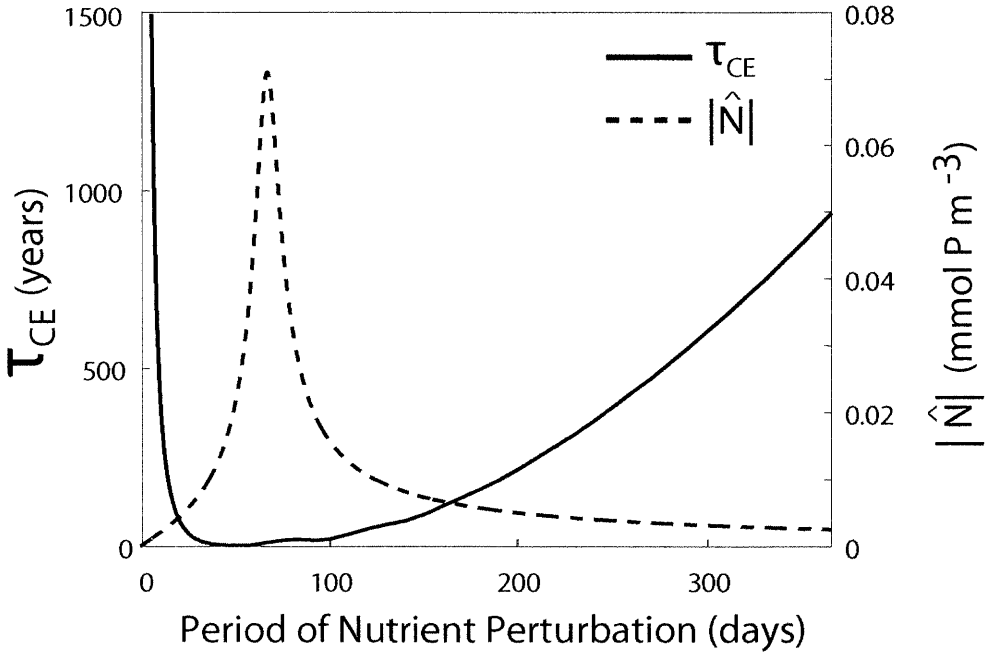

Figure 3A.3: The relationship between timescale of competitive exclusion (τ_{CE}, solid line) and period of nutrient variability. The magnitude of departures from R* ($|\hat{N}|$) are shown with a dashed line.

Armstrong, R.A., 1994. Grazing limitation and nutrient limitation in marine ecosystems: Steady state solutions of an ecosystem model with multiple food chains. Limnology and Oceanography 39(3), 597-608.

Bracco, A., et al., 2000. Mesoscale vortices and the paradox of the plankton. Proceedings of the Royal Society of London Biology, 267, 1795-1800.

Colwell, R.K., Hurtt, G.C., 1994. Nonbiological gradients in species richness and a spurious Rapoport effect. American Naturalist 144(4), 570-595.

Colwell, R.K., Lees, D.C., 2000. The mid-domain effect: geometric constraints on the geography of species richness. Trends in Ecology and Evolution 15(2), 70-76.

Colwell, R.K., et al., 2004. The mid-domain effect and species richness patterns: What have we learned so far? American Naturalist 163(3), E1-E23.

Currie, D.J., 1991. Energy and large-scale patterns of animal- and plant-species richness. American Naturalist 137(1), 27-49.

Dutkiewicz, S., Follows, M.J., Bragg, J.G., 2009. Modeling the coupling of ocean ecology and biogeochemistry. Global Biogeochemical Cycles 23, GB4017, doi:10.1029/2008GB003405.

Falkowski, P.G., Oliver, M.J., 2007. Mix and match: how climate selects phytoplankton. Nature Reviews Microbiology 5, 813-819.

Follows, M.J, et al., 2007. Emergent biogeography of microbial communities in a model ocean. Science 315, 1843-1846.

Fuhrman, J.A., 1999. Marine viruses and their biogeochemical and ecological effects. Nature 399, 541-548.

Grover, J.P., 1990. Resource competition in a variable environment: Phytoplankton growing according to Monod's model. American Naturalist 136(6), 771-789.

Holling, C.S., 1965. The functional response of predators to prey density and its role in mimicry and population regulation. Memoirs of the Entomological Society of Canada, 45.

Huisman, J., Weissing, R.J., 1999. Biodiversity of plankton by species oscillations and chaos. Nature 402, 407-410.

Huston, M.A., 1994. Biological Diversity: The Coexistence of Species on Changing Landscape, Cambridge University Press, Cambridge, UK, 708 pp.

Irigoien, X., Huisman, J., Harris R.P., 2004. Global biodiversity patterns of marine phytoplankton and zooplankton. Nature 429, 863-867.

MacArthur, R.H., MacArthur, J.W., 1961. On bird species diversity. Ecology 42(3), 594-598.

Paine, R.T., 1966. Food web complexity and species diversity. American Naturalist 100 (910), 65-75.

Rosenzweig, M.L., 1995. Species diversity in space and time. Cambridge University Press, Cambridge, UK, 436 pp.

Stewart, F.M., Levin, B.R., 1973. Partitioning of resources and the outcome of interspecific competition: A model and some general considerations. American Naturalist, 107(954), 171-198.

Tilman, D., 1981. Tests of resource competition theory using four species of Lake Michigan algae. Ecology 62(3), 802-815.

Torsvik, V., et al., 2002. Prokaryotic diversity-magnitude, dynamics, and controlling factors. Science 296, 1064-1066.

Zapata, F.A., et al., 2003. Mid-domain models of species richness gradients: assumptions, methods, and evidence. Journal of Animal Ecology 72, 677-690.

Chapter 4

The impact of turbulence on phytoplankton nutrient uptake rates and community structure

The collaborative work in this chapter is based upon the following publication in preparation: Barton, A.D., Ward, B.A., Follows, M.J., *in prep.* The impact of turbulence on phytoplankton nutrient uptake rates and community structure.

4.1 Summary

Fluid turbulence is thought to play an important role in structuring marine phytoplankton communities. We examine here the direct impact of small-scale fluid turbulence on nutrient uptake rates and community structure in an idealized community model where the traits describing each phytoplankton are constrained by their size. Turbulent flow distorts and erodes the diffusive boundary layers that often form around cells and therefore enhances the total flux of nutrients to the cell surface and subsequent nutrient uptake, and this effect is most pronounced for large cells in turbulent conditions. At high nutrient concentrations, however, nutrient uptake is limited not by flux of nutrients to the cell, but by the cell's inherent maximum rate of cross membrane transport. With grazing idealized as a linear loss term, we find that the smallest phytoplankton size outcompetes other, larger sizes, principally because of their ability to grow at lower nutrient concentrations than their larger competitors. In this case, the direct role of turbulence is minimal. With a non-linear, quadratic loss form of grazing, however, the extended coexistence of many model phytoplankton sizes was possible and turbulence played an important role in selecting the number of coexisting size classes and the dominant size class (in terms of biomass). We hypothesize that the positive impact of small-scale fluid turbulence on nutrient uptake in phytoplankton explains, in part, the persistence of large cells in the ocean. This effect may be most pronounced in relatively nutrient-deplete regions that experience episodic inputs of turbulent kinetic energy, such as the subtropical ocean or post-bloom conditions at higher latitudes.

4.2 Introduction

Relatively small (e.g., *Prochlorococcus*, picoeukaryotes) and motile phytoplankton (e.g., flagellates, dinoflagellates) typically dominate the strongly stratified, oligotrophic expanses of the global ocean, whereas larger phytoplankton (e.g., diatoms) are more conspicuous in weakly stratified, turbulent, and nutrient-rich conditions (Margalef, 1978; Cushing, 1989; Chisholm, 1992; Cullen et al., 2002; Kiørboe, 2008). This ecological differentiation between characteristic nutrient and turbulence regimes is evident in both the biogeography (Longhurst, 1995; Dutkiewicz et al., 2009) and seasonal succession of phytoplankton (Margalef, 1978), and has given rise to the hypothesis that turbulence plays a central role in structuring marine plankton communities (e.g., Margalef, 1978). Turbulence impacts phytoplankton through indirect and direct pathways, which we review here.

Turbulent mixing processes across a broad range of spatial and temporal scales play a crucial, but indirect role, in regulating phytoplankton populations by setting the background nutrient concentration that constrains phytoplankton population growth (Ferrari and Wunsch, 2009). Viewed from the perspective of a phytoplankton in the ocean surface, turbulent mixing tends to enhance nutrient concentrations by breaking down water column density stratification and mixing deep nutrients toward the surface, though turbulence and nutrients are not always correlated (Kiørboe, 1993). Phytoplankton of diverse size and taxonomy compete for these nutrients, with zooplankton grazing providing a top-down ecological control. To a large extent, turbulent mixing governs nutrient availability and therefore the structure of plankton communities. In oligotrophic regions, smaller cells dominate with respect to larger cells, principally because of their relatively high specific nutrient uptake rates (μmol N m^{-3} day^{-1}; Raven, 1998). In these conditions, motile microbes may also prosper by exploiting isolated nutrient patches (Seymour et al., 2009) or migrating vertically to seek out light, nutrients, or avoid predation (Klausmeier and Litchman, 2001). Here, the biomass of the small and motile cells tends to be tightly cropped by their relatively small, quickly growing predators (Hansen et al., 1994; Hansen et al., 1997). In relatively high nutrient conditions, large cells may become more abundant in both the steady state and transient dynamics. Using trait-based ecosystem models, both Armstrong (1994) and Ward et al. (2011b) predicted that in a steady state with high nutrients, both small and large cells may flourish because grazers keep small cells from outcompeting the larger cells (Armstrong, 1994; Ward et al., 2011b). When looking at a transient, or successional, response to a pulse of high nutrients, larger cells may bloom because their predators are larger and have slower response times, thereby opening a window in which large phytoplankton may become decoupled from top-down grazer control and become relatively more abundant than in resource-scarce conditions (Barber and Hiscock, 2006; Kiørboe, 2008). Turbulence plays an additional, indirect role by mediating the encounter rates of zooplankton predators and phytoplankton prey (Kiørboe, 1993; Kiørboe and Saiz, 1995).

Turbulent motion on the organism scale also impacts phytoplankton fitness in numerous other direct ways. The efficacy of motility and buoyancy strategies (Karp-Boss et al., 1996; Ruiz et al., 2004; Durham et al, 2009; Taylor et al., 2011), predator avoidance (Kiørboe, 2008), exposure to light (Kiørboe, 1993; Huisman et al., 2004; Taylor and Ferrari, 2011), and the uptake of nutrients are impacted by the small-scale turbulent motion (Karp-Boss et al., 1996; Metcalfe et al., 2004; Peters et al., 2006). Because competition for scarce resources, together with loss processes such as grazing, regulates phytoplankton community structure (Tilman, 1981; Dutkiewicz et al., 2009), here we focus on the direct impact of small-scale fluid turbulence on nutrient uptake rates, and how this can influence the community ecology

of competing phytoplankton. Though some have argued that this impact should be relatively unimportant when compared to other mechanisms, such as the size-dependence of specific nutrient uptake rates (Chisholm, 1992; Kiørboe, 2008), laboratory culture and modeling work suggest that this mechanism may indeed play a role in ecosystems, particularly for large cells (Mann and Lazier, 1996; Metcalfe et al., 2004; Peters et al., 2006). Thus, we ask under what levels of turbulence, and for what cell sizes, is the impact of turbulence on nutrient uptake rates important. And what impact, if any, might turbulent-driven nutrient uptake have on the biogeography and seasonal succession of phytoplankton?

To address these questions, we develop a size-structured phytoplankton community model where the organism traits are constrained by their cell size. The prescribed level of turbulence (turbulent kinetic energy dissipation rate, ϵ, $m^2\ s^{-3}$) determines the total flux of nutrients to the cell surface, which in turn impacts the realized uptake rates. The model considers spherical, non-motile photoautotrophs–possible analogs for important marine phytoplankton groups such as cyanobacteria, picoeukaryotes, coccolithophorids, and diatoms–but excludes motile species (flagellates, dinoflagellates) and other trophic strategies (mixotrophs, heterotrophs). We examine the impact of turbulence on community structure using simple linear and prey density-dependent, "quadratic" loss terms.

4.3 Turbulent and Phytoplankton Length Scales

Because it is not obvious why phytoplankton may be impacted by small-scale fluid turbulence, we first consider the length scales of the smallest turbulent motions and heterogeneities in the nutrient distribution in comparison to typical phytoplankton sizes. The schematics in Figs. 4.1-4.2 serve as a guide to the following discussion.

Energy imparted to the ocean by waves, wind, and tides is transfered from large to successively smaller eddies until ultimately it is dissipated by viscosity (Tennekes and Lumley, 1972). The dissipation rate of turbulent kinetic energy, or ϵ ($m^2\ s^{-3}$), is a commonly used measure of turbulence. In the ocean, ϵ varies rapidly in time and space by up to several orders of magnitude (MacKenzie and Leggett, 1993; Skyllingstad et al., 1999; D'Asaro et al., 2011), though certain regions are thought to have a characteristic range of values (Table 4.1). The length scale of the smallest eddies, or the transition point between inertial- and viscous-dominated regimes, is the Kolmogorov length scale, or η ($\eta = (\nu^3\epsilon^{-1})^{\frac{1}{4}}$), where ν is the kinematic viscosity of water ($\nu = 10^{-6}\ m^2\ s^{-1}$; Fig. 4.1). Larger values of ϵ generate smaller turbulent eddies. For the regimes considered in Table 4.1, η is approximately 300-10,000μm, which is larger than all but the very largest phytoplankton cells (Fig. 4.2). The diameter of diatoms, for example, varies from roughly $\sim 2 - 200\mu$m (Tomas et al., 1997), though aggregations of cells such as chains, colonies, and mats can be much larger (Villareal et al., 1993; Pahlow et al., 1997). The Kolmogorov length scale describes the smallest eddies, yet variations in the nutrient field occur below this length scale and are described by the Batchelor scale, or η_b ($= (\nu\kappa^2\epsilon^{-1})^{\frac{1}{4}}$ (Karp-Boss et al., 1996), where κ is the molecular diffusivity of the solute (e.g., $\kappa = 6.12\text{x}10^{-10}\ m^2\ s^{-1}$ for the phosphate ion). η_b is approximately 10-250μm, with higher turbulence driving heterogeneities on smaller scales (Table 4.1; Fig. 4.1). Here, there is significant overlap with much of the phytoplankton size spectrum (Fig. 4.2). Variations in the turbulent flow field (η) begin to affect the largest cells at high turbulence, and turbulence- and diffusion-driven variations in the nutrient field (η_b) affect a broad range of phytoplankton cell sizes. Thus, phytoplankton can "feel" turbulence in meaningful ways, and it is reasonable to further consider its impact on nutrient uptake.

Table 4.1: Characteristic values of turbulent kinetic energy dissipation rate (ϵ, $m^2\ s^{-3}$), the Kolmogorov length scale (η, μm), and the Batchelor length scale (η_b, μm) for differing ocean habitats. Adapted from Kiørboe and Saiz (1995).

Habitat	ϵ ($m^2\ s^{-3}$)	η (μm)	η_b (μm)
Open Ocean	$10^{-10} - 10^{-6}$	$1000 - 10000$	$25 - 247$
Shelf Seas	$10^{-7} - 10^{-6}$	$1000 - 1778$	$25 - 44$
Coastal Zones	$10^{-7} - 10^{-4}$	$316 - 1778$	$8 - 44$
Tidal Fronts	10^{-5}	562	14

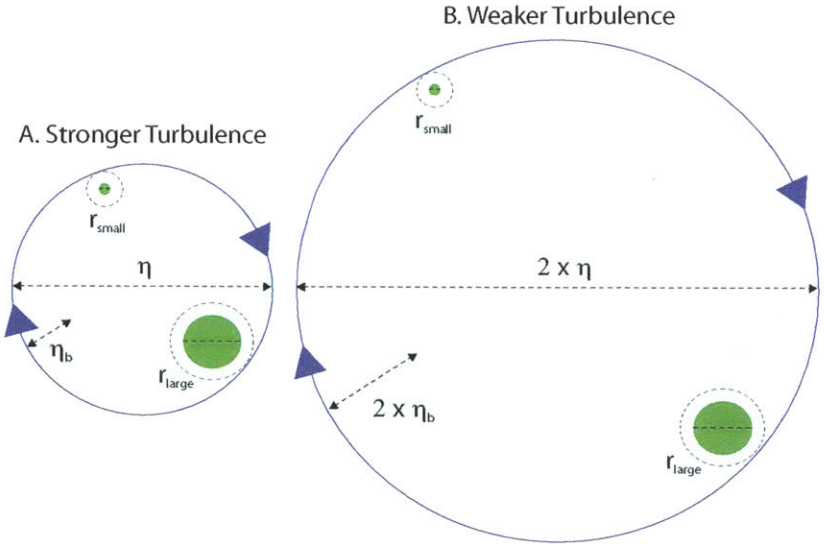

Figure 4.1: A large (r_{large}) and small (r_{small}) phytoplankton cell (green circles) embedded in a turbulent eddy (blue circle) of diameter A) η (stronger turbulence, higher ϵ) and B) 2η (weaker turbulence, lower ϵ). The length scale of nutrient patches (η_b) is smaller than η in both cases. Cells typically develop a nutrient depleted boundary layer around them (dashed circles). The relative motion between the cell and surrounding fluid enhances the flux of nutrients toward the cell by distorting the diffusive boundary layer around the cell, and this impact is more pronounced for larger cells in higher turbulence (Karp-Boss et al., 1996). Halving η and η_b is brought about by increasing ϵ by a factor of 16.

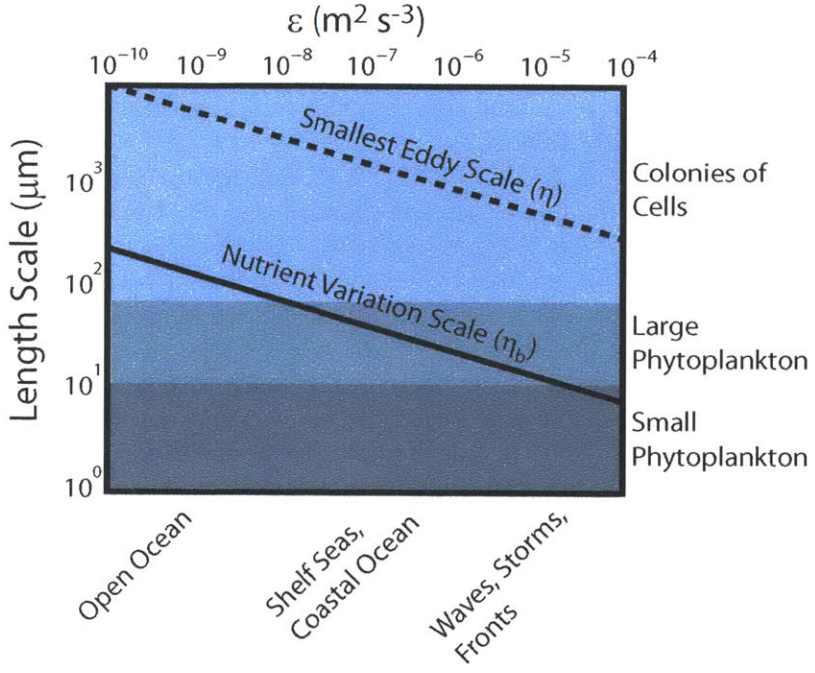

Figure 4.2: Kolmogorov (η) and Batchelor scales (η_b) for a range of turbulent kinetic energy dissipation rates (ϵ). As ϵ increases, both η and η_b decrease in size, and successively smaller phytoplankton are impacted by turbulent fluid motion and associated heterogeneities in the nutrient field.

4.4 Turbulence and Nutrient Uptake Rates

Here we describe a parameterization for the impact of small-scale turbulence on nutrient uptake in phytoplankton, a version of which has been previously used in algal growth models by Metcalfe et al. (2004) and Peters et al. (2006). Nutrient uptake (V, μmolN cell^{-1} day^{-1}) in phytoplankton is typically approximated as a Michaelis-Menten-like saturating function of nutrient concentration (N, μmolN m^{-3}), $V = V^{max}N(N+k)^{-1}$, where k (μmolN m^{-3}) is the half-saturation nutrient concentration and V^{max} (μmolN cell^{-1} day^{-1}) is the maximum uptake rate for a given cell (Pasciak and Gavis, 1974; Armstrong, 2008; Ward et al., 2011a; Fig. 4.3). With abundant nutrients ($N \gg k$), $V \approx V^{max}$. In this limit, it is the transport across the cell membrane that limits uptake. The number of nutrient handling sites per cell (n, cell^{-1}) and the time taken for each site to handle each μmol of nutrient (h, day μmolN^{-1}) is thought to define nutrient uptake ($V \approx V^{max} = (ah)^{-1}$; Aksnes and Egge, 1991). While there is evidence that V^{max} may vary in time through changes in transporter density (Aksnes et al., 2012), we assume here that this trait is fixed in time and scales with cell size (Litchman et al., 2007; Table 4.2).

In contrast, at low N ($N \ll k$), $V \approx V^{max}Nk^{-1}$, and uptake is not limited by cross-membrane transport but by the flux of nutrients toward the cell. Uptake increases linearly with N with a slope of the resource affinity, or α ($\alpha = V^{max}k^{-1}$; m^3 cell^{-1} day^{-1}). It is in this limit that turbulence plays a role by enhancing the flux of nutrients to the cell. At high nutrient levels, turbulence plays a limited role in uptake kinetics because the uptake saturates at V^{max}.

Thus, the parameterization for the impact of small-scale turbulence on uptake should modify the uptake at low resource concentrations by changing the apparent affinity (α). Because V^{max} is fixed and $k = V^{max}\alpha$, this impact is incorporated into k. If a cell takes up all nutrients arriving to its surface immediately, such that $N = 0$ at the cell surface, then $V = 4\pi r\kappa N$, where κ is the molecular diffusivity (m^2 s^{-1}; Berg and Purcell, 1977). In the presence of turbulent motion, the modified uptake rate is $V^T = 4\pi r\kappa ShN$, where Sh is the nondimensional Sherwood number, which is the ratio of the total flux of nutrients toward a sphere (diffusive plus turbulent fluxes) to the diffusive flux alone (Karp-Boss et al., 1996). We can incorporate the Sherwood number into a new, modified turbulent half-saturation constant k^T by noting that V^{max} is equal in still and turbulent conditions and that $N = k$ when $V = 0.5V^{max}$:

$$(4\pi r\kappa Shk^T)^{turb} = \frac{V^{max}}{2} = (4\pi r\kappa k)^{still} \tag{4.1}$$

Rearranging Eqn. 4.1, we can see that $k^T = kSh^{-1}$. In essence, turbulence increase resource affinity and allows cells to reach uptake saturation at lower resource concentrations (Metcalfe et al., 2004; Peters et al., 2006; Fig. 4.3).

We calculated Sh (and subsequently k^T) for range of cell radii and ϵ following Karp-Boss et al. (1996), who describe the analytical solutions for Sh as a function of the turbulent Péclet number, Pe. This is itself a function of cell radius (r), turbulent kinetic energy dissipation rate (ϵ), kinematic viscosity (ν), and molecular diffusivity (κ): $Pe = r^2\kappa^{-1}(\epsilon\nu^{-1})^{\frac{1}{2}}$. The Péclet number describes the relative importance of advective and diffusive processes to nutrient flux to the cell. In Fig. 4.4, we show Pe and Sh for a range of ϵ and cell radii. Pe, and consequently Sh, increases with cell size and ϵ, meaning the flux of nutrients due to turbulence is greater. For example, the total flux of nutrients to the surface of a 100 μm radius cell increases by a factor of three from a low to high turbulence environment (Fig. 4.4B). Based upon these calculations and as previously discussed by Mann and Lazier

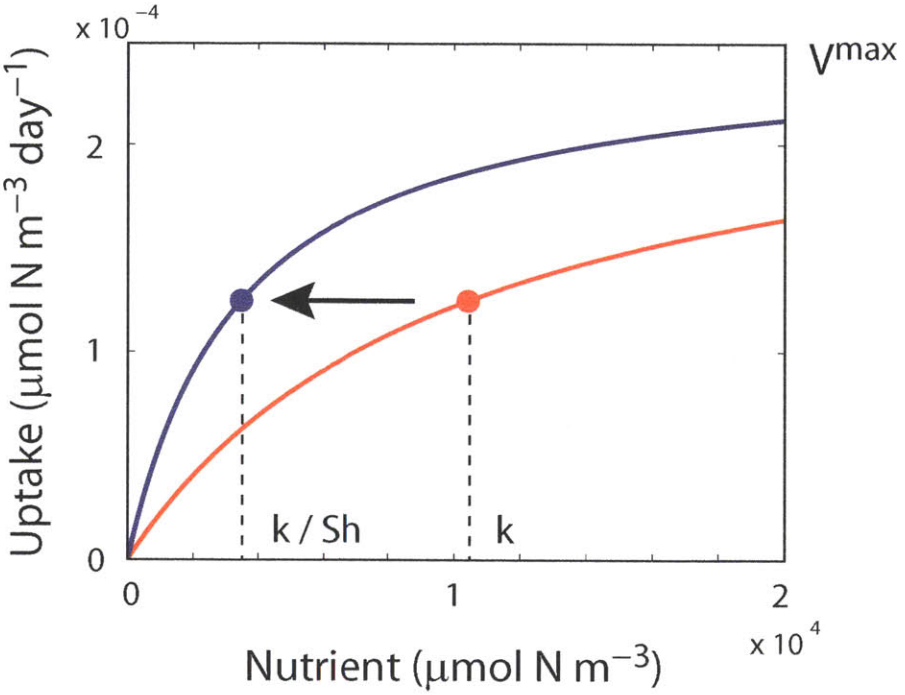

Figure 4.3: Nutrient uptake in turbulent (blue line) and quiescent (red line) conditions is a saturating function of nutrient concentration, $V = V^{max}N(N+k)^{-1}$. Turbulence decreases the half-saturation nutrient concentration (k) by kSh^{-1}. Maximum uptake rate (V^{max}) is unaffected by turbulence as this is a physiological property of the cell itself. Data are for a cell of 100 μm radius in turbulent conditions (ϵ=10^{-4} m^2 s^{-3}).

(1996), Karp-Boss et al. (1996), and others, the effect on nutrient uptake is greatest for large cells in turbulent conditions ($Sh > 1$), and negligible ($Sh \approx 1$) for small cells or in quiescent conditions.

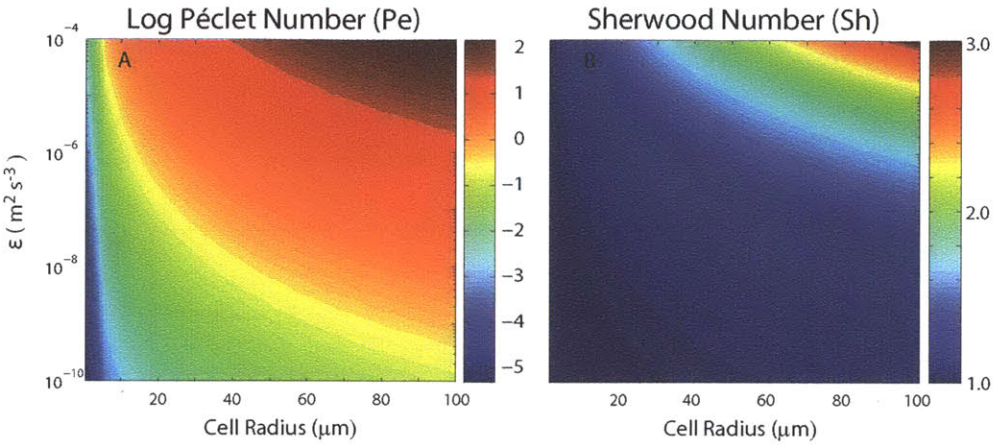

Figure 4.4: Péclet (A) and Sherwood (B) numbers for a range of cell radii (μm) and turbulence (ϵ, m^2 s^{-3}). The $\log_{10}$ of the Péclet (Pe) is shown. For $Pe > 1$, advective processes dominate, while for $Pe < 1$, diffusion dominates. Sh increases with cell size and turbulence, but is close to 1 for small cells or in quiescent environments. For $Pe \leq 0.01$, $Sh = 1 + 0.29Pe^{\frac{1}{2}}$; for $Pe \geq 100$, $Sh = 0.55Pe^{\frac{1}{3}}$; for $0.01 < Pe < 100$, Sh is the mean of $1.014 + 0.150Pe^{\frac{1}{2}}$ and $0.955 + 0.344Pe^{\frac{1}{3}}$ (Karp-Boss et al., 1996).

4.5 Phytoplankton Community Model

We now describe the inclusion of size- and turbulence-dependent traits in a size-structured community model with i phytoplankton types (X_i, cells m^{-3}) competing for one limiting nutrient (N, μmolN m^{-3}) in a chemostat. In all model simulations, we use 20 phytoplankton sizes, spaced evenly from 0.5-100μm in radius. As with previous chapters, we select discrete points in trait space to represent species rather than using a continuous distribution of traits representing all possible species (e.g., Bruggeman, 2009), and this methodology defines, in part, the equilibrium community structure. Unlike a Monod model of algal growth (Monod, 1950), in this quota-type or "internal stores" model (Droop, 1968), division is a function of internal nutrient quota (Q_i, μmolN cell^{-1}), not environmental concentration. Nutrient uptake (V_i, μmolN cell^{-1} day^{-1}) follows Michaelis-Menten kinetics, and the internal quota is depleted through cellular division (μ_i, day^{-1}). Cells die (m, day^{-1}) and are diluted (D, day^{-1}). The equations are:

$$\frac{dX_i}{dt} = \underbrace{\mu_i X_i}_{Division} - \underbrace{mX_i}_{Loss} - \underbrace{DX_i}_{Dilution} \tag{4.2}$$

Table 4.2: Model parameters and constants. Allometric traits scale with cell volume, or V.

Symbol	Parameter	Units	Value
N	Nutrient Concentration	μmolN m^{-3}	
X_i	Number Density	cells m^{-3}	
P_i	Biomass	μmolN m^{-3}	
Q_i	Internal Quota	μmolN cell^{-1}	
μ_i	Division Rate	day^{-1}	
μ_i^{max}	Maximum Division Rate	day^{-1}	$3.49V^{-0.15}$ *(a)*
V_i^{max}	Maximum Uptake Rate	μmolN cell^{-1} day^{-1}	$9.10\text{x}10^{-9}V^{0.67}$ *(b)*
Q_i^{min}	Minimum Internal Quota	μmolN cell^{-1}	$1.36\text{x}10^{-9}V^{0.77}$ *(b)*
k_i	Half-saturation Constant	μmolN m^{-3}	$0.17V^{0.27}$ *(b)*
k_i^T	Turbulent Half-saturation Constant	μmolN m^{-3}	$k(Sh)^{-1}$
α	Nutrient Affinity	m^3 cell^{-1} day^{-1}	$V_i^{max}(k_i^T)^{-1}$
D	Dilution Rate	day^{-1}	0.1
m	Phytoplankton Mortality	day^{-1}	0.1
m_z	Implicit Clearance Rate	m^3 cell^{-1} day^{-1}	$10^{-10} - 10^{-7}$
g_z	Zooplankton Clearance Rate	m^3 zoo^{-1} day^{-1}	$10^{-9} - 10^{-4}$ *(g)*
Z	Zooplankton Abundance	zoo m^{-3}	
γ	Proportionality Constant	zoo cells^{-1}	10^{-4}
N_o	Input Nutrient Concentration	μmolN m^{-3}	$8.0\text{x}10^3$
r	Cell Radius	μm	$0.5 - 100$
Sh	Sherwood Number	-	
Pe	Péclet Number	-	
ϵ	Turbulent Kinetic Energy Dissipation Rate	m^2 s^{-3}	$10^{-10} - 10^{-4}$ *(e,f)*
ν	Kinematic Viscosity of Water	m^2 s^{-1}	$1.004\text{x}10^{-6}$ *(c)*
κ	Molecular Diffusivity (Phosphate)	m^2 s^{-1}	$6.12\text{x}10^{-10}$ *(d)*

(a) Tang (1995), (b) Litchman et al. (2007), (c) Metcalfe et al. (2004), (d) Peters et al. (2006), (e) Schartau et al. (2003), (f) Kriest et al. (2010), (g) Hansen et al. (1997)

$$\frac{dQ_i}{dt} = \underbrace{V_i^{max}\frac{N}{N+k_i^T}}_{Uptake} - \underbrace{\mu_i Q_i}_{Division} \tag{4.3}$$

$$\frac{dN}{dt} = \underbrace{D(N_o - N)}_{Dilution} - \underbrace{\sum_i V_i^{max}\frac{N}{N+k_i^T}X_i}_{Uptake} \tag{4.4}$$

$$\mu_i = \mu_i^{max}(1 - \frac{Q_i^{min}}{Q_i}) \tag{4.5}$$

The turbulent half-saturation nutrient concentration, or k_i^T, depends on turbulence as described in Section 3, such that $k_i^T = k_i(Sh_{i,\epsilon})^{-1}$. The functional traits describing each model phytoplankton–maximum potential division rate (μ_i^{max}, day^{-1}), minimum internal nutrient quota (Q_i^{min}, μmolN cell^{-1}), maximum nutrient uptake rate (V_i^{max}, μmolN cell^{-1} day^{-1}), and the half-saturation nutrient concentration (k_i^T, μmolN m^{-3})–scale with cell volume: $x = bV^a$, where allometric coefficients a and b are taken from the literature and V is cell volume (Table 4.2). Nutrient input concentration (N_o, μmolN m^{-3}) is constant. Phytoplankton biomass (P_i, μmolN m^{-3}) is $X_i Q_i$. We implement the model in an idealized, zero-dimensional setting with constant dilution rate (D) and assume light does not limit growth. Turbulence and the supply of nutrients ($D(N_o - N)$) are not linked. See Table 4.2 for model parameters.

4.6 Competition with Linear Loss Form of Grazing

We ran the phytoplankton community model (Eqns. 4.2-4.5) with 20 size classes of phytoplankton at 20 different levels of ϵ (evenly log-spaced between $10^{-10} - 10^{-4}$ m^2 s^{-3}) for one year in each simulation, and found that the smallest phytoplankton class (r=0.5μm) dominates all other size classes at the end of one year for all ϵ (Fig. 4.5A). The abundance of larger cell sizes rapidly approaches zero, and they are effectively competitively excluded (defined here as $X_i < 1$ cell m^{-3}; Armstrong and McGehee, 1980). However, even in this case where all but the smallest cell size are rapidly excluded, increasing turbulence has a transient impact by enhancing the biomass of larger size classes in more turbulent conditions by as much as a factor of 50% or more (Fig. 4.5B). In effect, turbulence only delays the inevitable for larger cells. This effect is small in comparison with the massive difference in biomass between small and large cells after one year of model integration.

In order to demonstrate the differences in competitive ability for nutrients between differing size classes, we calculated R_i^* for each size class and turbulence level (Tilman, 1981; Irwin et al., 2006; Dutkiewicz et al., 2009; Ward et al., 2011a). R_i^* is the minimum, steady-state nutrient concentration at which growth and loss processes exactly balance were the species growing in isolation, and it is found by setting $\frac{d}{dt} = 0$ and solving Equations 4.2-4.5 for the steady state number density (X_i^*; the "*" denotes the steady state value), quota (Q_i^*), nutrient levels ($N_i^* = R_i^*$), and division rate (μ_i^*):

$$X_i(\mu_i - m - D) = 0 \Longrightarrow \mu_i^* = m + D \tag{4.6}$$

$$V_i^{max}\frac{N}{N+k_i^T} - \mu_i Q_i = 0 \Longrightarrow V_i^{max}\frac{R_i^*}{R_i^*+k_i^T} = \mu_i^* Q_i^* \tag{4.7}$$

$$D(N_o - N) - \sum_i V_i^{max} \frac{N}{N + k_i^T} X_i = 0 \Longrightarrow D(N_o - R_i^*) - V_i^{max} \frac{R_i^*}{R_i^* + k_i^T} X_i^* \tag{4.8}$$

$$\mu_i^* = \mu_i^{max}(1 - \frac{Q_i^{min}}{Q_i^*}) \tag{4.9}$$

Rearranging Equation 4.7 and 4.9, we solve for R_i^* and Q_i^*:

$$R_i^* = \frac{\mu_i^* Q_i^* k_i^T}{V_i^{max} - \mu_i^* Q_i^*} \tag{4.10}$$

$$Q_i^* = \frac{Q_i^{min} \mu_i^{max}}{\mu_i^{max} - \mu_i^*} \tag{4.11}$$

Combining Equations 4.10 and 4.11 we find R^*:

$$R_i^* = \frac{\mu_i^* \mu_i^{max} Q_i^* k_i^T}{V_i^{max}(\mu_i^{max} - \mu_i^*) - \mu_i^* \mu_i^{max} Q_i^*} \tag{4.12}$$

In Fig. 4.5C, we show the R^* for each cell size and ϵ, and find that the smallest phytoplankton have R^* values several orders of magnitude smaller than for the largest cells. This size structure in R^* originates from the allometric differentiation of phytoplankton traits (Q_i^{min}, k_i, V_i^{max}, and μ_i^{max}), and describes why the larger phytoplankton are excluded in model simulations (Fig. 4.5A). Simply put, larger cells need more nutrient to grow at the same rate as the smaller cells if all cells have equal mortality (m). For a given cell size, increasing turbulence lowers R^* by a factor of Sh^{-1}. This impact of turbulence is small in comparison to gross differences between large and small cells, and the larger cells are excluded as the system moves towards equilibrium. Much as others have argued previously (Chisholm, 1992; Kiørboe, 2008), the role of turbulence is negligible.

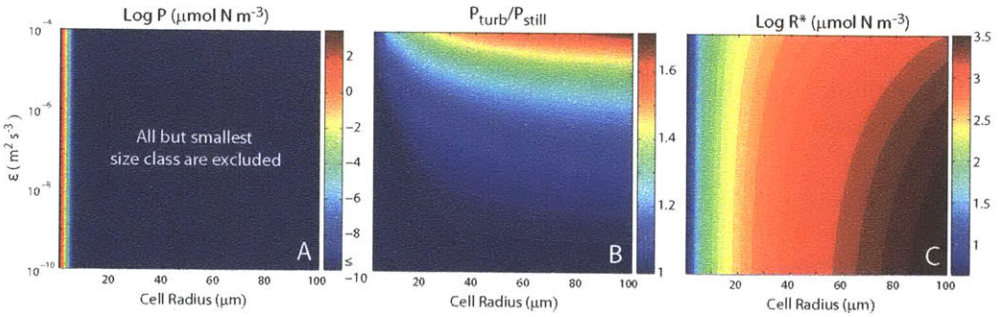

Figure 4.5: A) Log_{10} phytoplankton biomass (μmolN m^{-3}), B) the ratio of phytoplankton biomass in turbulent (ϵ) and still ($\epsilon = 10^{-10}$ m^2 s^{-3}) conditions, and C) the $\log_{10}$ of R^* (μmolN m^{-3}) for each size class and turbulence level. All but the smallest sized phytoplankton are rapidly outcompeted.

4.7 Competition with Quadratic Loss Form of Grazing

The numerical experiments in the previous section assumed a constant phytoplankton mortality rate (day^{-1}) for each size class and across a range of prey densities, such that the cell loss rate was $-mX_i$ (cells m^{-3} day^{-1}). While the prolonged coexistence of multiple size classes with size-dependent R^* is not possible with this form of loss (Fig. 4.5), numerous studies have shown that more realistic parameterizations of phytoplankton loss to zooplankton grazing enhance ecosystem stability and diversity (e.g., Vallina and LeQuéré, 2011). Here we implement one such idealized parameterization of zooplankton grazing, and assess the impact of turbulence on phytoplankton community structure in the presence of grazing.

Zooplankton grazing typically accounts for the majority of phytoplankton mortality (Calbet and Landry, 2004) and grazing rate, here defined as the number of phytoplankton consumed per zooplankton per time (phy zoo^{-1} day^{-1}), has been found to generally be a function of prey concentration (Holling, 1965; Gentleman et al., 2003). The grazing rate has also been called the specific ingestion rate (Hansen et al., 1997). Perhaps the simplest explicit grazing form is to assume that the grazing rate increases linearly with prey concentration X_i, such that Equation 4.6 becomes:

$$\frac{dX_i}{dt} = \mu_i X_i - DX_i - \overbrace{\underbrace{g_z X_i}_{Grazing} Z}^{Ingestion} \tag{4.13}$$

where Z is zooplankton abundance (zoo m^{-3}) and g_z (m^3 zoo^{-1} day^{-1}) is the zooplankton clearance rate. This form, also called the Holling type I functional response (Gentleman et al., 2003), allows grazing rates to increase with prey density, but does not saturate at high prey densities as might be expected (Hansen et al., 1997; Jeschke et al., 2004). Experiments have shown that the grazing rates of filter feeders, and possibly zooplankton employing other grazing strategies, can be approximated by this form (Mullin et al., 1975; Jeschke et al., 2004).

Here, for simplicity, we do not explicitly represent zooplankton, but assume that zooplankton and phytoplankton abundance are linked by a proportional constant γ (zoo cells^{-1}), such that $Z = \gamma X_i$. This form assumes also that each prey has its own predator whose abundance is determined by γ and X_i. This simplification allows us to represent grazing implicitly as follows:

$$\frac{dX_i}{dt} = \mu_i X_i - DX_i - m_z X_i X_i \tag{4.14}$$

where $m_z = g_z \gamma$ (m^3 cells^{-1} day^{-1}). This implicit grazing form, also called quadratic loss, has been used to represent grazing, losses to viral lysis, and density dependent self-limitation (Schartau and Oschlies, 2003; Kriest et al., 2010). These same studies give clearance rate values (m_z) of 10^{-9} and 10^{-8} m^3 cells^{-1} day^{-1}, respectively.

Next, we estimate γ and develop an independent calculation for m_z. If we assume that zooplankton predators are on average, 10 times larger in equivalent spherical diameter (ESD) than their phytoplankton prey (Hansen et al., 1994), we can evaluate the anticipated relative abundance of zooplankton and phytoplankton by using the allometric relationship between body volume (V, μm^3) and abundance (A, ind ml^{-1}), $A = bV^a$, where a is approximately equal to -1 and b is a constant (Finkel, 2007). Using this approach, $\gamma = \frac{A_z}{A_p} = \frac{V_p}{V_z} = \frac{1}{10^3}$, and $\gamma \approx 10^{-3}$. In other words, there are roughly 10^3 prey for

each predator. Hansen et al. (1997) report zooplankton maximum clearance rates (g_z, m^3 zoo^{-1} day^{-1}) of roughly $10^{-9} - 10^{-4}$, and recalling that $g_z = m_z\gamma$, we estimate that m_z should range from $10^{-12} - 10^{-7}$, which overlaps with the estimates of Schartau and Oschlies (2003) and Kriest et al. (2010). Considering this analysis, we consider a range of m_z, from $10^{-10} - 10^{-7}$, in the following experiments. The smallest value of m_z we consider is 10^{-10} because below that the results are essentially the same as for the linear loss case because the grazing loss approaches zero and the only loss is the constant dilution rate (Fig. 4.5).

In Fig. 4.6, we show a schematic comparing the quadratic loss form with the constant grazing pressure used in Fig. 4.5. At low prey concentrations, the linear loss term (cells m^{-3} day^{-1}) is greater than the quadratic loss term ($mX_i > m_z X_i X_i$). At high abundance, as is expected for small size classes, the quadratic loss exceeds the linear loss ($mX_i < m_z X_i X_i$). In essence, this parameterization of zooplankton grazing focuses predation upon the smaller, more abundant cells, thereby allowing the rarer, larger cells to become relatively more abundant than in the linear loss case.

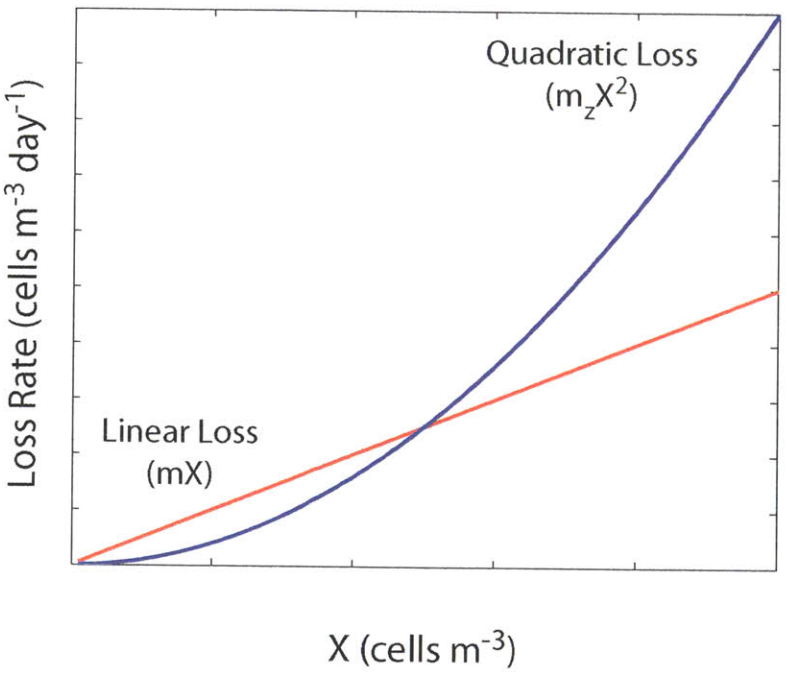

Figure 4.6: Schematic of linear (red line) and quadratic (blue line) loss rates indicating that at low concentrations, linear loss exceeds quadratic loss. The quadratic loss, in essence, allows less abundant, larger cells to compete with smaller, more abundant cells.

Using the same size classes, levels of turbulence, and allometrically-constrained traits as in the previous section, we integrate Equations 4.3-4.5 and 4.14 for 100 years, and show the equilibrium phytoplankton biomass in Fig. 4.7 for a range of clearance rates, or m_z. With relatively weak grazing pressure ($m_z = 10^{-10}$ m^3 $cell^{-1}$ day^{-1}; Fig. 4.7A), the smallest size classes dominate in terms of biomass, though unlike the experiment with linear loss (Fig. 4.5), several size classes may coexist (the white shaded areas indicate those size classes that are competitively excluded, or $X_i < 1$ cell m^{-3}). The dashed black line indicates the cell

size with the highest biomass at each level of turbulence. As grazing pressure increases (Fig. 4.7B,C), additional, larger size classes are able to coexist with the smaller cell sizes, and the impact of turbulence on equilibrium ecosystem structure becomes more apparent. For instance, in Fig. 4.7C, a change in ϵ from 10^{-10} to 10^{-4} enables even the largest cell sizes to coexist and causes the radius of the dominant phytoplankton (in terms of biomass) to be $\sim 20\mu$m larger. With the highest grazing pressure (Fig. 4.7D), all size classes coexist, and the largest cell size has the highest biomass at each level of turbulence.

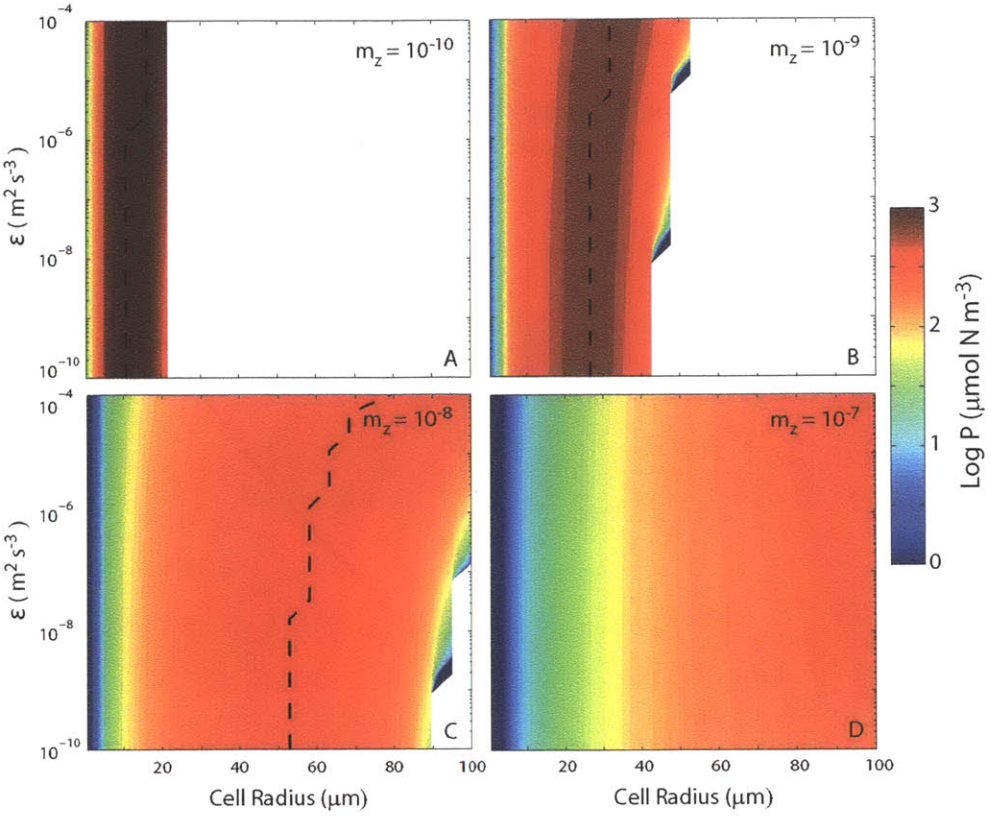

Figure 4.7: Equilibrium $\log_{10}$ phytoplankton biomass (μmolN m^{-3}) for each size class and turbulence level for a range of clearance rates, from lowest to highest (m^3 cells^{-1} day^{-1}): A) $m_z = 10^{-10}$, B) $m_z = 10^{-9}$, C) $m_z = 10^{-8}$, and D) $m_z = 10^{-7}$. White areas indicate competitively excluded sizes ($X_i < 1$ cell m^{-3}). The dashed black line indicates the radius of the cell with the highest biomass (located along the far right hand margin in D).

We can understand these equilibrium community structures by again considering the R^* for each size class at each level of turbulence. Much as was done by Dutkiewicz et al. (2009), we calculated a numerical, diagnostic R^* by substituting equilibrium (that is, after 100 years of integration) values for Q_i^*, X_i^*, and μ_i^* into Eqn. 4.12. Here, $\mu_i^* = D + m_z X_i^*$. We present the results in Fig. 4.8. For a given ϵ, all those size classes with the minimum R^* coexist, whereas those with higher R^* are excluded (Fig. 4.7). In Fig. 4.8D, all species can coexist because they all have equivalent, effective R^*, whereas at lower clearance rates (Fig. 4.8A-C), successively more larger size classes are excluded. In essence, grazing pressure modifies

the competitive structure, as indicated by R^*, and allows for increased coexistence. The R^* of coexisting sizes also increases with grazing pressure.

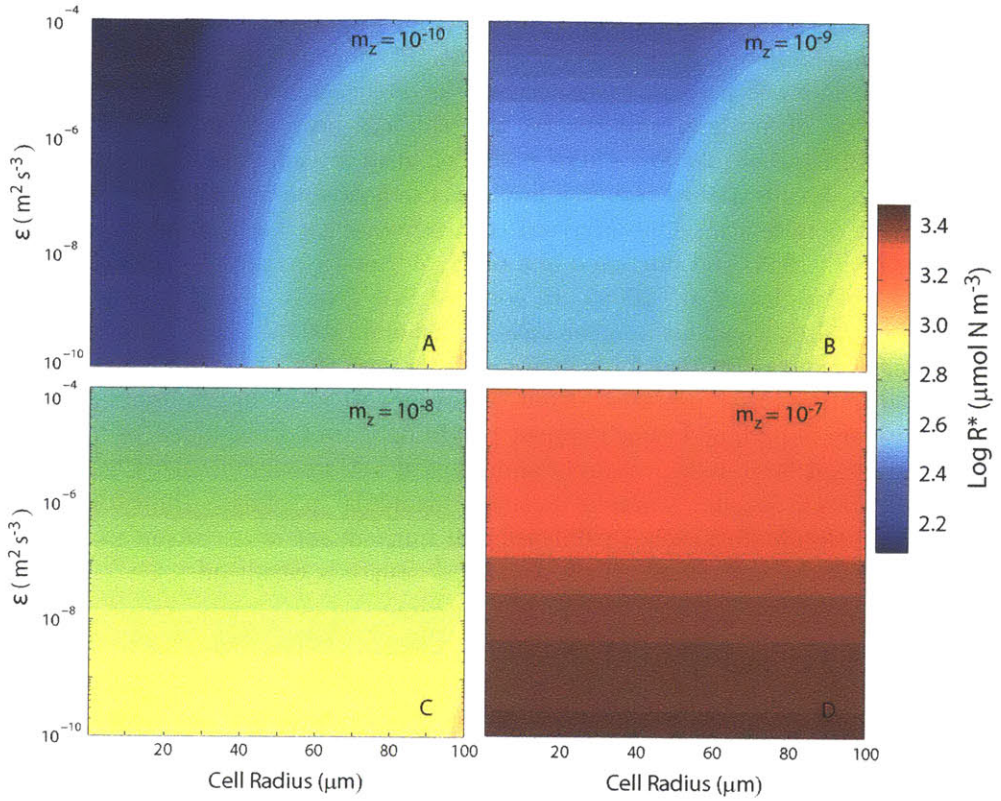

Figure 4.8: Log_{10} R^* (μmolN m^{-3}) for each size class and turbulence level for a range of clearance rates, from lowest to highest (m^3 cells^{-1} day^{-1}): A) $m_z = 10^{-10}$, B) $m_z = 10^{-9}$, C) $m_z = 10^{-8}$, and D) $m_z = 10^{-7}$.

4.8 Discussion

Using an idealized phytoplankton community model in a reduced-dimensional setting, we have demonstrated here that small-scale fluid turbulence can, under certain biological (cell size, grazing) and environmental conditions (level of turbulence), play a role in phytoplankton community dynamics via a direct impact on nutrient uptake rates. In the absence of prey density-dependent grazing pressure, the smallest cell always "wins" in this model and the impact of turbulence on nutrient uptake plays essentially no role in regulating community structure. With increasing prey density-dependent grazing pressure, however, additional, larger size cells may coexist, and turbulence becomes relevant in determining the community structure. We discuss here how the two sets of experiments–with linear loss and prey-density dependent grazing–complement the current understanding of the survival strategies of both large and small phytoplankton.

4.8.1 The Dominance of Small Cells, or "Small is Beautiful"

Using a linear loss parameterization of grazing in this allometric community model ($-mX_i$), the smallest size class of phytoplankton drives the ambient nutrient concentration to low levels at which other, larger sizes cannot compete (Fig. 4.5). Larger cells need more nutrient to survive (often several orders of magnitude higher R^*, depending on the cell size), and are rapidly excluded. Viewed from this perspective, the direct impact of turbulence on nutrient uptake is, at best, of minimal importance, and this has been argued in previous studies (Chisholm, 1992; Kiørboe, 2008). These small cell sizes are effective "gleaners", meaning they are adapted for life at low resource levels where nutrients are delivered primarily via diffusion. Their dominance in resource scarce conditions has been observed in the ocean (e.g., Zubkov et al., 1998) and predicted in a range of trait-based phytoplankton community models (e.g., Dutkiewicz et al., 2009). In contrast, the growth of larger cells tends to be more diffusion limited than for smaller cells (Chisholm, 1992). Thus, smaller cells tend to be more effective competitors for scarce nutrients, and this observation has formed the basis for interpreting other patterns. First, many investigators have observed that small cells are relatively abundant in low nutrient conditions, are not excluded in high nutrient conditions, and that large cells are rarely abundant at low resource levels (Chisholm, 1992; Irigoien et al., 2004). Second, Margalef's (1978) "mandala" paradigm argued that gleaners (and flagellates) dominate in low turbulence and nutrient regimes. Raven's (1998) iconic paper summarized the advantages of small cells as "Small is Beautiful."

4.8.2 "Big is Beautiful"

Despite their apparent limitation in terms of competition for scarce nutrients, large cells, such as diatoms, are found in a range of ocean habitats and conditions (e.g., Cermeño et al., 2006), though they are most conspicuous in periods of high turbulence and nutrients (Irigoien et al., 2004; Barber and Hiscock, 2006). Hypotheses explaining their survival are various (and not mutually exclusive), and we briefly mention several key hypotheses here before discussing the impact of turbulence on nutrient uptake rates. First is the grazing "loophole" hypothesis that explains why blooms of phytoplankton often have many large cells (Irigoien et al., 2005; Barber and Hiscock, 2006; Kiørboe, 2008). With the addition of inorganic nutrients, nutrient limitation is alleviated, and both small and large cells may grow. Because larger phytoplankton tend to have larger predators with slower growth rates, and smaller phytoplankton have smaller predators with faster growth rates (Hansen et al., 1994; Hansen et al., 1997), the result is often more large phytoplankton in bloom conditions. Second, we discuss a more steady state perspective. With low nutrient conditions, typically only smaller cells can grow because of their low R^*, and they are quickly grazed down by their predators. With additional nutrients, successively larger size cells may grow, and each prey is grazed by their own predator (or predators). The result is an ecosystem with both large and small phytoplankton (Armstrong, 1994; Ward et al., 2011b). Third, some larger phytoplankton, often with armored coverings, may be less palatable to predators.

In addition to this predation-focused perspective are several, more bottom-up hypotheses specific to large (here, non-motile) cells themselves. Large cells, particularly diatoms, have the capacity for "luxury uptake" and storage of nutrients in excess of their metabolic needs, which may allow them to weather nutrient-scarce periods and sequester nutrients away from competitors (Raven, 1987; Sunda and Huntsman, 1995; Tozzi et al., 2004). Also, the larger vacuoles of larger cells allow them to regulate buoyancy and increase their effective surface

area to volume ratio and specific nutrient uptake rates (Raven, 1987). Lastly, diatoms tend to have high maximum nutrient uptake and growth rates (Tang, 1995; Litchman et al., 2007), which may provide an advantage in variable nutrient and light conditions (Stewart and Levin, 1973; Grover, 1990).

4.8.3 Big Cells Benefit from Turbulence

Here, we have investigated an additional mechanism by which large phytoplankton increase their fitness. Small-scale fluid turbulence enhances the flux of nutrients to the cell surface by distorting the shape of the diffusive boundary layer surrounding cells, and nutrient uptake is increased particularly in turbulent conditions for large cells (Karp-Boss et al., 1996; Metcalfe et al., 2004; Peters et al., 2006). This enhancement is particularly relevant when we consider that the growth of large cells is quite often limited by diffusion of nutrients toward the cell (Chisholm, 1992; Ward et al., 2011a). The impact on the community structure is minimal for weak grazing pressure, but increases with higher clearance rates (Fig. 4.7). The idealized, quadratic parameterization of grazing used here ($-m_z X_i X_i$) levels the fitness landscape by focusing predation upon smaller, more numerous cells (Figs. 4.7, 4.8). Increasing the level of turbulence can then mean the difference between competitive exclusion and survival for a larger cell, and tends to enhance the biomass among the larger members of the phytoplankton community. Though we have considered only single, spherical cells, the benefits of turbulence may be more pronounced for larger colonies, mats, and chains of cells.

This mechanism is particularly meaningful when we consider the ubiquity and variability of turbulence in the ocean. In coastal and frontal zones, ϵ is generally higher than elsewhere, but is still quite variable (D'Asaro et al., 2011). Even in the more stratified, stable regions of the oceans that tend to have generally lower turbulence, ϵ can vary over several orders of magnitude in a period of days (e.g., MacKenzie and Leggett, 1993; Skyllingstad et al., 1999). Because phytoplankton growth timescales are similar to the timescales of periodically enhanced turbulence, we hypothesize that turbulence can have a quite immediate impact on phytoplankton community structure through the uptake mechanism outlined here. Our numerical experiments have suggested that this impact should be particularly strong where grazing pressure is relatively high, and negligible in the absence of strong grazing (high m_z). Next, if we consider habitats with extremely high resource levels, such as the high latitudes in spring, small-scale turbulence is unlikely to have a strong impact on community dynamics because nutrient uptake there is limited by cross-membrane exchange rather than flux towards the cell surface (Ward et al., 2011a).

Thus, the conceptual picture is that the direct impact turbulence has on nutrient uptake rates should play a key role in regions with relatively low nutrient levels and well-established predator populations. This scenario could be relevant to tropical and subtropical seas, as well as post-bloom conditions at higher latitudes. We hypothesize that episodic turbulence enhances the growth of large cells under these conditions, and may, in part, explain the persistence of large cells in apparently unfavorable habitats (Cermeño et al., 2006). We suggest that combined field measurements of phytoplankton community structure (including flow cytometry and microscopy; e.g., Irigoien et al., 2004) and fluid microstructure (ϵ; e.g., Gregg, 1989) may confirm or reject our hypotheses by targeting these relatively nutrient-deplete, yet periodically turbulent, conditions.

4.9 References

Aksnes, D., Egge, J., 1991. A theoretical model for nutrient uptake in phytoplankton. Marine Ecology Progress Series 70, 65-72.

Aksnes, D.L., Cao, F.J., 2011. Inherent and apparent traits in microbial nutrient acquisition. Submitted to Proceedings of the National Academy of Sciences.

Armstrong, R.A., McGehee, R., 1980. Competitive Exclusion. The American Naturalist 115(2), 151-170.

Armstrong, R.A., 1994. Grazing limitation and nutrient limitation in marine ecosystems: Steady state solutions of an ecosystem model with multiple food chains. Limnology and Oceanography 39(3), 597-608.

Armstrong, R. A., 2008. Nutrient uptake rate as a function of cell size and surface transporter density: A Michaelis-like approximation to the model of Pasciak and Gavis. Deep-Sea Research I 55, 1311-1317.

Barber, R.T., Hiscock, M.R., 2006. A rising tide lifts all phytoplankton: Growth response of other phytoplankton in diatom-dominated blooms. Global Biogeochemical Cycles 20, GB4S03, doi:10.1029/2006GB002726.

Berg, H.C., Purcell, E.M., 1977. Physics of chemoreception. Biophysical Journal 20, 193-219.

Bruggeman, J., 2009. Succession in plankton communities: A trait-based perspective. Ph.D. thesis, Vrije Universiteit, Amsterdam.

Calbet, A., Landry, M.R., 2004. Phytoplankton growth, microzooplankton grazing, and carbon cycling in marine systems. Limnology and Oceanography 49(1), 2004, 51-57.

Cermeño, P., et al., 2006. Invariant scaling of phytoplankton abundance and cell size in contrasting marine environments. Ecology Letters 9, 1210-1215.

Chisholm, S.W., 1992. Phytoplankton size. In Falkowski, P.G., Woodhead, A.D. (eds). Primary Productivity and Biogeochemical Cycles in the Sea. Plenum Press, New York.

Cullen, J.J., et al., 2002. Physical influences on marine ecosystem dynamics. In The Sea, Robinson, A., McCarthy, J.J., Rothschild, B.J., Eds. Wiley, New York, vol. 12, chap. 8.

Cushing, D.H., 1989. A difference in structure between ecosystems in strongly stratified waters and in those that are only weakly stratified. Journal of Plankton Research 11(1), 1-13.

D'Asaro, E., et al., 2011. Enhanced turbulence and energy dissipation at ocean fronts. Science 332, 318-322.

Droop, M.R., 1968. Vitamin B12 and marine ecology, IV. The kinetics of uptake, growth and inhibition in Monochrysis lutheri. Journal of the Marine Biological Association of the United Kingdom 48, 689-733.

Dutkiewicz, S., Follows, M.J., Bragg, J.G., 2009. Modeling the coupling of ocean ecology and biogeochemistry. Global Biogeochemical Cycles 23, GB4017, doi:10.1029/2008GB003405.

Falkowski, P.G., Oliver, M.J., 2007. Mix and match: how climate selects phytoplankton. Nature Reviews Microbiology 5, 813-819.

Finkel, Z.V., 2007. Does size matter? The evolution of modern marine food webs. In: The evolution of aquatic photoautotrophs. Eds. Falkowski, P.G., Knoll, A.H.. Academic Press. Chapter 15, 333-350.

Ferrari, R., Wunsch, C., 2009. Ocean circulation kinetic energy: reservoirs, sources, and sinks. Annual Reviews in Fluid Mechanics 41, 253-282.

Follows, M.J, et al., 2007. Emergent biogeography of microbial communities in a model ocean. Science 315, 1843-1846.

Gargett, A., 1989. Ocean turbulence. Annual Review of Fluid Mechanics 21, 419-451.

Gentleman, W., et al., 2003. Functional responses for zooplankton feeding on multiple resources: a review of assumptions and biological dynamics. Deep-Sea Research II 50, 2847-2875.

Gregg, M.C., 1989. Scaling turbulent dissipation in the thermocline. Journal of Geophysical Research 94(C7), 9686-9698.

Grover, J.P., 1990. Resource competition in a variable environment: phytoplankton growing according to Monod's model. The American Naturalist 136(6), 771-789.

Hansen, P.J., Bjørnsen, P.K., Hansen, B.W., 1994. The size ratio between planktonic predators and their prey. Limnology and Oceanography 39(2), 395-403.

Hansen, P.J., Bjørnsen, P.K., Hansen, B.W., 1997. Zooplankton grazing and growth: Scaling within the 2-2,000μm body size range. Limnology and Oceanography 42(4), 687-704.

Holling, C.S., 1965. The functional response of predators to prey density and its role in mimicry and population regulation. Memoirs of the Entomological Society of Canada, 45.

Huisman, J., et al., 2004. Changes in turbulent mixing shift competition for light between phytoplankton species. Ecology 85(11), 2960-2970.

Irigoien, X., et al., 2004. Global biodiversity patterns of marine phytoplankton and zooplankton. Nature 429, 863-867.

Irigoien, X., Flynn, K.J., Harris, R.P., 2005. Phytoplankton blooms: a loophole in microzooplankton grazing impact? Journal of Plankton Research 27(4), 313-321.

Irwin, A.J., et al., 2006. Scaling-up from nutrient physiology to the size-structure of phytoplankton communities. Journal of Plankton Research 28(5), 459-471.

Jeschke, J.M., Kopp, M., Tollrian, R., 2004. Consumer-food systems: why type I functional responses are exclusive to filter feeders. Biological Review 79, 337-349.

Karp-Boss, L., Boss, E., Jumars, P.A., 1996. Nutrient fluxes to planktonic osmotrophs in the presence of fluid motion. Oceanography and Marine Biology: an Annual Review 34, 71-107.

Kiørboe, T., Saiz, E., 1995. Planktiverous feeding in calm and turbulent environments, with emphasis on copepods. Marine Ecology Progress Series 122, 135-145.

Kiørboe, T., 2008. A Mechanistic Approach to Plankton Ecology. Princeton University Press.

Klausmeier, C.A., Litchman, E., 2001. Algal games: The vertical distribution of phytoplankton in poorly mixed water columns. Limnology and Oceanography 46(8), 1998-2007.

Kriest, I., Khatiwala, S., Oschlies, A., 2010. Towards an assessment of simple global marine biogeochemical models of different complexity. Progress in Oceanography 86, 337-360.

Longhurst, A.R., 1998. Ecological geography of the sea, San Diego, Academic Press.

MacKenzie, B.R., Leggett, W.C., 1993. Wind-based models for estimating the dissipation rates of turbulent energy in aquatic environments: empirical comparisons. Marine Ecology Progress Series 94, 207-216.

Mann, K.H., Lazier, J.R.N., 1996. Dynamics of marine ecosystems: biological-physical interactions in the oceans. Blackwell Publishing, Malden, MA, USA.

Margalef, R., 1978. Life-forms of phytoplankton as survival alternatives in an unstable environment. Oceanologica acta 1(4), 493-509.

Metcalfe, A.M., Pedley, T.J., Thingstad, T.F., 2004. Incorporating turbulence into a plankton foodweb model. Journal of Marine Systems 49, 105-122.

Monod, J., 1950. La technique de culture continue, théorie et applications. Ann. Inst. Pasteur (Paris) 79, 390-410.

Mullin, M., Stewart, E.F., Fuglister, F.J., 1975. Ingestion by planktonic grazers as a function of concentration of food. Limnology and Oceanography 20(2), 259-262.

Pahlow, M., Riebesell, U., Wolf-Gladrow, D.A., 1997. Impact of cell shape and chain formation on nutrient acquisition by marine diatoms. Limnology and Oceanography 42(8), 1660-1672.

Pasciak, W.J., Gavis, J., 1974. Transport limitation of nutrient uptake in phytoplankton. Limnology and Oceanography 19(6), 881-888.

Peters, F., Marrasé, C., 2000. Effects of turbulence on plankton: an overview of experimental evidence and some theoretical considerations. Marine Ecology Progress Series 205, 291-306.

Peters, F., et al., 2006. Effects of small-scale turbulence on the growth of two diatoms of different size in a phosphorus-limited medium. Journal of Marine Systems 61, 134-148.

Raven, J.A., 1987. The role of vacuoles. New Phytologist 106(3), 357-422.

Raven, J.A., 1998. The Twelfth Tansley Lecture, Small is Beautiful: The Picophytoplankton. Functional Ecology 12(4), 503-513.

Ruiz, J., Macías, D., Peters, R., 2004. Turbulence increases the average settling velocity of phytoplankton cells. Proceedings of the National Academy of Sciences 101(58), 17720-17724.

Seymour, J.R., Marcos, Stocker, R., 2009. Resource patch formation and exploitation throughout the marine microbial food web. The American Naturalist 173(1), E15-E29.

Schartau, M., Oschlies, A., 2003. Simultaneous data-based optimization of a 1D-ecosystem model at three locations in the North Atlantic: Part IMethod and parameter estimates. Journal of Marine Research 61, 765-793.

Skyllingstad, E.D., et al., 1999. Upper-ocean turbulence during a westerly wind burst: A comparison of large-eddy simulation results and microstructure measurements. Journal of Physical Oceanography 29, 5-28.

Stewart, F.M., Levin, B.R., 1973. Partitioning of resources and the outcome of interspecific competition: A model and some general considerations. American Naturalist 107(954), 171-198.

Sunda, W.G., Huntsman, S.A., 1995. Iron uptake and growth limitation in oceanic and coastal phytoplankton. Marine Chemistry 50, 189-206.

Tang, E.P.Y., 1995. The allometry of algal growth rates. Journal of Plankton Research 17 (6), 1325-1335.

Taylor J.R., Stocker, R., 2011. Trade-offs of chemotactic foraging in turbulence. In prep.

Taylor J.R., Ferrari, R., 2011. Shutdown of turbulent convection as a new criterion for the onset of spring phytoplankton blooms. In prep.

Tennekes, H., Lumley,J.L., 1972. A first course in turbulence. Cambridge: The MIT Press.

Tilman, D., 1981. Tests of Resource Competition Theory Using Four Species of Lake Michigan Algae. Ecology 62(3), 802-815.

Tomas, C., et al., 1997. Identifying marine phytoplankton. Academic Press.

Tozzi, S., Schofield, O., Falkowski, P., 2004. Historical climate change and ocean turbulence as selective agents for two key phytoplankton functional groups. Marine Ecology Progress Series 274, 123-132.

Vallina, S.M., LeQuéré, C., 2011. Stability of complex food webs: Resilience, resistance and the average interaction strength. Journal of Theoretical Biology 272, 160-173.

Villareal, T.A., Altabet, M.A., Culver-Rymsza, K., 1993. Nitrogen transport by vertically migrating diatom mats in the North Pacific Ocean. Nature 363, 709-712.

Ward, B.A., Barton, A.D., Dutkiewicz, S., Follows, M.J., 2011a. Biophysical aspects of mixotrophic resource acquisition and competition. Accepted, The American Naturalist.

Ward, B.A., Dutkiewicz, S., Follows, M.J., 2011b. Size-structured food webs in the global ocean: theory, model, and observations. Submitted, Marine Ecology Progress Series.

Zubkov, M.V., et al., 1998. Picoplanktonic community structure on an Atlantic transect from 50N to 50S. Deep-Sea Research I 45, 1339-1355.

Chapter 5

Summary and Future Directions

5.1 Overview

In the preceding chapters, I sought to understand how the functional traits of constituent species and the marine environment jointly regulate the community ecology of phytoplankton. In Chapter 2, I examined field observations from the Continuous Plankton Recorder (CPR) of the abundances of diatoms and dinoflagellates in the North Atlantic Ocean and interpreted their ecological dynamics in terms of functional traits, as inferred from compilations of laboratory- and field-based data. In Chapter 3, I diagnosed the patterns of phytoplankton diversity that emerged in a complex global ecosystem model, and interpreted these patterns by using an idealized, zero-dimensional model of competition for resources among phytoplankton with a range of traits. In Chapter 4, I investigated–again using an idealized, phytoplankton resource competition model–how small-scale fluid turbulence affects phytoplankton nutrient uptake rate and community structure. In this section, I summarize the main findings and limitations of each chapter (Chapters 2-4) and pose what I believe are compelling, unanswered questions that stem from the work. Despite the general focus on bottom-up processes in the thesis, a recurring theme throughout is that both bottom-up and top-down (zooplankton grazing) processes jointly regulate the community ecology of phytoplankton (see also the Introduction section on grazing). As a result, in this section I discuss how I could build upon the initial bottom-up focus by exploring top-down processes more thoroughly. Lastly, in the "Future Directions" Section, I describe several avenues for future research that build upon the work in this thesis and begin to answer some of the unanswered questions.

5.2 Chapter Summary

5.2.1 Chapter 2: The Continuous Plankton Recorder

Ecologists have long examined the CPR survey data for long-term ecological change (e.g., Barton et al., 2003), temporal species succession (Colebrook, 1979), biogeographical patterns (Barnard et al., 2004), invasive species (Reid et al., 2007), and phenological change (Edwards and Richardson, 2004). Here, my collaborators and I have interpreted, for the first time, the successional patterns in terms of the functional traits of the surveyed taxa, which we inferred from a large range of published studies. The main findings of Chapter 2 are:

- We have assembled an extensive cell size database of surveyed phytoplankton taxa, which can be used to infer other phytoplankton traits, such as maximum growth rate (μ^{max}). To our knowledge, it is the most comprehensive database of its kind.

- We have assembled a database describing the trophic strategies of surveyed phytoplankton taxa. To our knowledge, this is the first effort of its kind. The majority of survey dinoflagellates appear to be mixotrophic (n=44), and a few are pure heterotrophs (n=7). None are pure photoautotrophs in this classification scheme.

- There is a seasonal succession from photoautotrophic diatoms to mixotrophic and then heterotrophic dinoflagellates in the North Atlantic Ocean. Photoautotrophs dominate in spring with abundant nutrients and light, heterotrophs dominate later with abundant prey, and mixotrophs reach their maximum in between these two extremes. We hypothesize that this characteristic pattern in mixotrophs occurs because they exploit multiple resources.

- During nutrient-deplete periods (i.e., summer), there is a shift toward smaller cells among both diatoms and dinoflagellates. We hypothesize that this shift occurs because smaller cells are more competitive in low nutrient conditions than larger cells. For dinoflagellates, smaller prey in summer may favor smaller over larger dinoflagellates.

- On the timescale measured by the survey ($\sim$1 month), there is no relationship between maximum net growth (μ^{net}) and cell size or taxonomy. This suggests that growth and loss processes nearly balance across a wide range of cell sizes and between diatoms and dinoflagellates.

In addition to these findings, I highlight here a number of limitations of the study. First, though the methodology is consistent through space and time, the density of data sampling by the CPR survey is inconsistent through space and time. Second, the CPR abundance data are not reported in the more standard units of cells m^{-3}, but instead cells per generic volume. Both of these points limit the utility of the CPR database. Third, rather than analyzing zooplankton abundance and nutrient data that are co-located with the phytoplankton abundance data, we instead discussed their generic, mean seasonal patterns, as reported by previous studies. This simplification could be improved upon by incorporating additional data, which I discuss below.

In the process of conducting research for Chapter 2, a number of questions arose that merit further consideration, some of which I revisit below in the "Future Directions" section:

Q1 Dinoflagellates have lower maximum growth rates (μ^{max}) than diatoms in laboratory conditions (Tang, 1995). Is this because they are grown as though they are photoautotrophs, when in fact they are often mixotrophic? If their heterotrophic nutrition is considered, do they still grow more slowly than diatoms?

Q2 We largely considered the spatial and temporal mean successional patterns in Chapter 2. How do these patterns vary in space (i.e., latitude and longitude)? In time (i.e., the whole survey period, 1958-2006)?

Q3 Is it possible to diagnose which functional traits are favored where and when? In other words, is it possible to make a "trait map" showing the likelihood of a given trait being favored at a given place and period?

Q4 Would it be possible to better constrain phytoplankton grazing losses by examining the zooplankton data in the CPR survey? The zooplankton community is quite well-sampled by the survey.

Q5 Would it be possible to better understand the shifts in phytoplankton size structure if we were able to compare co-located nutrient, zooplankton, and phytoplankton data? While the nutrient and CPR data are sparse, there is the possibility of including nutrient data from long-term monitoring sites such as Helgoland and ocean weather ships.

5.2.2 Chapter 3: Phytoplankton Diversity

Ecologists have long debated over the mechanisms regulating the meridional decrease in species diversity, and there is no single, accepted explanation. This is particularly true of marine phytoplankton. Here, my collaborators and I have found an emergent meridional diversity gradient in a complex marine ecosystem model (Follows et al., 2007) that resembles the meridional patterns seen among more well-studied marine and terrestrial taxa, and which is consistent with the limited available data describing phytoplankton diversity. Using an idealized resource competition model, we developed hypotheses for the spatial diversity gradients seen in the global model. The main findings of Chapter 3 are:

- In the modeled subpolar oceans, strong seasonal variability of the environment leads to competitive exclusion of phytoplankton with slower growth rates and subsequently to lower diversity.
- The relatively weak seasonality of the stable subtropical and tropical oceans in the global model enables long exclusion timescales and the prolonged coexistence of multiple phytoplankton with comparable fitness, as measured by R^*.
- Superimposed on this equator-to-pole diversity decrease are "hot spots" of enhanced diversity in some regions of energetic ocean circulation which reflect a strong influence of lateral dispersal.

In addition to these findings, I highlight here a number of limitations of the study. First, the treatments of grazing in the global and 0-D models are not the same, making direct inter-comparison impossible. However, the simple linear loss grazing in the 0-D model highlights the role environmental, rather than top-down processes, in shaping community diversity and is therefore illuminating. More realistic grazing schemes not used in either the global or 0-D models would likely have an important, unresolved impact on diversity (see below). Second, the Monod model of algal growth used in both the global and 0-D model does not allow for internal storage of nutrients and does not differentiate between algal growth (change in cell biomass) and division (change in number of cells). As a result, we have adopted a quota model for later chapters.

In the process of conducting research for Chapter 3, a number of questions arose that merit further consideration, some of which I revisit below in the "Future Directions" section:

Q6 What roles does zooplankton grazing play in determining the diversity of phytoplankton? How might different grazing behaviors and food chain structures affect phytoplankton diversity? How might our hypotheses concerning the maintenance of

diversity change if we considered more realistic grazing? For instance, in Chapter 4 I employed a non-linear loss that allowed many different size classes to coexist with the same R*. How would such a parameterization of grazing change the results in Chapter 3?

Q7 Over what distances may mixing and advection enhance phytoplankton diversity? On what timescales? How does the importance of these dispersal processes compare to *in situ* growth and loss processes?

Q8 There does not appear to be a strong relationship between the amount of primary productivity and diversity in the global model, though this has often been discussed in the literature (e.g., Irigoien et al., 2004). Why might this be the case?

5.2.3 Chapter 4: Turbulence and Nutrient Uptake

Turbulence is thought to play a key role in structuring marine ecosystems by setting the background nutrient concentration and through the direct impacts of small-scale fluid motion on cells themselves. Here, my collaborators and I investigated the direct impact that small-scale fluid turbulence has on nutrient uptake rates and phytoplankton community structure using a quota-type allometric model configured in an idealized, zero-dimensional setting. Whereas numerous other investigators have concluded that the impact of fluid turbulence on nutrient uptake is largely irrelevant, we find that it is important under certain biological and physical conditions. The main findings of Chapter 4 are:

- Turbulence enhances the total flux of nutrients to the cell surface and nutrient uptake above what is possible in still conditions, and this effect is most pronounced for large cells in turbulent conditions.
- In the absence of prey density-dependent grazing pressure (or linear loss), turbulence plays little role in regulating community structure and the smallest cell size outcompetes all others because of its relatively low R^*.
- With prey density-dependent grazing pressure (or quadratic loss), the coexistence of many phytoplankton sizes was possible and turbulence played a role in selecting the number of coexisting size classes and the dominant size class.
- We hypothesize that the impact of turbulence on community structure may be greatest in relatively nutrient-deplete regions that experience episodic inputs of turbulent kinetic energy.

In addition to these findings, I highlight here a number of limitations of the study. First, we considered only non-motile, spherical, photoautotrophic cells. This simplification excludes a large range of phytoplankton morphologies and behaviors, including motility, chain and colony formation, and non-spherical geometries. Second, we considered only the steady state solutions describing resource competition between phytoplankton at different, constant levels of turbulence. Though instructive, it may be more realistic to examine variable turbulence and the transient phytoplankton dynamics.

In the process of conducting research for Chapter 4, a number of questions arose that merit further consideration, some of which I revisit below in the "Future Directions" section:

Q9 Would it be possible to parameterize small-scale fluid turbulence in a global ocean and ecosystem model (using surface winds and water column density structure; e.g., MacKenzie and Leggett, 1993) and evaluate in a regional or global setting the impact of small-scale turbulence on community structure?

Q10 Using a similar method to parameterize the enhanced flux of nutrients toward the cell caused by swimming (Karp-Boss et al., 1996), can we model the effect of swimming in turbulent flows on nutrient uptake? This experiment would be relevant to motile phytoplankton, including dinoflagellates, and allow for quantification of some of the suspected advantages provided by swimming.

5.3 Future Directions

While it would be impossible to reasonably outline a path to answering all these outstanding and other closely related questions, several feasible and immediate projects build well upon the work I and my collaborators conducted for this thesis. With the exception of Chapter 3 where I examined phytoplankton diversity in a global model, much of the analyses in this thesis focused on large spatial- and temporal-scale averages of field observations (e.g., Chapter 2) or idealized models configured in a zero-dimensional setting (Chapters 3, 4). Though informative, these approaches lose important spatial and temporal information. Below, I briefly propose several follow-on projects that build upon this thesis by considering in greater detail how community structure, and the mechanisms regulating community structure, vary in time and space. The descriptions of each project are intended to be brief but detailed enough to highlight the main hypotheses and methodologies.

5.3.1 Putting Functional Traits on the Map

An analysis of CPR phytoplankton and trait data, conducted in collaboration with Zoe Finkel of Mt. Allison University and Mick Follows of MIT.

The CPR survey roughly spans the transition zone between subpolar and subtropical ocean habitats, and includes coastal and pelagic zones. The data are therefore well-suited for discerning not only what types of phytoplankton inhabit each region, but also which traits or combination of traits tend to enable those phytoplankton to grow in particular environmental conditions. In effect, the idea of the proposed work is to build a better spatial understanding of how and why traits vary in the ocean, and thereby enhance understanding of phytoplankton biogeography. To this end, there are two complementary goals: a) build maps of how the expression of particular functional traits, such as cell size, maximum growth rate (μ^{max}), or trophic strategy, varies over the North Atlantic basin and b) quantify characteristic assemblages of phytoplankton species with known traits and assess how these change in space.

The first goal is an extension of the CPR analyses presented in this thesis, but I plan to reevaluate the CPR phytoplankton abundance and trait data in a spatial context. Several large-scale field surveys of the phytoplankton community (e.g., Atlantic Meridional Transect; Johnson et al., 2006) and trait-based models of phytoplankton communities (e.g., Follows et al., 2007; Dutkiewicz et al., 2009) have begun to unravel the mechanisms that determine phytoplankton biogeography, but in the CPR data, combined with the database

we have built of phytoplankton traits, there is a great opportunity to make additional advances in this area. The second goal is a clustering exercise to identify those taxa that covary (e.g., Keister and Peterson, 2003; Peterson and Keister, 2003), and to determine how these characteristic assemblages vary in space.

In this project, we address the following hypotheses:

- Particular associations of phytoplankton taxa consistently and predictably co-occur, and these patterns are based upon the functional traits of each species, biotic interactions such as grazing, and environmental conditions.
- Cell size is an important phytoplankton trait that varies in space and time. Smaller phytoplankton cells should be most conspicuous in regions and times with relatively low nutrients, such as the northern margin of the subtropical gyre and during summer in the subpolar gyre. Because of the relatively high nutrient levels in coastal zones, the competitive advantage of smaller cells there should be minimal.
- Trophic strategy is an important phytoplankton trait that varies in time and space. Because of their "bet hedging" and utilization of multiple resources, mixotrophs should be most successful in regions that have rapidly evolving physical conditions or relatively low nutrient levels (e.g., Ward et al., 2011b).

5.3.2 Long-term Ecological Variability in the North Atlantic Ocean

An analysis of CPR phytoplankton, trait, hydrographic, and meteorological data and a basin-scale ecosystem model, conducted in collaboration with Susan Lozier of Duke University and Mick Follows, Stephanie Dutkiewicz, and Ben Ward of MIT.

The relative abundance of diatoms and dinoflagellates and the total phytoplankton biomass have varied considerably over the many decades covered by the CPR survey, and it is thought that these changes may be linked to decadal-scale climate variations (e.g., Barton et al., 2003; Leterme et al., 2005). However, the causes of these coordinated, long-term changes are poorly understood. Here, we propose to combine analyses of CPR abundance and species-specific trait data and hydrographic and meteorological data with basin-scale models of the North Atlantic Ocean in order to develop greater understanding of how long-term variability in the marine environment brings about observable changes in the North Atlantic Ocean phytoplankton community.

First, we propose to characterize the long-term variability in the abundance of the phytoplankton species measured by the CPR over the survey area. This analysis is an extension of the CPR work done in this thesis, but it will focus more on the long-term temporal change in phytoplankton communities rather than on seasonal cycles. Second, using retrospective hydrographic and meteorological data, we will evaluate, to the extent possible, variability of important physical processes, including local stratification (Dave and Lozier, 2010), lateral Ekman transport (Williams and Follows, 1998; Ayers and Lozier, 2010), and production and advection of subtropical mode water (Palter et al., 2005). We seek correlations between the relevant physical processes and ecosystem properties and species abundances, and use these analyses to inform experiments with a coupled ocean and ecosystem model. We propose to configure the size-structured phytoplankton community model of Ward et al. (2011a), with the addition of important taxonomic differences between dinoflagellates and diatoms, in a

realistic physical representation of the North Atlantic basin (after Wunsch and Heimbach, 2007; 20°S-70°N, 1°x1° resolution, 23 vertical levels for years 1992-2010). After running the ecosystem model on top of the physical setting to attain relatively stable, repeating annual cycles of phytoplankton biomass, we then excite the physical model with idealized wind and buoyancy forcing in order to recreate characteristic climate-linked physical regimes seen in the observational record, such as the North Atlantic Oscillation. In this manner, we can evaluate the model ecosystem response to idealized forcing and examine more closely the causal mechanisms linking environmental and ecosystem changes. In other words, we propose to use the model to interpret the long-term patterns seen in the CPR record.

In this project, we address the following hypotheses:

- Phytoplankton species, and groups of species such as diatoms and dinoflagellates, show spatially coherent, long-term variability in the CPR survey.
- Patterns in long-term community structure and total biomass of phytoplankton can be linked to coherent shifts in physical forcing such as local stratification, Ekman transport, and production and advection of subtropical mode water.
- Shifts in phytoplankton community structure can be reproduced in a coupled ocean and ecosystem model that is forced with idealized conditions in a manner to bring about physical processes that are consistent with the observational record. For instance, by modifying model surface wind stresses and thereby driving differing Ekman transports, can we bring about an ecosystem response that is consistent with what is seen in the observational record?

5.3.3 The Importance of Bottom-up and Top-down Regulation of Phytoplankton Community Ecology

An analysis of CPR phytoplankton, zooplankton, and associated trait data and a basin-scale ecosystem model, conducted in collaboration with Neil Banas and Julie Keister of the University of Washington and Mick Follows, Stephanie Dutkiewicz, and Ben Ward of MIT.

In this thesis and elsewhere, progress has been made toward modeling and understanding the bottom-up role of functional traits and the environment in structuring marine phytoplankton communities (e.g., Follows et al., 2007). Yet throughout this thesis, top-down processes, including zooplankton grazing, also played an important role in regulating community ecology. However, there remain a number of unanswered questions regarding how top-down pressure impacts plankton community structure, several of which we address here.

As with the preceding project, here we propose both an analysis of CPR data and basin-scale ecosystem models. First, we consider the CPR data to determine the spatial, seasonal, interannual, and climate-scale patterns of phytoplankton abundance, but now also analyze the zooplankton abundance data. We use statistical methods to determine community associations, predator-prey co-occurrence, and link these associations to their traits and the environment (Keister and Peterson, 2003; Peterson and Keister, 2003). For instance, do small phytoplankton covary with the smallest zooplankton? Fortunately, the sizes of survey zooplankton are relatively well-known (Richardson et al., 2006), and we can estimate many of their relevant traits, such as growth and clearance rates, using their size (Hansen et al., 1994; Hansen et al., 1997). Second, we build a size-structured model

of a diverse phytoplankton and zooplankton ecosystem such that the interplay of bottom-up and top-down ecological processes can be assessed (e.g., Armstrong, 1994; Baird and Suthers, 2007; Fuchs and Franks, 2010; Banas, 2011; Prowe et al., 2011; Ward et al., 2011a). We implement this model in a zero-dimensional test case and in a more realistic three-dimensional configuration of the North Atlantic basin, as described above. However, rather than forcing the ocean-ecosystem model with idealized climate states as above, here we examine the ecosystem during the period for which we have an ocean state estimate, 1992-2010.

In this project, we address the following hypotheses:

- Particular associations of phytoplankton and zooplankton taxa consistently and predictably co-occur, and these patterns are based upon the functional traits of each species, their interactions, and environmental conditions.
- The abundance of relatively small, quickly-growing predators should closely track the abundance of relatively small prey, whereas the abundance of larger prey and larger, more slowly-growing predators should be, at times, decoupled. This hypothesis is called the "grazing loophole", and though we cannot diagnose predation directly from the survey data, we look for patterns that are consistent with the "grazing loophole" hypothesis in the CPR data. The size-structured model allows for more direct consideration of this hypothesis.
- Various models have predicted that zooplankton grazing enhances phytoplankton diversity. We look for evidence of this in the CPR data by quantifying the number of species present and evenness of abundance distribution among phytoplankton in relation to attendant zooplankton populations. We also experiment with the ecosystem model to see how diversity varies in response to accepted grazing schemes.

5.4 References

Ayer, J.M., Lozier, M.S., 2010. Physical controls on the seasonal migration of the North Pacific transition zone chlorophyll front. Journal of Geophysical Research 115, C05001, doi:10.1029/2009JC005596.

Baird, M.E., Suthers, I.M., 2007. A size-resolved pelagic ecosystem model. Ecological Modelling 203, 185-203.

Banas, N.S., 2011. Adding rich trophic interactions to a size-spectral plankton model: Emergent diversity patterns and limits on predictability. Submitted to Ecological Modeling. Also http://faculty.washington.edu/banasn/papers/banas-astrocat-submitted.pdf

Barnard, R., et al., 2004. Continuous Plankton Records: plankton atlas of the North Atlantic Ocean (1958-1999). II. Biogeographical Charts. Marine Ecology Progress Series Supplement, 11-75.

Barton, A.D., et al., 2003. The Continuous Plankton Recorder survey and the North Atlantic Oscillation: Interannual- to Multidecadal-scale patterns of phytoplankton variability in the North Atlantic Ocean. Progress in Oceanography 58, 337-358.

Colebrook, J.M., 1979. Continuous Plankton Records: seasonal cycles of phytoplankton and copepods in the North Atlantic Ocean and North Sea. Marine Biology 51, 23-32.

Dave, A., Lozier, M.S., 2010. Local stratification control of marine productivity in the subtropical North Pacific. Journal of Geophysical Research 115, C12032, doi:10.1029/2010JC006507.

Dutkiewicz, S., Follows, M.J., Bragg, J.G., 2009. Modeling the coupling of ocean ecology and biogeochemistry. Global Biogeochemical Cycles 23, GB4017, doi:10.1029/2008GB003405.

Edwards, M., Richardson, A.J., 2004. Impact of climate change on marine pelagic phenology and trophic mismatch. Nature 430, 881-884.

Follows, M.J, et al., 2007. Emergent biogeography of microbial communities in a model ocean. Science 315, 1843-1846.

Fuchs, H.L., Franks, P.J.S., 2010. Plankton community properties determined by nutrients and size-selective feeding. Marine Ecology Progress Series 413, 1-15.

Hansen, P.J., Bjørnsen, P.K., Hansen, B.W., 1994. The size ratio between planktonic predators and their prey. Limnology and Oceanography 39(2), 395-403.

Hansen, P.J., Bjørnsen, P.K., Hansen, B.W., 1997. Zooplankton grazing and growth: Scaling within the 2-2,000um body size range. Limnology and Oceanography 42(4), 687-704.

Irigoien, X., Huisman, J., Harris R.P., 2004. Global biodiversity patterns of marine phytoplankton and zooplankton. Nature 429, 863-867.

Johnson, Z.I., et al., 2006. Niche partitioning among *Prochlorococcus* ecotypes along ocean-scale environmental gradients. Science 311, 1737-1740.

Karp-Boss, L., Boss, E., Jumars, P.A., 1996. Nutrient fluxes to planktonic osmotrophs in the presence of fluid motion. Oceanography and Marine Biology: an Annual Review 34, 71-107.

Keister, J.E., Peterson, W.T., 2003. Zonal and seasonal variations in zooplankton community structure off the central Oregon coast, 1998-2000. Progress in Oceanography 57, 341-361.

Leterme, S.C., et al., 2005. Decadal basin-scale changes in diatoms, dinoflagellates, and phytoplankton color across the North Atlantic. Limnology and Oceanography 50(4), 1244-1253.

MacKenzie, B.R., Leggett, W.C., 1993. Wind-based models for estimating the dissipation rates of turbulent energy in aquatic environments: empirical comparisons. Marine Ecology Progress Series 94, 207-216.

Palter, J.B., Lozier, M.S., Barber, R.T., 2005. The effect of advection on the nutrient reservoir in the North Atlantic Subtropical Gyre. Nature 437(7059), 687-692.

Peterson, W.T., Keister, J.E., 2003. Interannual variability in copepod community composition at a coastal station in the northern California Current: a multivariate approach. Deep-Sea Research II 50, 2499-2517.

Prowe, A.E., et al., 2011. Top-down control of marine phytoplankton diversity in a global ecosystem model. Submitted to Progress in Oceanography.

Reid, P.C., et al., 2007. A biological consequence of reducing Arctic ice cover: arrival of the Pacific diatom Neodenticula seminae in the North Atlantic for the first time in 800000 years. Global Change Biology 13, 1910-1921.

Richardson, A.J., et al., 2006. Using continuous plankton recorder data. Progress in Oceanography 68, 27-74.

Tang, E.P.Y., 1995. The allometry of algal growth rates. Journal of Plankton Research 17(6), 1325-1335.

Ward, B.A., Dutkiewicz, S., Follows, M.J., 2011a. Size-structured food webs in the global ocean: theory, model, and observations. Submitted, Marine Ecology Progress Series.

Ward, B.A., et al, 2011b. Biophysical aspects of mixotrophic resource acquisition and competition. Accepted, The American Naturalist.

Williams, R.G., Follows, M.J., 1998. The Ekman transfer of nutrients and maintenance of new production over the North Atlantic. Deep Sea Research Part I 45(2-3), 461-489.

Wunsch, C., Heimbach, P., 2007. Practical global ocean state estimation. Physica D 230, 197-208.